

AD-A223 221

MTL TR 90-26

AD

2

# A SUMMARY OF MEASUREMENTS OF PERMITTIVITIES AND PERMEABILITIES OF SOME MICROWAVE ABSORBING MATERIALS

W. A. SPURGEON

U.S. ARMY MATERIALS TECHNOLOGY LABORATORY  
CERAMICS RESEARCH BRANCH

M. EL RAYESS, P. DORSEY, and C. VITTORIA  
DEPARTMENT OF ELECTRICAL AND COMPUTER ENGINEERING  
NORTHEASTERN UNIVERSITY, BOSTON, MA

May 1990

Approved for public release; distribution unlimited.

Co



US ARMY  
LABORATORY COMMAND  
MATERIALS TECHNOLOGY LABORATORY

U.S. ARMY MATERIALS TECHNOLOGY LABORATORY  
Watertown, Massachusetts 02172-0001

90 00 25 174

The findings in this report are not to be construed as an official Department of the Army position, unless so designated by other authorized documents.

Mention of any trade names or manufacturers in this report shall not be construed as advertising nor as an official indorsement or approval of such products or companies by the United States Government.

**DISPOSITION INSTRUCTIONS**

Destroy this report when it is no longer needed.  
Do not return it to the originator.

UNCLASSIFIED

SECURITY CLASSIFICATION OF THIS PAGE (When Data Entered)

DD FORM 1 JAN 73 1473

EDITION OF 1 N. V 85 IS OBSOLETE

UNCLASSIFIED

SECURITY CLASSIFICATION OF THIS PAGE (When Data Entered)

**UNCLASSIFIED**

SECURITY CLASSIFICATION OF THIS PAGE (When Data Entered)

Block No. 20

**ABSTRACT**

This report presents results of measurements of permittivities (see Glossary) and permeabilities of assorted materials collected by the U.S. Army Office of Low Observables Technology and Applications (LOTA), and by the U.S. Army Materials Technology Laboratory (MTL). This will be one of a planned series of annual reports prepared by MTL for LOTA describing the results of such tests.

The samples fell into the following categories:

1. Pure materials (teflon, plexiglasses and casting plastic).
2. Metal-coated microspheres.
3. Carbospheres, both uncoated and metal coated.
4. Ferrites.
5. Magnetic metal flake.
6. Ceramic matrix composites.
7. A standard paint.

The data and its limitations and plans for additional testing are presented in the text. The most interesting results were obtained for a Rockwell Ferrite and for a 50/50 ferronickel flake which showed magnetic loss from 2 to 18 GHz.

**UNCLASSIFIED**

SECURITY CLASSIFICATION OF THIS PAGE (When Data Entered)

## CONTENTS

	Page
INTRODUCTION .....	1
EXPERIMENTAL .....	1
RESULTS	
Pure Materials .....	1
Metal-Coated Microspheres .....	2
Carbospheres .....	6
Ferrites .....	7
Magnetic Metal Flake .....	11
Ceramic Matrix Composites .....	12
A Standard Paint .....	12
CONCLUSIONS AND RECOMMENDATIONS .....	13
GLOSSARY .....	13



Accession For	
1. THIS COPY	<input checked="" type="checkbox"/>
2. OTHER	<input type="checkbox"/>
3. INDEX	<input type="checkbox"/>
4. FILE	<input type="checkbox"/>
5. STAMP	<input type="checkbox"/>
6. OTHER	<input type="checkbox"/>
7. INDEX	<input type="checkbox"/>
8. FILE	<input type="checkbox"/>
9. STAMP	<input type="checkbox"/>
10. OTHER	<input type="checkbox"/>
11. INDEX	<input type="checkbox"/>
12. FILE	<input type="checkbox"/>
13. STAMP	<input type="checkbox"/>
14. OTHER	<input type="checkbox"/>
15. INDEX	<input type="checkbox"/>
16. FILE	<input type="checkbox"/>
17. STAMP	<input type="checkbox"/>
18. OTHER	<input type="checkbox"/>
19. INDEX	<input type="checkbox"/>
20. FILE	<input type="checkbox"/>
21. STAMP	<input type="checkbox"/>
22. OTHER	<input type="checkbox"/>
23. INDEX	<input type="checkbox"/>
24. FILE	<input type="checkbox"/>
25. STAMP	<input type="checkbox"/>
26. OTHER	<input type="checkbox"/>
27. INDEX	<input type="checkbox"/>
28. FILE	<input type="checkbox"/>
29. STAMP	<input type="checkbox"/>
30. OTHER	<input type="checkbox"/>
31. INDEX	<input type="checkbox"/>
32. FILE	<input type="checkbox"/>
33. STAMP	<input type="checkbox"/>
34. OTHER	<input type="checkbox"/>
35. INDEX	<input type="checkbox"/>
36. FILE	<input type="checkbox"/>
37. STAMP	<input type="checkbox"/>
38. OTHER	<input type="checkbox"/>
39. INDEX	<input type="checkbox"/>
40. FILE	<input type="checkbox"/>
41. STAMP	<input type="checkbox"/>
42. OTHER	<input type="checkbox"/>
43. INDEX	<input type="checkbox"/>
44. FILE	<input type="checkbox"/>
45. STAMP	<input type="checkbox"/>
46. OTHER	<input type="checkbox"/>
47. INDEX	<input type="checkbox"/>
48. FILE	<input type="checkbox"/>
49. STAMP	<input type="checkbox"/>
50. OTHER	<input type="checkbox"/>
51. INDEX	<input type="checkbox"/>
52. FILE	<input type="checkbox"/>
53. STAMP	<input type="checkbox"/>
54. OTHER	<input type="checkbox"/>
55. INDEX	<input type="checkbox"/>
56. FILE	<input type="checkbox"/>
57. STAMP	<input type="checkbox"/>
58. OTHER	<input type="checkbox"/>
59. INDEX	<input type="checkbox"/>
60. FILE	<input type="checkbox"/>
61. STAMP	<input type="checkbox"/>
62. OTHER	<input type="checkbox"/>
63. INDEX	<input type="checkbox"/>
64. FILE	<input type="checkbox"/>
65. STAMP	<input type="checkbox"/>
66. OTHER	<input type="checkbox"/>
67. INDEX	<input type="checkbox"/>
68. FILE	<input type="checkbox"/>
69. STAMP	<input type="checkbox"/>
70. OTHER	<input type="checkbox"/>
71. INDEX	<input type="checkbox"/>
72. FILE	<input type="checkbox"/>
73. STAMP	<input type="checkbox"/>
74. OTHER	<input type="checkbox"/>
75. INDEX	<input type="checkbox"/>
76. FILE	<input type="checkbox"/>
77. STAMP	<input type="checkbox"/>
78. OTHER	<input type="checkbox"/>
79. INDEX	<input type="checkbox"/>
80. FILE	<input type="checkbox"/>
81. STAMP	<input type="checkbox"/>
82. OTHER	<input type="checkbox"/>
83. INDEX	<input type="checkbox"/>
84. FILE	<input type="checkbox"/>
85. STAMP	<input type="checkbox"/>
86. OTHER	<input type="checkbox"/>
87. INDEX	<input type="checkbox"/>
88. FILE	<input type="checkbox"/>
89. STAMP	<input type="checkbox"/>
90. OTHER	<input type="checkbox"/>
91. INDEX	<input type="checkbox"/>
92. FILE	<input type="checkbox"/>
93. STAMP	<input type="checkbox"/>
94. OTHER	<input type="checkbox"/>
95. INDEX	<input type="checkbox"/>
96. FILE	<input type="checkbox"/>
97. STAMP	<input type="checkbox"/>
98. OTHER	<input type="checkbox"/>
99. INDEX	<input type="checkbox"/>
100. FILE	<input type="checkbox"/>
101. STAMP	<input type="checkbox"/>
102. OTHER	<input type="checkbox"/>
103. INDEX	<input type="checkbox"/>
104. FILE	<input type="checkbox"/>
105. STAMP	<input type="checkbox"/>
106. OTHER	<input type="checkbox"/>
107. INDEX	<input type="checkbox"/>
108. FILE	<input type="checkbox"/>
109. STAMP	<input type="checkbox"/>
110. OTHER	<input type="checkbox"/>
111. INDEX	<input type="checkbox"/>
112. FILE	<input type="checkbox"/>
113. STAMP	<input type="checkbox"/>
114. OTHER	<input type="checkbox"/>
115. INDEX	<input type="checkbox"/>
116. FILE	<input type="checkbox"/>
117. STAMP	<input type="checkbox"/>
118. OTHER	<input type="checkbox"/>
119. INDEX	<input type="checkbox"/>
120. FILE	<input type="checkbox"/>
121. STAMP	<input type="checkbox"/>
122. OTHER	<input type="checkbox"/>
123. INDEX	<input type="checkbox"/>
124. FILE	<input type="checkbox"/>
125. STAMP	<input type="checkbox"/>
126. OTHER	<input type="checkbox"/>
127. INDEX	<input type="checkbox"/>
128. FILE	<input type="checkbox"/>
129. STAMP	<input type="checkbox"/>
130. OTHER	<input type="checkbox"/>
131. INDEX	<input type="checkbox"/>
132. FILE	<input type="checkbox"/>
133. STAMP	<input type="checkbox"/>
134. OTHER	<input type="checkbox"/>
135. INDEX	<input type="checkbox"/>
136. FILE	<input type="checkbox"/>
137. STAMP	<input type="checkbox"/>
138. OTHER	<input type="checkbox"/>
139. INDEX	<input type="checkbox"/>
140. FILE	<input type="checkbox"/>
141. STAMP	<input type="checkbox"/>
142. OTHER	<input type="checkbox"/>
143. INDEX	<input type="checkbox"/>
144. FILE	<input type="checkbox"/>
145. STAMP	<input type="checkbox"/>
146. OTHER	<input type="checkbox"/>
147. INDEX	<input type="checkbox"/>
148. FILE	<input type="checkbox"/>
149. STAMP	<input type="checkbox"/>
150. OTHER	<input type="checkbox"/>
151. INDEX	<input type="checkbox"/>
152. FILE	<input type="checkbox"/>
153. STAMP	<input type="checkbox"/>
154. OTHER	<input type="checkbox"/>
155. INDEX	<input type="checkbox"/>
156. FILE	<input type="checkbox"/>
157. STAMP	<input type="checkbox"/>
158. OTHER	<input type="checkbox"/>
159. INDEX	<input type="checkbox"/>
160. FILE	<input type="checkbox"/>
161. STAMP	<input type="checkbox"/>
162. OTHER	<input type="checkbox"/>
163. INDEX	<input type="checkbox"/>
164. FILE	<input type="checkbox"/>
165. STAMP	<input type="checkbox"/>
166. OTHER	<input type="checkbox"/>
167. INDEX	<input type="checkbox"/>
168. FILE	<input type="checkbox"/>
169. STAMP	<input type="checkbox"/>
170. OTHER	<input type="checkbox"/>
171. INDEX	<input type="checkbox"/>
172. FILE	<input type="checkbox"/>
173. STAMP	<input type="checkbox"/>
174. OTHER	<input type="checkbox"/>
175. INDEX	<input type="checkbox"/>
176. FILE	<input type="checkbox"/>
177. STAMP	<input type="checkbox"/>
178. OTHER	<input type="checkbox"/>
179. INDEX	<input type="checkbox"/>
180. FILE	<input type="checkbox"/>
181. STAMP	<input type="checkbox"/>
182. OTHER	<input type="checkbox"/>
183. INDEX	<input type="checkbox"/>
184. FILE	<input type="checkbox"/>
185. STAMP	<input type="checkbox"/>
186. OTHER	<input type="checkbox"/>
187. INDEX	<input type="checkbox"/>
188. FILE	<input type="checkbox"/>
189. STAMP	<input type="checkbox"/>
190. OTHER	<input type="checkbox"/>
191. INDEX	<input type="checkbox"/>
192. FILE	<input type="checkbox"/>
193. STAMP	<input type="checkbox"/>
194. OTHER	<input type="checkbox"/>
195. INDEX	<input type="checkbox"/>
196. FILE	<input type="checkbox"/>
197. STAMP	<input type="checkbox"/>
198. OTHER	<input type="checkbox"/>
199. INDEX	<input type="checkbox"/>
200. FILE	<input type="checkbox"/>
201. STAMP	<input type="checkbox"/>
202. OTHER	<input type="checkbox"/>
203. INDEX	<input type="checkbox"/>
204. FILE	<input type="checkbox"/>
205. STAMP	<input type="checkbox"/>
206. OTHER	<input type="checkbox"/>
207. INDEX	<input type="checkbox"/>
208. FILE	<input type="checkbox"/>
209. STAMP	<input type="checkbox"/>
210. OTHER	<input type="checkbox"/>
211. INDEX	<input type="checkbox"/>
212. FILE	<input type="checkbox"/>
213. STAMP	<input type="checkbox"/>
214. OTHER	<input type="checkbox"/>
215. INDEX	<input type="checkbox"/>
216. FILE	<input type="checkbox"/>
217. STAMP	<input type="checkbox"/>
218. OTHER	<input type="checkbox"/>
219. INDEX	<input type="checkbox"/>
220. FILE	<input type="checkbox"/>
221. STAMP	<input type="checkbox"/>
222. OTHER	<input type="checkbox"/>
223. INDEX	<input type="checkbox"/>
224. FILE	<input type="checkbox"/>
225. STAMP	<input type="checkbox"/>
226. OTHER	<input type="checkbox"/>
227. INDEX	<input type="checkbox"/>
228. FILE	<input type="checkbox"/>
229. STAMP	<input type="checkbox"/>
230. OTHER	<input type="checkbox"/>
231. INDEX	<input type="checkbox"/>
232. FILE	<input type="checkbox"/>
233. STAMP	<input type="checkbox"/>
234. OTHER	<input type="checkbox"/>
235. INDEX	<input type="checkbox"/>
236. FILE	<input type="checkbox"/>
237. STAMP	<input type="checkbox"/>
238. OTHER	<input type="checkbox"/>
239. INDEX	<input type="checkbox"/>
240. FILE	<input type="checkbox"/>
241. STAMP	<input type="checkbox"/>
242. OTHER	<input type="checkbox"/>
243. INDEX	<input type="checkbox"/>
244. FILE	<input type="checkbox"/>
245. STAMP	<input type="checkbox"/>
246. OTHER	<input type="checkbox"/>
247. INDEX	<input type="checkbox"/>
248. FILE	<input type="checkbox"/>
249. STAMP	<input type="checkbox"/>
250. OTHER	<input type="checkbox"/>
251. INDEX	<input type="checkbox"/>
252. FILE	<input type="checkbox"/>
253. STAMP	<input type="checkbox"/>
254. OTHER	<input type="checkbox"/>
255. INDEX	<input type="checkbox"/>
256. FILE	<input type="checkbox"/>
257. STAMP	<input type="checkbox"/>
258. OTHER	<input type="checkbox"/>
259. INDEX	<input type="checkbox"/>
260. FILE	<input type="checkbox"/>
261. STAMP	<input type="checkbox"/>
262. OTHER	<input type="checkbox"/>
263. INDEX	<input type="checkbox"/>
264. FILE	<input type="checkbox"/>
265. STAMP	<input type="checkbox"/>
266. OTHER	<input type="checkbox"/>
267. INDEX	<input type="checkbox"/>
268. FILE	<input type="checkbox"/>
269. STAMP	<input type="checkbox"/>
270. OTHER	<input type="checkbox"/>
271. INDEX	<input type="checkbox"/>
272. FILE	<input type="checkbox"/>
273. STAMP	<input type="checkbox"/>
274. OTHER	<input type="checkbox"/>
275. INDEX	<input type="checkbox"/>
276. FILE	<input type="checkbox"/>
277. STAMP	<input type="checkbox"/>
278. OTHER	<input type="checkbox"/>
279. INDEX	<input type="checkbox"/>
280. FILE	<input type="checkbox"/>
281. STAMP	<input type="checkbox"/>
282. OTHER	<input type="checkbox"/>
283. INDEX	<input type="checkbox"/>
284. FILE	<input type="checkbox"/>
285. STAMP	<input type="checkbox"/>
286. OTHER	<input type="checkbox"/>
287. INDEX	<input type="checkbox"/>
288. FILE	<input type="checkbox"/>
289. STAMP	<input type="checkbox"/>
290. OTHER	<input type="checkbox"/>
291. INDEX	<input type="checkbox"/>
292. FILE	<input type="checkbox"/>
293. STAMP	<input type="checkbox"/>
294. OTHER	<input type="checkbox"/>
295. INDEX	<input type="checkbox"/>
296. FILE	<input type="checkbox"/>
297. STAMP	<input type="checkbox"/>
298. OTHER	<input type="checkbox"/>
299. INDEX	<input type="checkbox"/>
300. FILE	<input type="checkbox"/>
301. STAMP	<input type="checkbox"/>
302. OTHER	<input type="checkbox"/>
303. INDEX	<input type="checkbox"/>
304. FILE	<input type="checkbox"/>
305. STAMP	<input type="checkbox"/>
306. OTHER	<input type="checkbox"/>
307. INDEX	<input type="checkbox"/>
308. FILE	<input type="checkbox"/>
309. STAMP	<input type="checkbox"/>
310. OTHER	<input type="checkbox"/>
311. INDEX	<input type="checkbox"/>
312. FILE	<input type="checkbox"/>
313. STAMP	<input type="checkbox"/>
314. OTHER	<input type="checkbox"/>
315. INDEX	<input type="checkbox"/>
316. FILE	<input type="checkbox"/>
317. STAMP	<input type="checkbox"/>
318. OTHER	<input type="checkbox"/>
319. INDEX	<input type="checkbox"/>
320. FILE	<input type="checkbox"/>
321. STAMP	<input type="checkbox"/>
322. OTHER	<input type="checkbox"/>
323. INDEX	<input type="checkbox"/>
324. FILE	<input type="checkbox"/>
325. STAMP	<input type="checkbox"/>
326. OTHER	<input type="checkbox"/>
327. INDEX	<input type="checkbox"/>
328. FILE	<input type="checkbox"/>
329. STAMP	<input type="checkbox"/>
330. OTHER	<input type="checkbox"/>
331. INDEX	<input type="checkbox"/>
332. FILE	<input type="checkbox"/>
333. STAMP	<input type="checkbox"/>
334. OTHER	<input type="checkbox"/>
335. INDEX	<input type="checkbox"/>
336. FILE	<input type="checkbox"/>
337. STAMP	<input type="checkbox"/>
338. OTHER	<input type="checkbox"/>
339. INDEX	<input type="checkbox"/>
340. FILE	<input type="checkbox"/>
341. STAMP	<input type="checkbox"/>
342. OTHER	<input type="checkbox"/>
343. INDEX	<input type="checkbox"/>
344. FILE	<input type="checkbox"/>
345. STAMP	<input type="checkbox"/>
346. OTHER	<input type="checkbox"/>
347. INDEX	<input type="checkbox"/>
348. FILE	<input type="checkbox"/>
349. STAMP	<input type="checkbox"/>
350. OTHER	<input type="checkbox"/>
351. INDEX	<input type="checkbox"/>
352. FILE	<input type="checkbox"/>
353. STAMP	<input type="checkbox"/>
354. OTHER	<input type="checkbox"/>
355. INDEX	<input type="checkbox"/>
356. FILE	<input type="checkbox"/>
357. STAMP	<input type="checkbox"/>
358. OTHER	<input type="checkbox"/>
359. INDEX	<input type="checkbox"/>
360. FILE	<input type="checkbox"/>
361. STAMP	<input type="checkbox"/>
362. OTHER	<input type="checkbox"/>
363. INDEX	<input type="checkbox"/>
364. FILE	<input type="checkbox"/>
365. STAMP	<input type="checkbox"/>
366. OTHER	<input type="checkbox"/>
367. INDEX	<input type="checkbox"/>
368. FILE	<input type="checkbox"/>
369. STAMP	<input type="checkbox"/>
370. OTHER	<input type="checkbox"/>
371. INDEX	<input type="checkbox"/>
372. FILE	<input type="checkbox"/>
373. STAMP	<input type="checkbox"/>
374. OTHER	<input type="checkbox"/>
375. INDEX	<input type="checkbox"/>
376. FILE	<input type="checkbox"/>
377. STAMP	<input type="checkbox"/>
378. OTHER	<input type="checkbox"/>
379. INDEX	<input type="checkbox"/>
380. FILE	<input type="checkbox"/>
381. STAMP	<input type="checkbox"/>
382. OTHER	<input type="checkbox"/>
383. INDEX	<input type="checkbox"/>
384. FILE	<input type="checkbox"/>
385. STAMP	<input type="checkbox"/>
386. OTHER	<input type="checkbox"/>
387. INDEX	<input type="checkbox"/>
388. FILE	<input type="checkbox"/>
389. STAMP	<input type="checkbox"/>
390. OTHER	<input type="checkbox"/>
391. INDEX	<input type="checkbox"/>
392. FILE	<input type="checkbox"/>
393. STAMP	<input type="checkbox"/>
394. OTHER	<input type="checkbox"/>
395. INDEX	<input type="checkbox"/>
396. FILE	<input type="checkbox"/>
397. STAMP	<input type="checkbox"/>
398. OTHER	<input type="checkbox"/>
399. INDEX	<input type="checkbox"/>
400. FILE	<input type="checkbox"/>
401. STAMP	<input type="checkbox"/>
402. OTHER	<input type="checkbox"/>
403. INDEX	<input type="checkbox"/>
404. FILE	<input type="checkbox"/>
405. STAMP	<input type="checkbox"/>
406. OTHER	<input type="checkbox"/>
407. INDEX	<input type="checkbox"/>
408. FILE	<input type="checkbox"/>
409. STAMP	<input type="checkbox"/>
410. OTHER	<input type="checkbox"/>
411. INDEX	<input type="checkbox"/>
412. FILE	<input type="checkbox"/>
413. STAMP	<input type="checkbox"/>
414. OTHER	<input type="checkbox"/>
415. INDEX	<input type="checkbox"/>
416. FILE	<input type="checkbox"/>
417. STAMP	<input type="checkbox"/>
418. OTHER	<input type="checkbox"/>
419. INDEX	<input type="checkbox"/>
420. FILE	<input type="checkbox"/>
421. STAMP	<input type="checkbox"/>
422. OTHER	<input type="checkbox"/>
423. INDEX	<input type="checkbox"/>
424. FILE	<input type="checkbox"/>
425. STAMP	<input type="checkbox"/>
426. OTHER	<input type="checkbox"/>
427. INDEX	<input type="checkbox"/>
428. FILE	<input type="checkbox"/>
429. STAMP	<input type="checkbox"/>
430. OTHER	<input type="checkbox"/>
431. INDEX	<input type="checkbox"/>
432. FILE	<input type="checkbox"/>
433. STAMP	<input type="checkbox"/>
434. OTHER	<input type="checkbox"/>
435. INDEX	<input type="checkbox"/>
436. FILE	<input type="checkbox"/>
437. STAMP	<input type="checkbox"/>
438. OTHER	<input type="checkbox"/>
439. INDEX	<input type="checkbox"/>
440. FILE	<input type="checkbox"/>
441. STAMP	<input type="checkbox"/>
442. OTHER	<input type="checkbox"/>
443. INDEX	<input type="checkbox"/>
444. FILE	<input type="checkbox"/>
445. STAMP	<input type="checkbox"/>
446. OTHER	<input type="checkbox"/>
447. INDEX	<input type="checkbox"/>
448. FILE	<input type="checkbox"/>
449. STAMP	<input type="checkbox"/>
450. OTHER	<input type="checkbox"/>
451. INDEX	<input type="checkbox"/>
452. FILE	<input type="checkbox"/>
453. STAMP	<input type="checkbox"/>
454. OTHER	<input type="checkbox"/>
455. INDEX	<input type="checkbox"/>
456. FILE	<input type="checkbox"/>
457. STAMP	<input type="checkbox"/>
458. OTHER	<input type="checkbox"/>
459. INDEX	<input type="checkbox"/>
460. FILE	<input type="checkbox"/>
461. STAMP	<input type="checkbox"/>
462. OTHER	<input type="checkbox"/>
463. INDEX	<input type="checkbox"/>
464. FILE	<input type="checkbox"/>
465. STAMP	<input type="checkbox"/>
466. OTHER	<input type="checkbox"/>
467. INDEX	<input type="checkbox"/>
468. FILE	<input type="checkbox"/>
469. STAMP	<input type="checkbox"/>

## INTRODUCTION

This report presents results of measurements of permittivities (see Glossary) and permeabilities of assorted materials collected by the U. S. Army Office of Low Observables Technology and Applications (LOTA), and by the U. S. Army Materials Technology Laboratory (MTL). This will be the first in a planned series of annual reports prepared by MTL for LOTA describing the results of such tests.

The samples fell into the following categories:

1. Pure materials (teflon, plexiglasses and casting plastic).
2. Metal-coated microspheres.
3. Carbospheres, both uncoated and metal coated.
4. Ferrites.
5. Magnetic metal flake.
6. Ceramic matrix composites.
7. A standard paint.

The data and its limitations and plans for additional testing are presented in what follows.

## EXPERIMENTAL

Most of the samples were powders which were hand mixed with an acrylic-polyester binder (Castolite CP, Castolite Co., Woodstock, IL) and formed into toroidal samples machined to fit a 7 millimeter OD, 3 millimeter ID coaxial airline for measurements of epsilon and mu from 2 to 18 GHz with a Hewlett-Packard 8510 - A Vector Network Analyzer (VNA). A Hewlett-Packard 8510-B VNA, which will permit future extension of the measurement range to 40 GHz using a K<sub>A</sub> band waveguide, was acquired about halfway through the project and used to measure about half of the samples. The measurement procedure and equations for data analysis are described in a Hewlett-Packard Product Note.<sup>1</sup> A few free-space reflectivity measurements using millimeterwave test apparatus (26-40, 40-60, and 75-110 GHz) are also reported.

## RESULTS

### Pure Materials

The permittivities and permeabilities of several pure materials were measured at the start of the project validate the measurement techniques. The materials included teflon, ordinary plexiglass, a leaded plexiglass, and the Castolite casting plastic selected for use as the base material for composite studies. This casting plastic was selected on the basis of convenient working characteristics and commercial availability.

1. Hewlett-Packard Product Note 8510 -3- Materials Measurement. Hewlett-Packard Corporation, 3000 Hanover Street, Palo Alto, CA 94304.

Although the teflon sample could possibly have been better machined, the experimental values of epsilon and mu (see Figures 1a, 1b, 1c, and 1d) agree reasonably well with the nominal values of (2.03, 0) and (1.0, 0.0), respectively. The average value of epsilon prime was  $2.03 \pm 0.04$  on this determination and  $2.03 \pm 0.03$  on another. The original open literature articles on the vector network analyzer technique are apparently by Weir,<sup>2</sup> and by Nicholson and Ross;<sup>3</sup> their measurements show the same type of scatter in the permittivity and permeability observed in the current results. X-band (8 to 12 GHz) test results for teflon and nylon are also reported in the Hewlett-Packard product Note;<sup>1</sup> the Hewlett-Packard results actually show a small ( $\pm 1.5\%$ ) systematic error in epsilon prime.

Since the teflon was hard to machine, two types of plexiglass were also tested. The first, a standard material on hand, had a frequency independent dielectric constant of  $2.602 \pm 0.006$ , as expected.<sup>3</sup> Leaded plexiglasses can also be obtained; they were an early solution to the X-ray emission problem in color televisions manufactured in the 1960s. A leaded plexiglass sample on hand had a frequency independent dielectric constant of  $3.25 \pm 0.07$ .

Data for the real part of the dielectric constant of Castolite is shown in Figure 2. This data reproduces reasonably well. The average dielectric constant was  $(2.685 \pm 0.06, -0.15 \pm 0.054)$  in one run, and  $(2.70 \pm 0.12, -0.15 \pm 0.07)$  in another.

#### Metal-Coated Microspheres

Many of the samples tested were metal-coated microspheres. These particles were expected to be interesting since, if properly made, they can have permeability which is frequency dependent in the microwave range as a consequence of eddy current effects. Although the theory of the permeability of a solid metal particle has long been available in the literature,<sup>5</sup> no similar analysis for a spherical shell could be found so the relevant expressions were derived from classical electromagnetic theory. The results are detailed in a companion paper which will be made available as an MTL Technical Report.<sup>4</sup> The particles tested were about 50 microns in diameter, and many were silver coated so that no ferromagnetism was present to obscure the results. A magnetic loss that was relatively small, but measurable and possibly useful, and a mu prime less than one were expected for composites of these particles.

The permittivity of a metal-dielectric composite is comparatively hard to predict as a consequence of the nearly infinite dielectric constant of the metal at these frequencies. One possible approach<sup>5</sup> is to use a common mixture formula such as the Maxwell-Garnett expression, which for this case (metal particles of very high dielectric constant) reduces to

$$E_c = E_b (1 + 2F)/(1 - F), \quad (1)$$

2. WEIR, W. B. *Automatic Measurement of Complex Dielectric Constant and Permeability at Microwave Frequencies*. Proceedings of the IEEE, v. 62, no. 1, 1974, p. 33-36.
3. NICHOLSON, A. M., and ROSS, G. F. *Measurement of the Intrinsic Properties of Materials by Time Domain Techniques*. IEEE Transactions of Instrumentation and Measurement, v. IM-19, no. 4, 1970, p. 377-382.
4. HOW, H., SPURGEON, W. A., and VITTORIA, C. *The Microwave Permeability of a Conducting Spherical Shell*. U.S. Army Materials Technology Laboratory, MTL TR 90-7, February 1990.
5. CARR, G. L., HENRY, R. L., RUSSELL, N. E., GARLAND, J. C., and TANNER, D. B. *Anomalous Far-infrared Absorption in Random Small Particle Composites*. Physical Review B24, no. 2, 1981, p. 777-786.

where  $E_c$  is the dielectric constant of the composite,  $E_b$  is the dielectric constant of the binder, and  $F$  is the volume fraction of the particles. Note that this predicts a low-loss dielectric; the use of metal particles in preparing artificial low-loss dielectrics dates at least back to the 1950s. At high concentrations, this behavior will change as particle-particle contact effects become important, leading to a nonlinear (and hard to model) increase in the dielectric constant and loss.

The actual experimental results are best illustrated for a series of samples of nickel-coated microspheres obtained from Novamet, Inc., 10 Lawlins Park, Wyckoff, NJ 07481. These are approximately 50 micron-diameter particles with an estimated nickel thickness of 2 microns deposited by a chemical vapor deposition process. Although nickel is ferromagnetic, the ferromagnetic resonance (FMR) frequency is quite low (about 0.75 GHz for a sphere), and since there is actually very little nickel on the particles, the major effects expected are those of the eddy current losses, not those of ferromagnetic interactions.

At low particle concentrations  $\epsilon'$  for the composite increases with the weight fraction in a linear manner up to about 20 weight % of particles (see Figure 3). The dielectric loss is low, as expected. Also,  $\mu'$  is less than one, and the magnetic loss is too small to measure. This is the expected behavior which one can at least attempt to model.

At high particle concentrations (30 weight % or more),  $\epsilon'$  increases in a very nonlinear manner, as expected, but also shows an unexpected resonant behavior. This is illustrated for a 30 weight % sample in Figures 4a and 4b.  $\mu'$  for the sample is less than one (Figure 4c), and the magnetic loss is too small to measure reliably. Several attempts were made to prepare composites with higher particle concentration; the reproducibility of the results was very poor and the results are not worth reporting.

The quantities of the uncoated and other metal-coated microspheres (Samples 1 through 9) were quite limited. Where possible, results were obtained at one high loading level, which was determined as the highest level which would mix properly with the Castolite binder, and one or more lower concentrations if enough of the sample remained. Sample 5 was totally consumed in an unsuccessful attempt to prepare the high concentration sample, which turned out too powdery for reliable measurements. The data for the other metal-coated microsphere samples are presented below.

#### Sample 1 - Carolina Solvents Microspheres, Untreated

Hollow-glass microspheres can be made from a variety of glasses and have dielectric constants which depend on the type of glass and its thickness and the particle diameter. Composites of 15 and 45 weight % (26 and 64 volume %) of this sample were prepared with the Castolite binder. The average frequency independent dielectric constants of these composites were  $2.488 \pm 0.06$  and  $2.207 \pm 0.04$ , respectively. A more interesting parameter is the dielectric constant of the particles, which was extracted from the composite data using the Maxwell-Garnett expression for the dielectric constant of the composite,

$$E_C = E_B + \frac{E_B F(E_B - E_P)}{(1 - F)E_P + (2 + F)E_B}, \quad (2)$$

where  $E_C$  is the dielectric constant of the composite,  $E_B$  is the dielectric constant of the binder,  $E_P$  is the dielectric constant of the composite, and  $F$  is the volume fraction of the particles. Values for  $E_P$  of 1.87 and 1.91 were obtained from the 15 and 45 weight % composites, respectively.

#### Sample 2 - Carolina Solvents Silver-Coated Microspheres, 20/30

Although the microspheres comprising this sample appeared to be silver coated, they tested out quite differently. A 15 weight % composite in Castolite had a dielectric constant of  $2.675 \pm 0.1$ , which indicates that the dielectric constants of the particle and binder are essentially the same. The permeability was (1.0, 0.0) and there was no additional dielectric loss in these composites within the experimental error.

#### Sample 3 - Carolina Solvents Silver-Coated Microspheres, 20/26

The real and imaginary parts of the dielectric constant for a 45 weight % composite of this sample are shown in Figures 5a and 5b. In view of the relative constancy of the real part of the dielectric constant of the composite, we applied the Maxwell-Garnett expression above and find a value of  $E_P$  of 6.0, although this analysis may not be entirely appropriate because of the semiconducting nature of the particles.  $\mu$  prime for this sample was one within experimental error, and  $\mu$  double prime measured slightly positive and should be regarded as zero. It should be noted that separation of the dielectric and magnetic losses is difficult when one component is considerably larger than the other.

#### Sample 4 - Carolina Solvents Silver-Coated Microspheres, 34/94

Two composites of this sample were prepared, one at 15 weight % and one at 45 weight %. The 15 weight % sample was low-loss dielectric with an average dielectric constant of  $(6.65 \pm 0.18, -0.17 \pm 0.12)$ , and an average permeability of  $(0.95 \pm 0.03, 0.03 \pm 0.03)$ . No clear frequency dependence was noticed in the data. The 45 weight % composite showed a strong dielectric resonance (Figures 6a and 6b), as anticipated. The behavior of  $\mu$  (Figures 6c and 6d) is somewhat puzzling in that the large decrease in  $\mu$  prime should be accompanied by a larger peak in  $\mu$  double prime. The dielectric constant is going through a resonance, and the data are very noisy and not particularly reliable when this happens, or when the sample is a half wavelength thick. Scattering within the sample is likely to be very high as well, which may account for some of the observed behavior. The data follows the metal-dielectric composite behavior for which the notion of a particle dielectric constant is not appropriate.

#### Sample 6 - Carolina Solvents Silver-Coated Microspheres, 200/10

Behavior similar to that of the 45 weight % composite of Sample 4 was obtained in a 35 weight % composite of Sample 6. A 25 weight % sample also showed a strong dielectric resonance (Figures 7a and 7b), but the behavior of

$\mu$  was somewhat different (Figures 7c and 7d). Again, the reasons for this behavior are not clear.

#### Sample 7 - Carolina Solvents Nickel-Coated Microspheres

A 15 weight % composite of this sample was again a low-loss dielectric with a  $\mu$  prime that was nearly one, and a  $\mu$  double prime that was too small to measure. Twenty-five and 45 weight % composites showed dielectric resonances similar to those described above; the results from these composites were regarded as unreproducible and uninteresting. The behavior of these particles was generally similar to that of the nickel-coated microspheres from Novamet described above.

#### Sample 8 - Mobay Chemical Silver-Coated Microspheres

A 15 weight % composite of these microspheres was a low-loss dielectric, as expected, with a dielectric constant of  $(5.68 +/- 0.18, -0.15 +/- 0.10)$ . In contrast, a 25 weight % composite had a dielectric resonance at about 11 GHz (see Figures 8a and 8b), with a  $\mu$  of  $(0.71 +/- 0.04, -0.02 +/- 0.03)$ .

#### Sample 9 - Mobay Chemical Iron-Coated Microspheres

Composites of 15, 25, and 40 weight % of these particles were prepared. As expected, the 15% composite was a moderate-loss dielectric with  $\epsilon = (7.1 +/- 0.24, -0.54 +/- 0.09)$ , and  $\mu$  prime =  $0.94 +/- 0.08$ .  $\mu$  double prime was zero within experimental error. The 25 weight % composite had a modest dielectric resonance, shown in Figures 9a and 9b. The average  $\mu$  prime for this sample was  $0.74 +/- 0.03$ , and  $\mu$  double prime was unmeasurably small. The 40% composite had a stronger dielectric resonance (Figures 9c and 9d) and a  $\mu$  prime of only  $0.19 +/- 0.03$  with no measurable magnetic loss.

The question of the possible utility of these particles is hard to answer in a completely satisfactory manner. Since they are very light compared to solid metal particles of the same size, they could certainly be used to fabricate light-weight, low-loss, artificial dielectrics. The theory of the dielectric constant, particularly the imaginary part, in the high concentration region is quite inadequate, and the scaling with concentration is too nonlinear for modelling absorptive materials. Only very small quantities of particles were provided, which necessitated testing small, hand-mixed batches of materials, which demonstrated highly variable, poorly reproducible results at high concentrations. Proceeding empirically would require analyzing large machine-mixed batches of material to generate working curves and would certainly be laborious. This is not of clear value given the uncertainty in the outcome. The large increase in the dielectric constant with particle concentration is partially offset by the decrease in the permeability, which would make the material behave as though it had a comparatively low dielectric constant in a quarterwave absorber; i.e., it would have a better bandwidth than a material in which the dielectric constant had been increased when made lossy by adding carbon black, so the idea of using these particles is not entirely without basis. The route to making a broadband absorber from them is not clear, however.

Since the lossy composites require particle-to-particle contact, anything that changes the degree of contact, such as aging of the polymer or thermal expansion, would also be likely to alter the absorption characteristics, which is clearly undesirable.

Particles similar to these, if properly metal coated, could be of use in magnetic absorbers. Since these materials would have magnetic loss without a Curie point, a possible application is in high temperature materials.

### **Carbospheres**

The samples of carbospheres tested were very light, spherical, carbon particles manufactured by Versar Manufacturing Company, 1412A Sullyfield Circle, Chantilly, VA 22021.

#### **Type A Carbospheres**

Composites of 3, 6.5, and 10 weight % of the Type A carbospheres were prepared and analyzed. Figures 10a and 10b show the average values of epsilon prime and epsilon double prime. The permeability was (1,0) within the 5% experimental error.

The dielectric behavior of these particles is qualitatively similar to that which would be expected for carbon black powder. The use of a simple mixture formula for the dielectric constant of a composite of the particles is not appropriate. If practical use of them were to be attempted, an empirical curve of dielectric constant versus loading similar to Figures 10a and 10b would have to be generated for composites with the base material. As a first approximation, the change in dielectric constant with particle loading should be proportional to the dielectric constant of the base material.

#### **Type D Carbospheres**

The dielectric behavior of the Type D carbospheres was similar to that of the Type A carbospheres, although the dielectric loss at low concentrations was higher. Figures 11a and 11b show the concentration dependence of the dielectric of composites of these particles in Castolite.

#### **Type E Carbospheres**

A 10 weight % composite of these particles in Castolite was a low-loss dielectric with a dielectric constant of (5.32 +/- 0.12, -0.08 +/- 0.07). Since this behavior was very similar to that of the metal-coated microspheres, no other composites were prepared.

#### **Type MS-1000 Carbospheres**

Type MS-1000 carbospheres are conductive to a DC ohmmeter, and are roughly one millimeter in average diameter. Since this particle size is too large for a composite which would be homogeneous on the scale of the 7 millimeter

diameter coaxial transmission line, the sample could not be measured. The size of the particles may lead to some interesting scattering effects in the 100 GHz range.

#### Type ME-27 Cobalt-Coated Carbospheres

The cobalt-coated carbospheres seemed comparatively heavy, which was taken as an indication that the cobalt coating was reasonably thick. They were strongly magnetic to a test with a laboratory permanent magnet. Hexagonal close-packed cobalt has an anisotropy field,  $H_A$ , of around 15 kilooersteds, so that the FMR frequency should be about 45 GHz, which is well beyond the current 2 to 18 GHz measurement range. A 25 weight % composite of these particles had a  $\mu$  of one within experimental error from 2 to 18 GHz. The average dielectric constant of the composite was (4.2 +/- 0.15, -0.15 +/- 0.06).

#### Type MA-26 Iron-Coated Carbospheres

Figures 12a, 12b, 12c, and 12d show, respectively, the averages of three determinations of the real and imaginary parts of the permittivity and permeability of a 25 weight % composite of these particles in Castolite. This was the highest concentration that could be prepared. Although a small ferromagnetism may be present, as evidenced by the slight drop in  $\mu$  prime with frequency and the small  $\mu$  double prime, it does not appear to be large enough to be useful in an absorber.

#### Type MA-28 Nickel-Coated Carbospheres

Figures 13a and 13b show, respectively, the real and imaginary parts of the permittivity and permeability of a 20 weight % (again, the highest concentration that could be prepared) composite of these particles in Castolite. Note the very large dielectric resonance. This did not reproduce well in a second experiment.  $\mu$  was not well resolved, but it was clear that any magnetic loss, if present, was very small. Since the overall electromagnetic behavior of the composite is dominated by the dielectric constant, it did not appear that further analysis was merited.

The possible advantages of using the carbospheres instead of a carbon black powder to introduce dielectric loss in a plastic are not clear. The metal-coated carbospheres were disappointing in that no useful magnetic loss was found.

#### Ferrites

The selection of samples from the LOTA Office included an assortment of ferrites. Details regarding the nature of the ferrites and their sources may be obtained from the LOTA Office.

The imaginary parts of the permittivity and permeability of ferrite composites can be relatively small so composites in comparatively high concentrations (50 weight % or more) were prepared in order to get good measurements of these parameters. A description of the results obtained is provided below.

Tables of  $\mu$  values for those samples which demonstrated significant magnetic loss are provided in Appendix A.

#### Sample 10 - Rockwell Ferrites

The most interesting of the ferrites was Sample 10 from Rockwell. A 60 weight % (20.4 volume %) composite of this ferrite had a modest magnetic loss from 2 to 18 GHz, as shown in Figures 14a and 14b. The fact that  $\mu$  prime is still greater than one at 18 GHz suggests that the loss should extend to higher frequencies, possibly through  $K_A$  band. The data for  $\mu$  also suggests that the sample is actually a mixture of ferrites. The dielectric constant of the composite was frequency independent in this range within the experimental errors and is plotted as a function of volume % of particles in Figure 14c.

The more interesting parameters are  $\epsilon$  and  $\mu$  for the particles. Unfortunately, extracting these parameters is not as straightforward as one would hope. In particular, application of Maxwell-Garnett theory for spherical particles does not result in realistic values for the real part of the dielectric constant of the particle: a value of 47.5 would be obtained for the 60 weight (20.4 volume %) composite described above. A problem with the Maxwell-Garnett theory is that it is not very sensitive to the particle dielectric constant when this is much above 10 (typical values for ferrites are in the 10 to 30 range). This is illustrated in Figure 14d which shows a plot of the dielectric constant of a composite of 20 volume % of particles in a binder of dielectric constant 2.7 as a function of the dielectric constant of the particle. Note that the dielectric constant of the composite increases from 3.55 to 3.82 as the particle dielectric constant increases from 10 to 15, and a 3.5% error in the composite dielectric constant becomes a 20% error in that for the particle. Also, note that the composite dielectric constant can never exceed 4.725 for this volume fraction in the binder. This actually happened for several of the samples described below.

Another problem in applying the Maxwell-Garnett theory for spherical particles is that the particles were not spherical for nearly all of the samples. The apparent exception was Sample 10, which was composed of micron sized particles which looked reasonably spherical under a 500-power microscope. Such small particles are quite difficult to completely disperse, and one cannot be certain what the depolarization factor for the particle aggregates should be. A more general Maxwell-Garnett expression for nonspherical particles is given by

$$\epsilon_C = \epsilon_B + \frac{F(\epsilon_P - \epsilon_B)}{(1 - F)(1 + (L/\epsilon_B)(\epsilon_P - \epsilon_B)) + F} \quad (3)$$

where  $L$  is a depolarizing factor which is 1/3 for a sphere. Given the general irregularity of the particle shapes, no value of  $L$  which would lead to a reasonable value of the particle dielectric constant could be justified.

In view of the near linearity of the composite dielectric constant with volume loading shown in Figure 14c, and the above discussion, the use of a simple expression for the composite dielectric constant,

$$E_C = E_P F + (1 - F) E_B , \quad (4)$$

to extract values of the particles seemed justified and, accordingly, was employed. The values obtained are reasonable for ferrites, and are usable for modelling purposes with the above expression. Accurate values of the particle dielectric constant (and permeability) are best obtained from dense, sintered samples. A calibration curve for the dielectric constants of composites should always be prepared if one were to try to make useful materials from them.

The permeability constant for a composite should also follow a formula similar to the Maxwell-Garnett expression. However, for ferromagnetic particles a micron or more in diameter, the depolarizing factor is determined by domain interactions within the particles, and is generally taken to be zero. In this case, the generalized Maxwell-Garnett expression reduces to

$$\mu_U C = \mu_U P F + (1 - F) . \quad (5)$$

Epsilon for the particles of Sample 10 was calculated to be (16.9 +/- 1.4, -0.9 +/- 0.6). The calculated values of mu prime and mu double prime are shown in Figures 14e and 14f, respectively; these values are accurate to +/- 20%.

#### Sample 11 - Titan Ferrites FCX-1535

Sample 11 was strongly magnetic when tested with a laboratory magnet suggesting that it may be a high frequency hexagonal ferrite. The average permeability of a 50 weight % (19.7 volume %) composite was 1.11 +/- 0.05 (1.40 +/- 0.2 for the particle) in the 2 to 18 GHz range, which is what would be expected for such ferrites at low frequencies. The imaginary part of mu was too small for a reliable measurement. The real part of the dielectric constant was (5.78 +/- 0.15, -0.59 +/- 0.2) for the composite, (17.6 +/- 1.8, -2.4 +/- 1.4) for the particle.

#### Sample 12 - Titan Ferrites FCX-1536

Sample 12 was prepared in a 65 weight % (32 volume %) composite, and was rather difficult to measure. The average dielectric constant of the composite was (7.19 +/- 0.17, -0.98 +/- 0.22). The corresponding values for the particle are (16.8 +/- 0.7, 3.6 +/- 0.75). The average value of the real part of the permeability was 1.15 +/- 0.03 (1.47 +/- 0.2 for the particle). No magnetic loss was evident although it is possible that a small magnetic loss would be obscured by the comparatively large dielectric loss.

#### Sample 13 - Titan Ferrites FCX-1537

Although magnetic, Sample 13 exhibited only a hint of ferromagnetic behavior in a 31 weight % (9.8 volume %) composite in the 2 to 6 GHz range (Figures 15a and 15b). An attempt to prepare a higher concentration sample failed; the specimen was too crumbly. The frequency independent dielectric constant was (3.32 +/- 0.06, -0.08 +/- 0.05) for the composite. The real part of the dielectric constant of the particle works out to 9.2 +/- 1.4, and the loss is

negligible. Values for  $\mu$  of the particles were calculated and are shown in Figures 15c and 15d. The accuracy of the values is limited to about  $\pm$  50% by the low volume loading.

#### Sample 14 - Titan Ferrites FCX-1538

Sample 14 was a low frequency ferrite, with most of the magnetic loss below 7.5 GHz in a 50 weight % (18.9 volume %) composite (Figures 16a and 16b). The values of  $\mu$  for the particles inferred from the composite data are shown in Figures 16c and 16d. These values are accurate to about  $\pm$  20% in this and subsequent determinations. The real part of the dielectric constant was frequency independent from 2 to 18 GHz (3.54  $\pm$  0.06 for the composite, 7.2  $\pm$  1.5 for the particle). The imaginary part of the dielectric constant of the composite was -0.12  $\pm$  0.05 which is comparable to that of the base plastic.

#### Sample 15 - Titan Ferrites FCX-1539

Sample 15 had a modest magnetic loss from 6 to 18 GHz. The permeability of a 20.1 volume % composite is shown in Figures 17a and 17b, and that of the particle is shown in Figures 17c and 17d. The frequency-independent dielectric constant was 3.97  $\pm$  0.06 for the composite and (9.0  $\pm$  1.5) for the particle. The dielectric loss of the particle was too small to measure.

#### Sample 16 - Titan Ferrites FCX-1540

Sample 16 was a low-frequency ferrite with most of the magnetic loss below 7.5 GHz in a 40 volume % composite (Figures 18a and 18b). The values of  $\mu$  for the particles inferred from the composite data are shown in Figures 18c and 18d. The real part of the dielectric constant was frequency independent from 2 to 18 GHz (6.00  $\pm$  0.06 for the composite, 11.0  $\pm$  0.34 for the particle) and the imaginary part was too small to measure.

#### Sample 17 - Titan Ferrites FCX-1541

A composite was prepared at 45.3 volume % which had a magnetic loss that may be useful in the 2 to 8 GHz range (Figures 19a and 19b).  $\mu$  for the particle is shown in Figures 19c and 19d. The frequency-independent dielectric constant was found to be 8.1  $\pm$  0.1 for the particle (5.13  $\pm$  0.10 for the composite). The dielectric loss of the particle was unmeasurably small.

#### Sample 18 - Titan Ferrites FCX-1542

Sample 18 had a very broad peak in  $\mu$  double prime from 2 to about 12 GHz in a 34 volume % composite (Figures 20a and 20b). The values of  $\mu$  for the particles inferred from the composite data are shown in Figures 20c and 20d. The real part of the dielectric constant was frequency independent from 2 to 18 GHz (5.12  $\pm$  0.10 for the composite, 9.8  $\pm$  1.3 for the particle) and the imaginary part was too small to measure.

### Sample 19 - Titan Ferrites FCX-1543

Sample 19 was strongly magnetic when tested with a laboratory magnet. However, a 50 weight % (10.4 volume %) composite in Castolite had an average permeability of  $0.98 \pm 0.04$ , with an unmeasurably small magnetic loss, indicating that the FMR frequency was out of the 2 to 18 GHz measurement range. The real part of the dielectric constant was  $3.93 \pm 0.06$  for the composite ( $9.1 \pm 1.5$  for the particle) and the imaginary part was too small to measure.

### Sample 20 - Titan Ferrites FCX-1544

Sample 20 was a low-frequency ferrite, with most of the magnetic loss below 7.5 GHz (Figures 21a and 21b) in a 50 weight % (21.7 volume %) composite. The values of  $\mu$  for the particles inferred from the composite data are shown in Figures 21c and 21d. The real part of the dielectric constant was frequency independent from 2 to 18 GHz ( $3.90 \pm 0.04$  for the composite,  $8.3 \pm 1.4$  for the particle) and the imaginary part was too small to measure.

### Sample 21 - Titan Ferrites FCX-1545

Sample 21 was **not** magnetic when tested with a three-kilooersted laboratory permanent magnet. The real part of the dielectric constant of a 50 weight % (20.8 volume %) composite in Castolite was  $4.25 \pm 0.04$  ( $10.2 \pm 1.5$  for the particle). The imaginary part of the permittivity was zero and the permeability was (1.0, 0.0) within the experimental error.

### Sample 22 - Titan Ferrites FCX-1546

Sample 22, like Sample 20, was a low-frequency ferrite with most of its magnetic loss below 10 GHz. The permeability of a 18.1 volume % composite of the particles in Castolite is shown in Figures 22a and 22b. Figures 22c and 22d show the corresponding values for the particles. The average dielectric constant was ( $5.75 \pm 0.11$ ,  $-0.35 \pm 0.1$ ) for the composite, and ( $19.6 \pm 1.9$ ,  $-1.5 \pm 1.0$ ) for the particles.

### Sample 23 - Titan Ferrites FCX-1547

Sample 23 was similarly a low-frequency ferrite with most of its magnetic loss below 10 GHz. The permeability of a 19.5 volume % composite of the particles in Castolite is shown in Figures 23a and 23b. Figures 23c and 23d show the corresponding values for the particles. The average dielectric constant was ( $5.83 \pm 0.21$ ,  $-0.21 \pm 0.09$  for the composite, ( $18.8 \pm 2.0$ ,  $-0.67 \pm 0.4$ ) for the particles.

### Magnetic Metal Flake

Magnetic metal flake offers a possible alternative to needles or whiskers as a means of reducing the weight of magnetic metal needed in absorbing composites. Flakes could be cheaper than needles or whiskers since they are made by a relatively simple hammering process which will work with varying degrees of

success for most metals. MTL has purchased quantities of permalloy, carbonyl iron, cobalt, nickel, several ferronickels, and stainless steels for evaluation from Novamet, Inc., Wycoff, NJ. One unfortunate problem these samples have is that they contain a relatively high percentage of fines (particles two microns or less in diameter and only slightly flattened) in addition to the flakes for which the aspect ratios are not uniform. The analysis of most of these samples is still in progress. As an example of the results, data are presented for a 50/50 ferro-nickel sample, which includes both fines and flake. Given the irregularity in the particle sizes and shapes, the data is presented in terms of weight % of metal.

The effect of the metal flake on the dielectric constant of the composite is shown in Figure 24a. Note that the behavior is essentially linear to about 25 weight % metal (about 5 volume %), at which point the dielectric constant increases in a highly nonlinear fashion.

The effect permeability of the composite is shown in Figures 24b and 24c. This is interesting in that magnetic loss is present from 2 to 18 GHz.

### Ceramic Matrix Composites

At the suggestion of the Chief of MTL's Ceramics Research Branch, representative samples of several light armor ceramic materials were tested for reflectivity in the 26 to 40 and 75 to 110 GHz range. All proved to have metallic reflectivity; they were later found to be conductive to a DC ohmmeter. Although introducing microwave absorption in light armor materials seems desirable, the prognosis for doing so in a practical manner is not clear at this time.

The samples were as follows:

- 6.1 Boron carbide ( $B_4C$ ) from Ceradyne, Costa Mesa, CA.
- 6.2 Silicon carbide (SiC) from Cercom, Vista, CA.
- 6.3 SiC whisker-reinforced alumina ( $Al_2O_3$ ) from Advanced Composite Materials Corporation, Greer, SC.

### A Standard Paint

A matter which will need more attention than it has apparently had is determining the electromagnetic properties of standard (decorative) paint samples. The real part of the dielectric constant is the most important parameter to be determined. In many cases it may not be possible to fabricate free standing samples and, therefore, a method to analyze a supported sample was devised. To do this, one looks for the downward shift in the half-wave frequency (determined from the open circuit reflection coefficient,  $S_{11}$ ) of a Castolite sample when a layer of paint is added, as indicated in Figure 25. The accuracy of the method depends in large part on the thickness and dielectric constant of the paint and the quality of the data; in most cases, epsilon prime can probably be determined to plus or minus 5% or better.

To test out this method, samples of an old acrylic green paint were prepared. A batch of the paint was also cast in a relatively flat sheet, from which cut a free standing sample for the 7mm transmission line was cut. A dielectric

constant of  $4.2 \pm 0.2$  was obtained in both free standing sample tests and in the test described in the previous paragraph. The imaginary part was on the order of -0.3 in the driest sample (thick layers of paint take a long time to cure; this one had cured for about a month and so may not have been fully cured).

Several samples of low emissivity paints of Taiwanese manufacture are planned for test in this manner. These are expected to be very high dielectric constant materials as a consequence of their metal flake content, and an  $\epsilon\mu$  product (which would be useful in most cases) may be all that can be obtained from the experiments. Other standard paints in common Army use should also be tested.

### CONCLUSIONS AND RECOMMENDATIONS

Permittivity and permeability data for a variety of materials and its limitations have been presented above. Results for simple dielectric materials are satisfactory, as expected. Many of the samples were metal-coated glass microspheres, for which the composite permeability data is in qualitative agreement with theoretical models, but for which the composite dielectric constant shows unexplained resonances at high volume percentages of particles. The potential utility of the particles tested in composites for absorbing microwave radiation would depend on the ability to make stable, reproducible, high-volume fraction composites of them. At a minimum, this would require large machine-mixed batches of material, which were not available for this study. The carbospheres tested behaved rather like carbon black particles in composites, although the weight percentage of them needed to introduce dielectric loss was comparatively small. Carbospheres coated with several magnetic metals showed no useful magnetic loss.

Of the ferrites tested, only a sample from Rockwell showed potentially useful magnetic loss from 2 to 18 GHz, as did a sample of 50/50 ferronickel flakes. Several ceramic composites proved to be too conductive to absorb microwave radiation. A method for determining the dielectric constant of paints was developed and should be exploited.

The data reduction for the vector network analyzer was not automated at the time these experiments were performed. This is the next problem to be addressed. An improved technique for measuring small values of  $\mu$  is also needed and will be explored.

### GLOSSARY

GHz - Gigahertz (10<sup>9</sup> cycles per second)

K<sub>A</sub> Band - 26.5 to 40 GHz

Permeability - The permeability,  $\mu$ , of a material is a measure of the extent to which an applied magnetic field is increased or decreased within the material as a consequence of its interactions with magnetic dipoles in the material.

Mathematically, one writes  $B = \mu H$ , where  $B$  is the field within the material (in units of gauss) and  $H$  is the applied magnetic field (in oersteds). At microwave frequencies, the magnetic dipoles within the material become unable to follow the changes in the magnetic field, and the material becomes lossy (i.e., it can absorb radiation).  $\mu$  is, thus, generally a complex number, with a real part  $\mu'$  and an imaginary part  $\mu''$  (or  $\mu_{double\ prime}$ ). The notation ( $\mu'$ ,  $\mu''$ ) for such complex numbers has been used in the text.

Permittivity - The permittivity, or dielectric constant,  $\epsilon$ , of a material is a measure of the extent to which an applied electric field is increased or decreased within the material as a consequence of its interactions with electric dipoles in the material. In a manner analogous to magnetic materials, one writes  $D = \epsilon E$ , where  $D$  is the electric displacement within the material, and  $E$  is the applied field. The dielectric constant is often a complex number at microwave frequencies, for which the notation ( $\epsilon'$ ,  $\epsilon''$ ) has been used in the text.

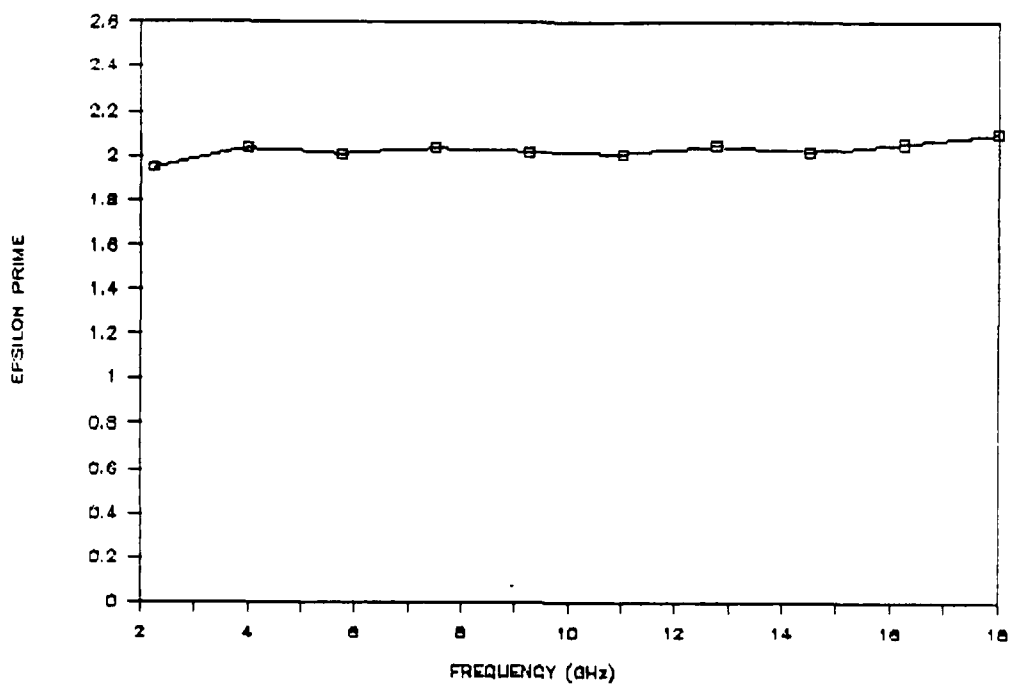


Figure 1a. The measured real part of the dielectric constant of teflon.

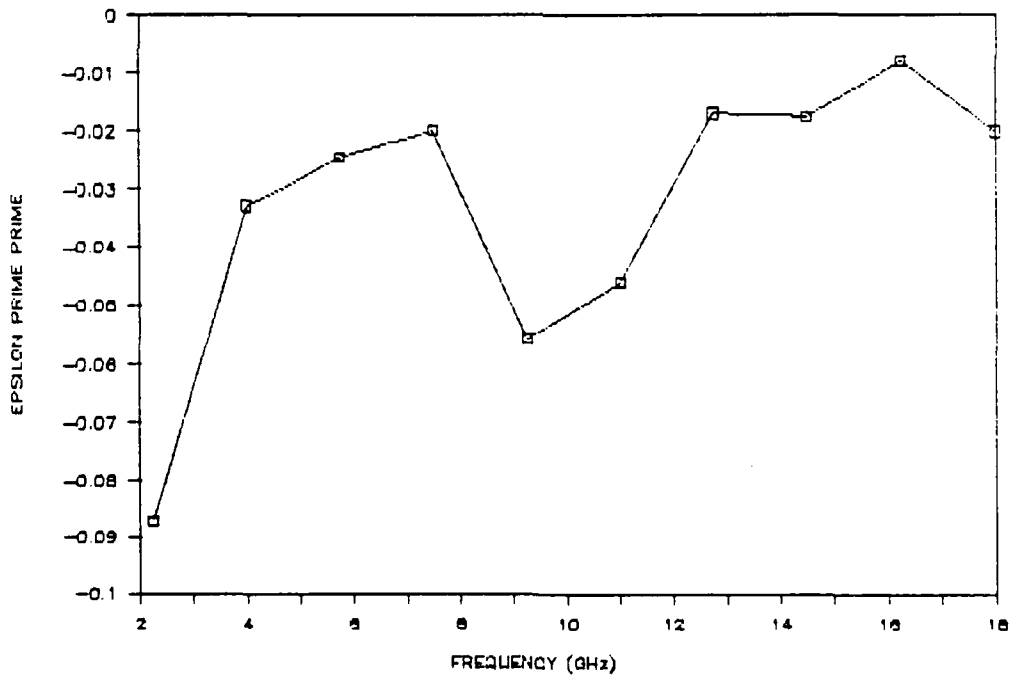


Figure 1b. The measured imaginary part of the dielectric constant of teflon.

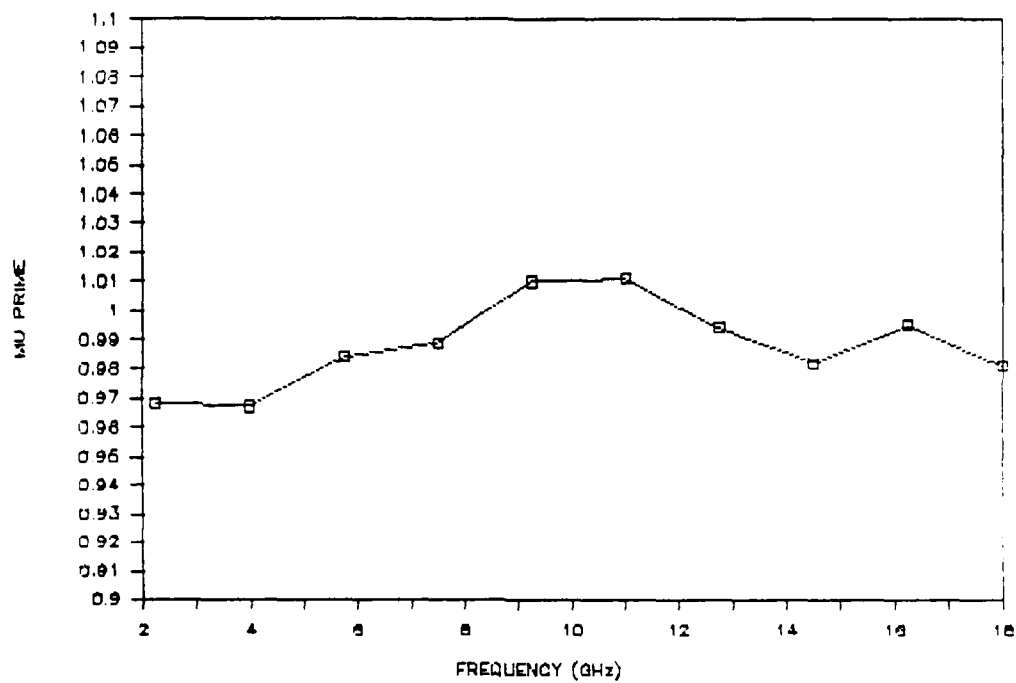


Figure 1c. The measured real part of the permeability of teflon.

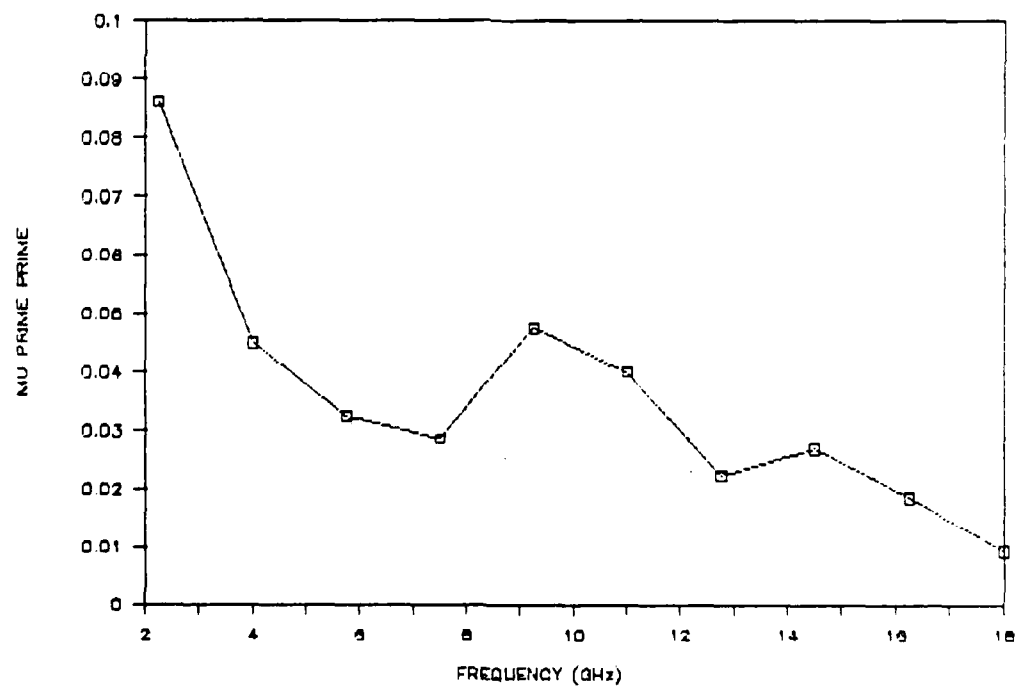


Figure 1d. The measured imaginary part of the permeability of teflon.

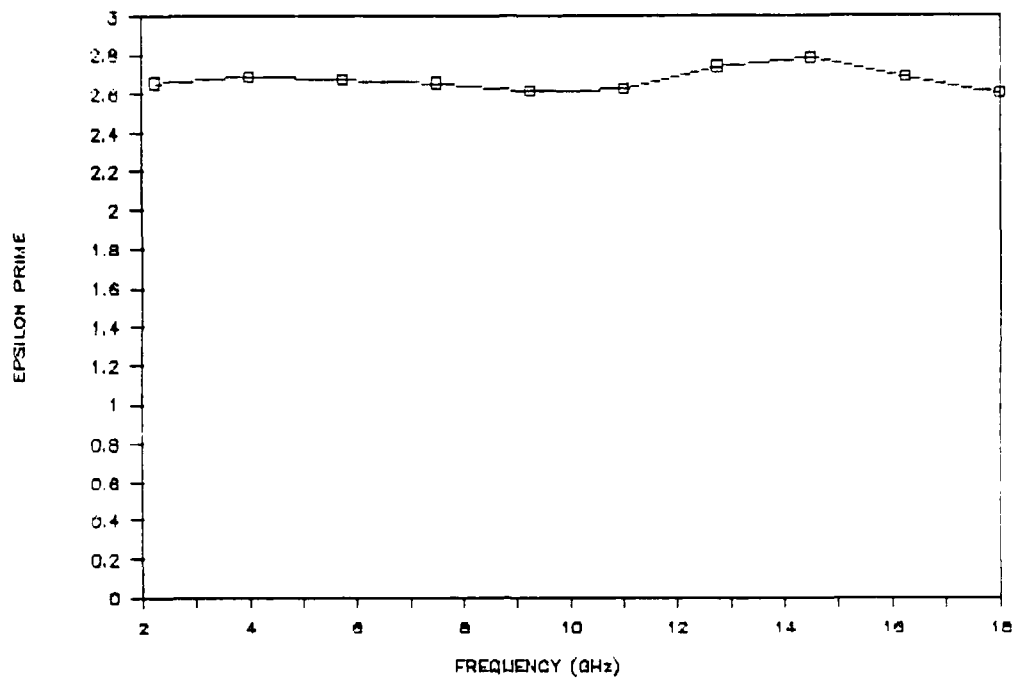


Figure 2. The measured real part of the dielectric constant of the Castolite casting plastic.

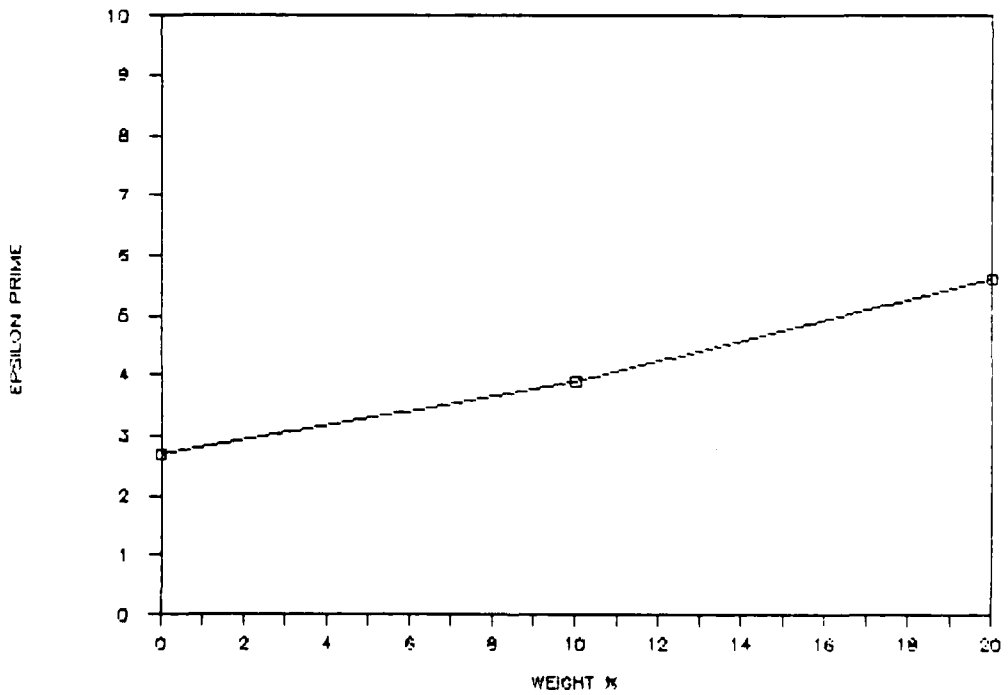


Figure 3. Variation of the real part of the dielectric constant of Castolite, nickel-coated microsphere composites as a function of particle concentration.

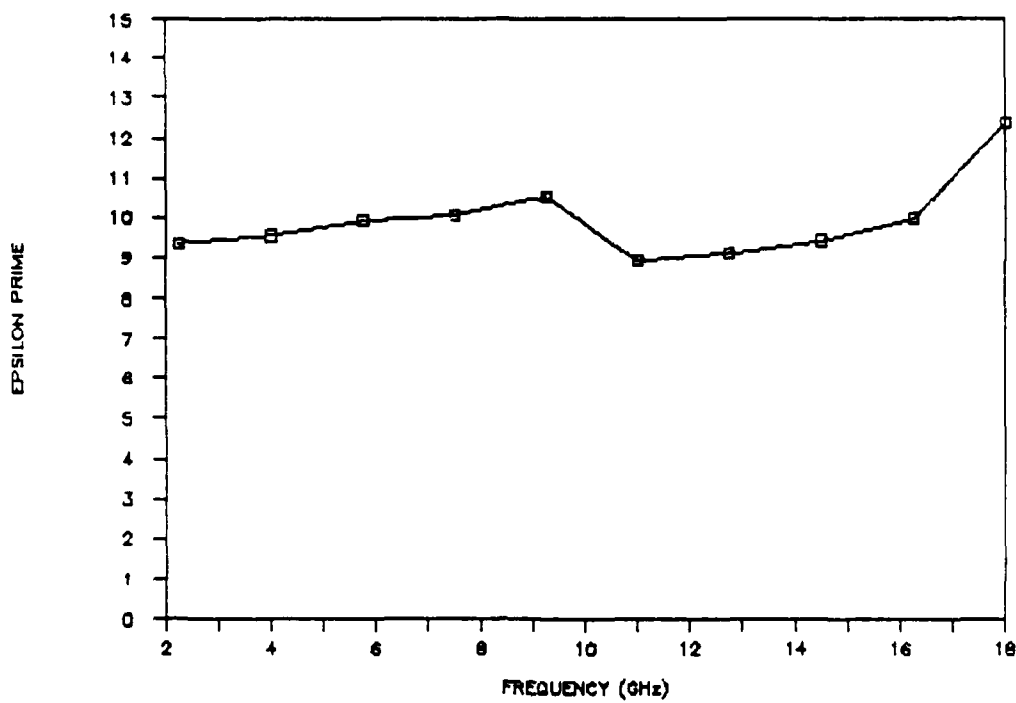


Figure 4a. The real part of the dielectric constant for a 30 weight % composite of nickel-coated microspheres in a Castolite binder.

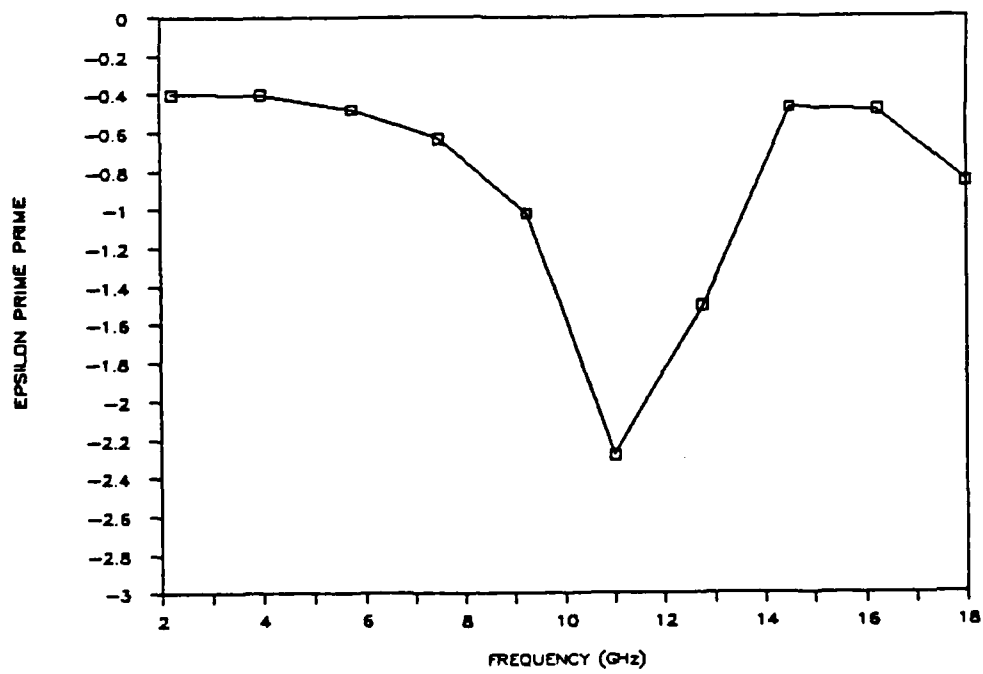


Figure 4b. The imaginary part of the dielectric constant for a 30 weight % composite of nickel-coated microspheres in a Castolite binder.

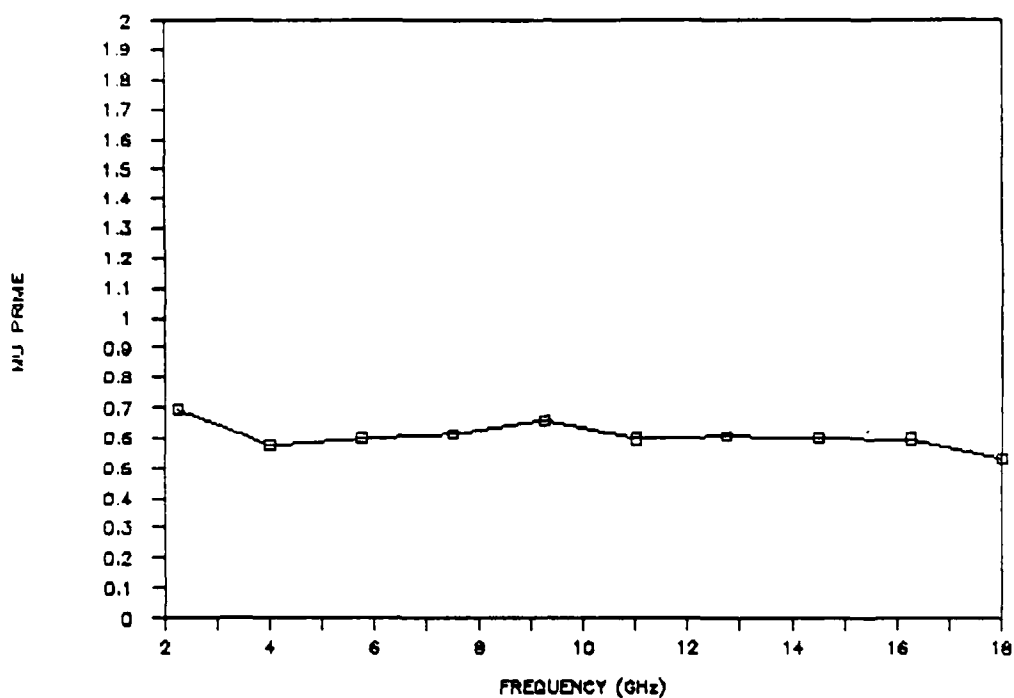


Figure 4c. The real part of the permeability constant for a 30 weight % composite of nickel-coated microspheres in a Castolite binder.

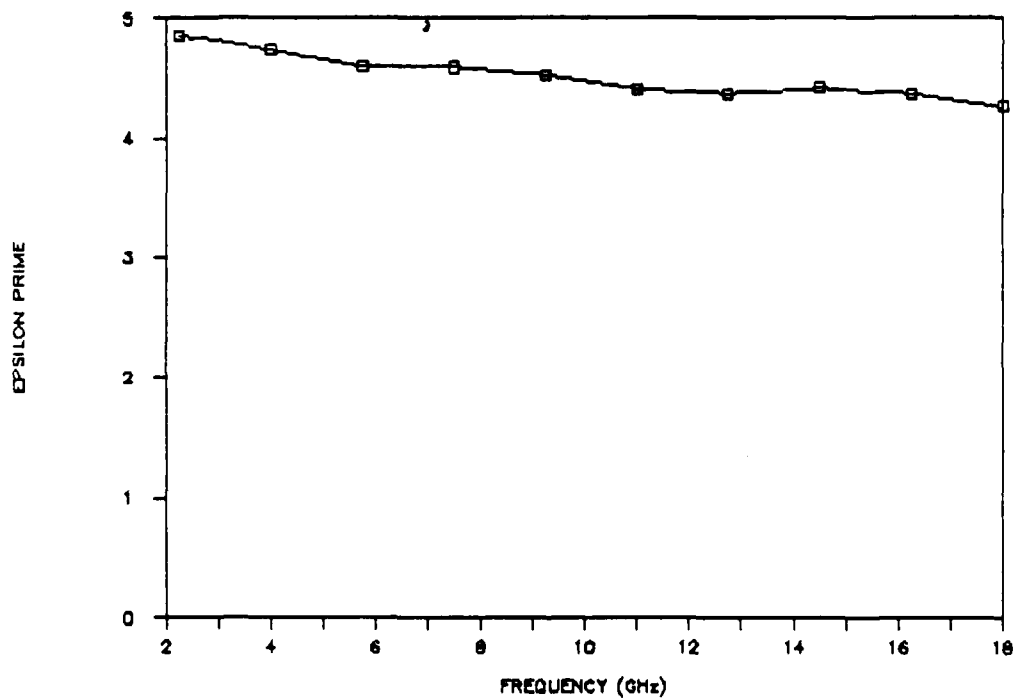


Figure 5a. The real part of the dielectric constant for a 45 weight % composite of Sample 3 (Carolina Solvents Silver-Coated Microspheres, 20/26) in a Castolite binder.

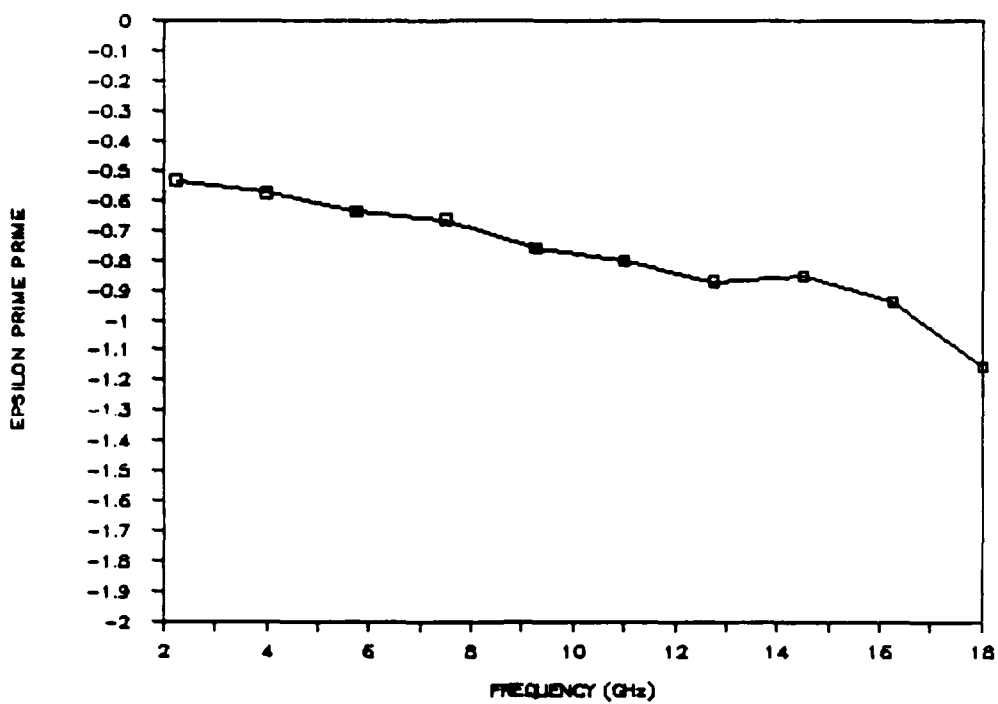


Figure 5b. The imaginary part of the dielectric constant for a 45 weight % composite of Sample 3 (Carolina Solvents Silver-Coated Microspheres, 20/26) in a Castolite binder.

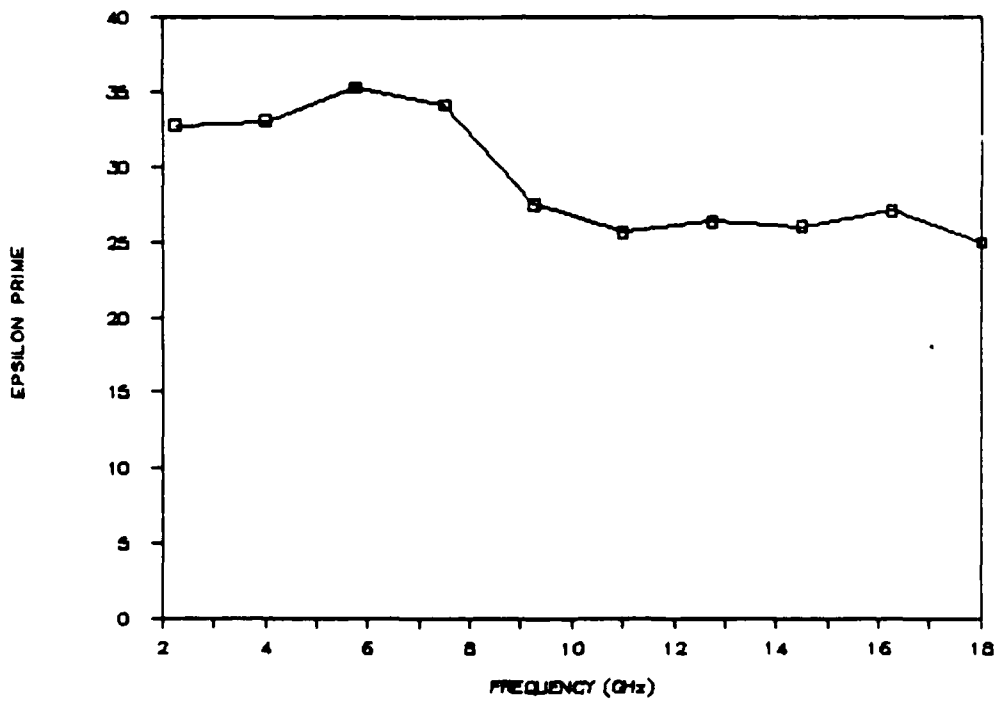


Figure 6a. The real part of the dielectric constant for a 45 weight % composite of Sample 4 (Carolina Solvents Silver-Coated Microspheres, 34/94) in a Castolite binder.

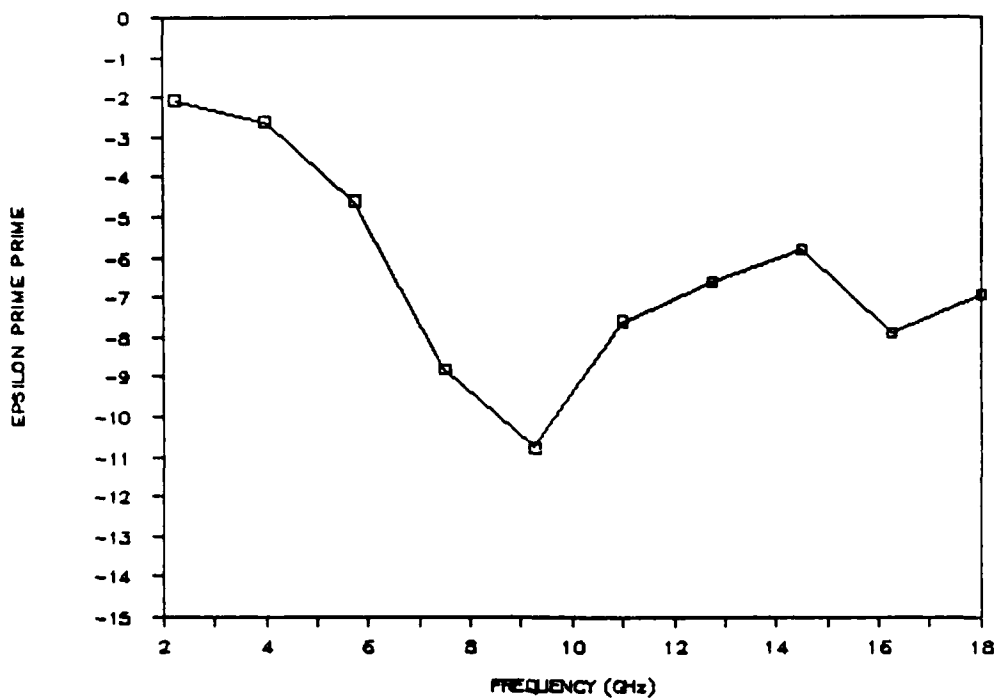


Figure 6b. The imaginary part of the dielectric constant for a 45 weight % composite of Sample 4 (Carolina Solvents Silver-Coated Microspheres, 34/94) in a Castolite binder.

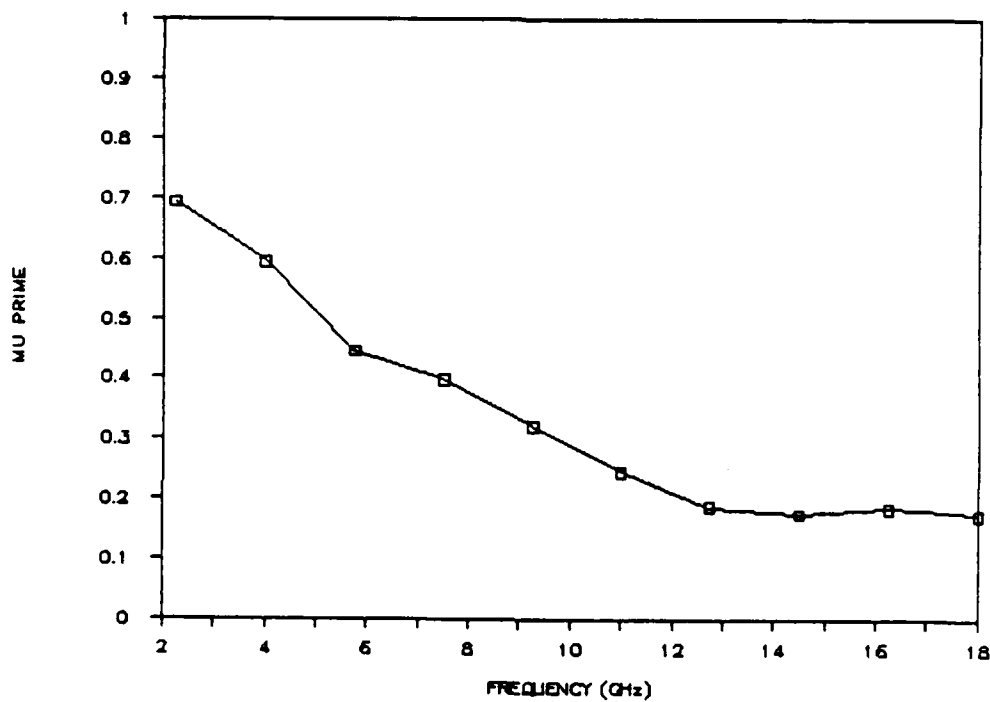


Figure 6c. The real part of the permeability constant for a 45 weight % composite of Sample 4 (Carolina Solvents Silver-Coated Microspheres, 34/94) in a Castolite binder.

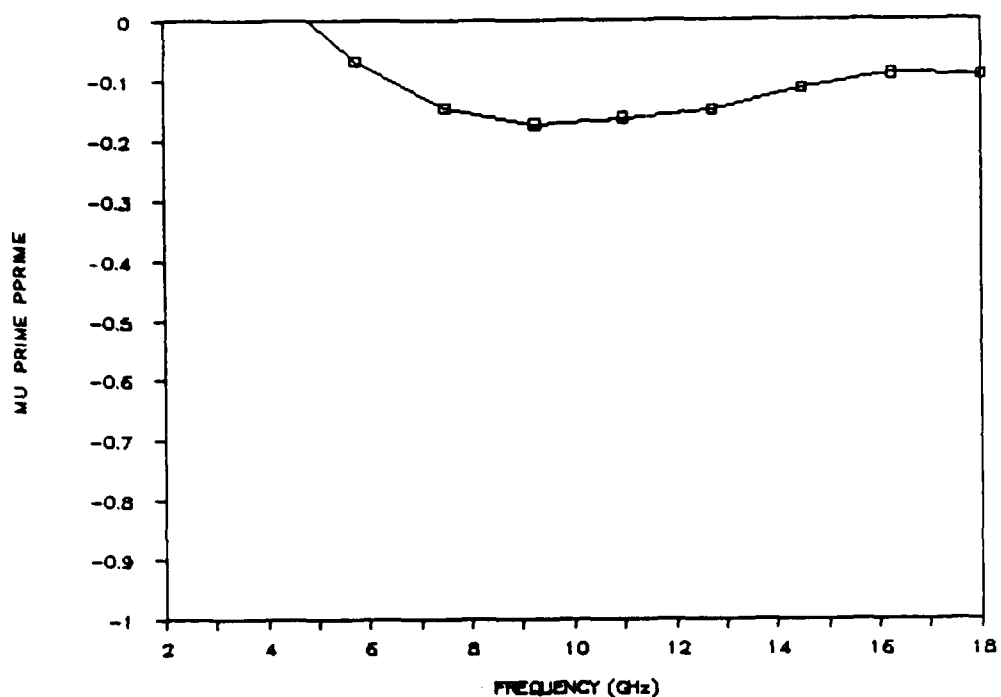


Figure 6d. The imaginary part of the permeability constant for a 25 weight % composite of Sample 4 (Carolina Solvents Silver-Coated Microspheres, 34/94) in a Castolite binder.

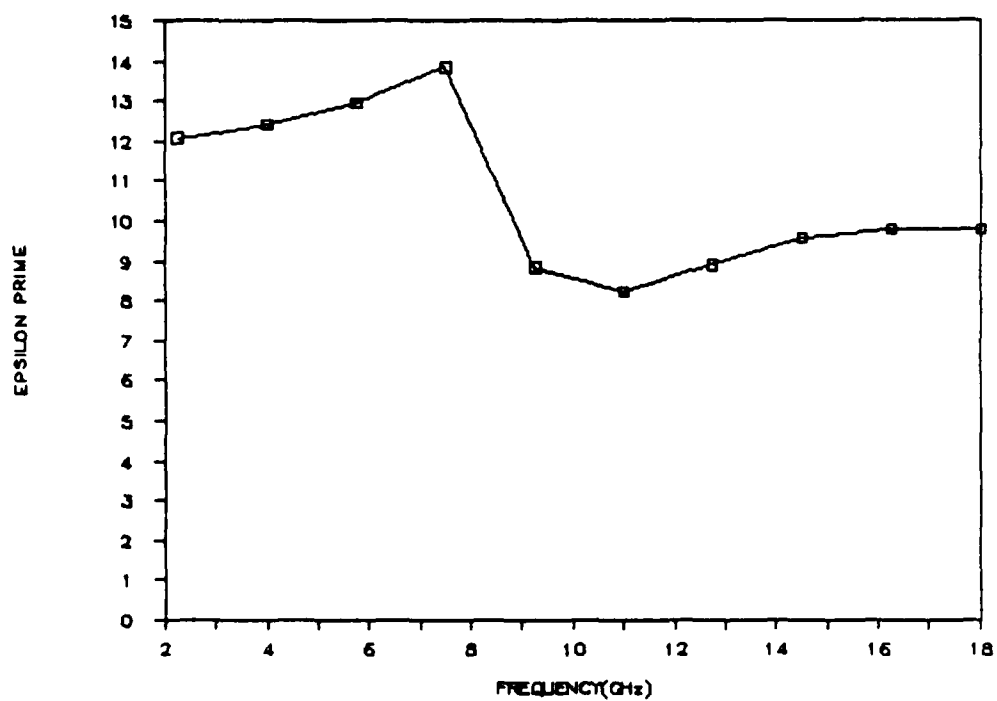


Figure 7a. The real part of the dielectric constant for a 25 weight % composite of Sample 6 (Carolina Solvents Silver-Coated Microspheres, 200/10) in a Castolite binder.

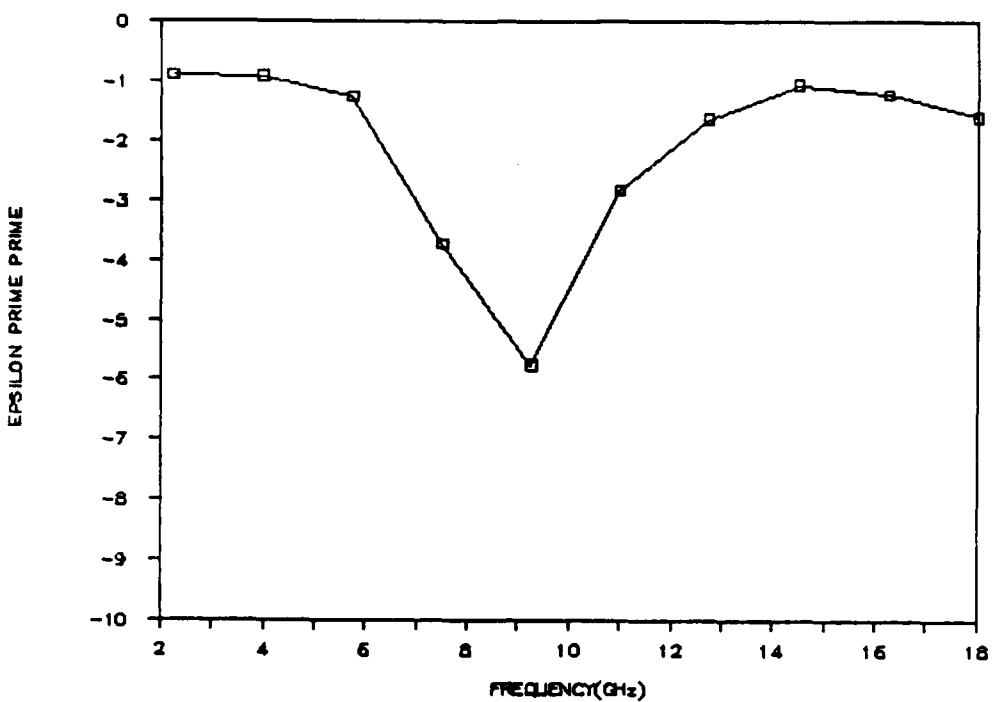


Figure 7b. The imaginary part of the dielectric constant for a 25 weight % composite of Sample 6 (Carolina Solvents Silver-Coated Microspheres, 200/10) in a Castolite binder.

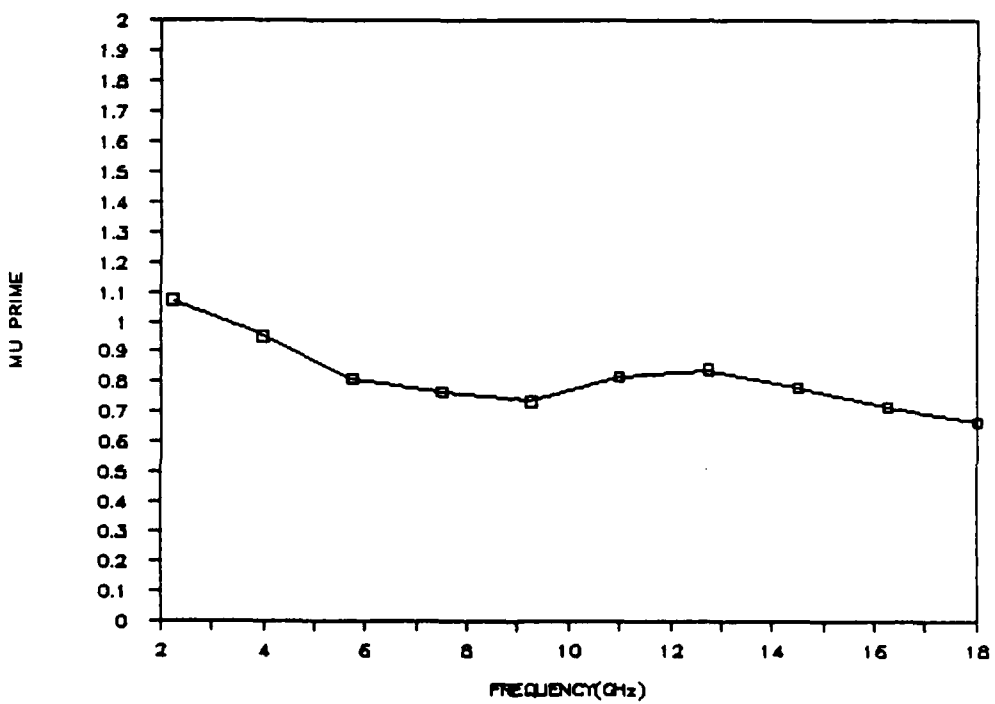


Figure 7c. The real part of the permeability constant for a 25 weight % composite of Sample 6 (Carolina Solvents Silver-Coated Microspheres, 200/10) in a Castolite binder.

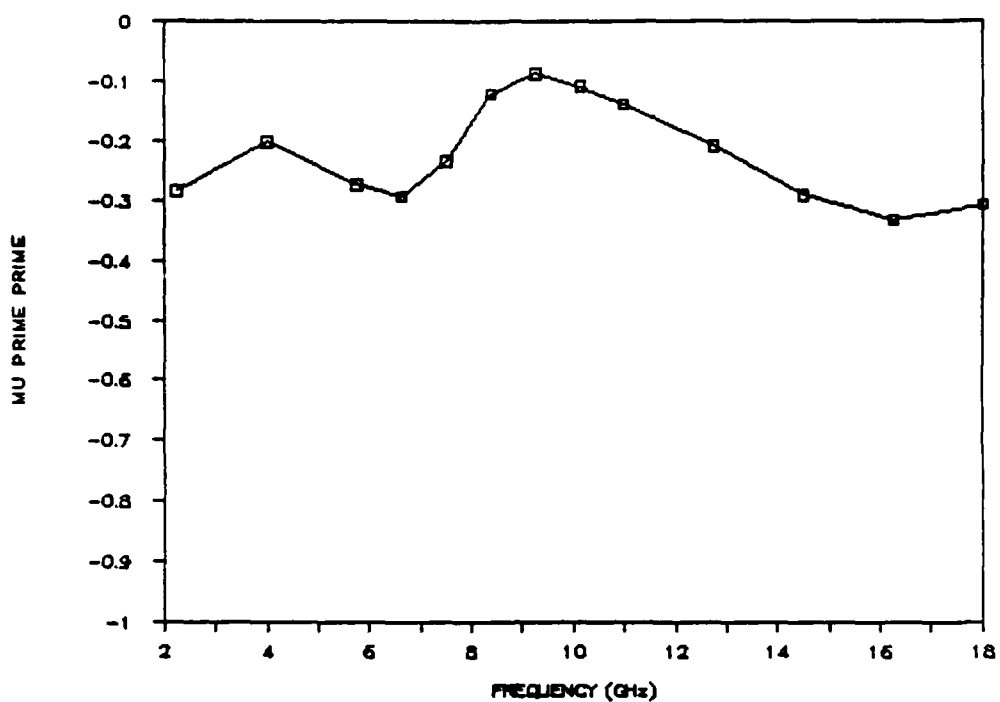


Figure 7d. The imaginary part of the permeability constant for a 45 weight % composite of Sample 6 (Carolina Solvents Silver-Coated Microspheres, 200/10) in a Castolite binder.

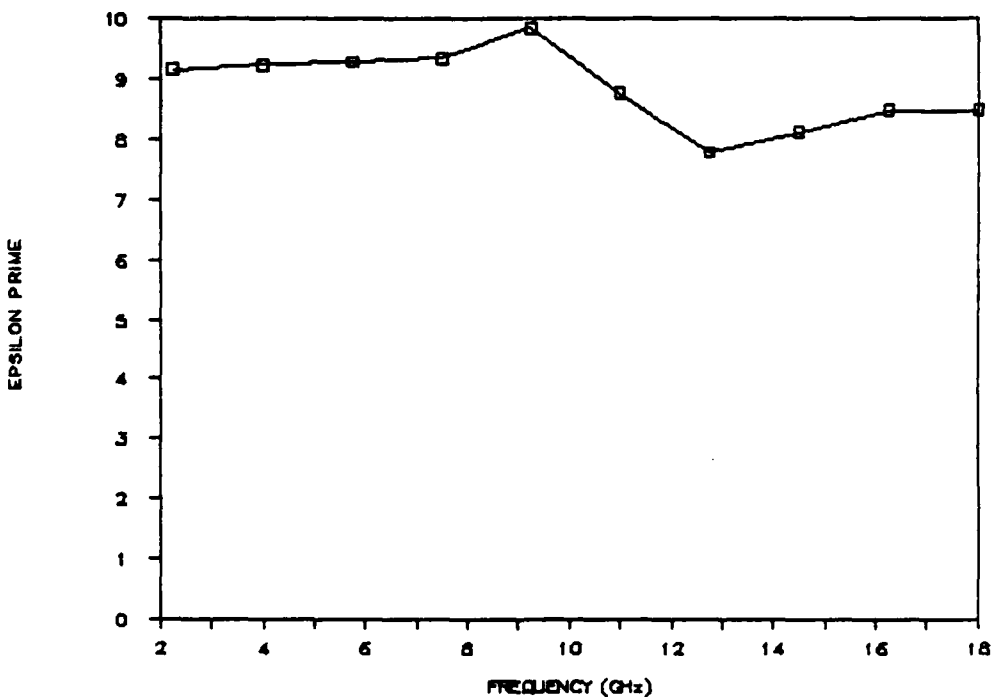


Figure 8a. The real part of the dielectric constant for a 25 weight % composite of Sample 8 (Mobay Chemical Silver-Coated Microspheres) in a Castolite binder.

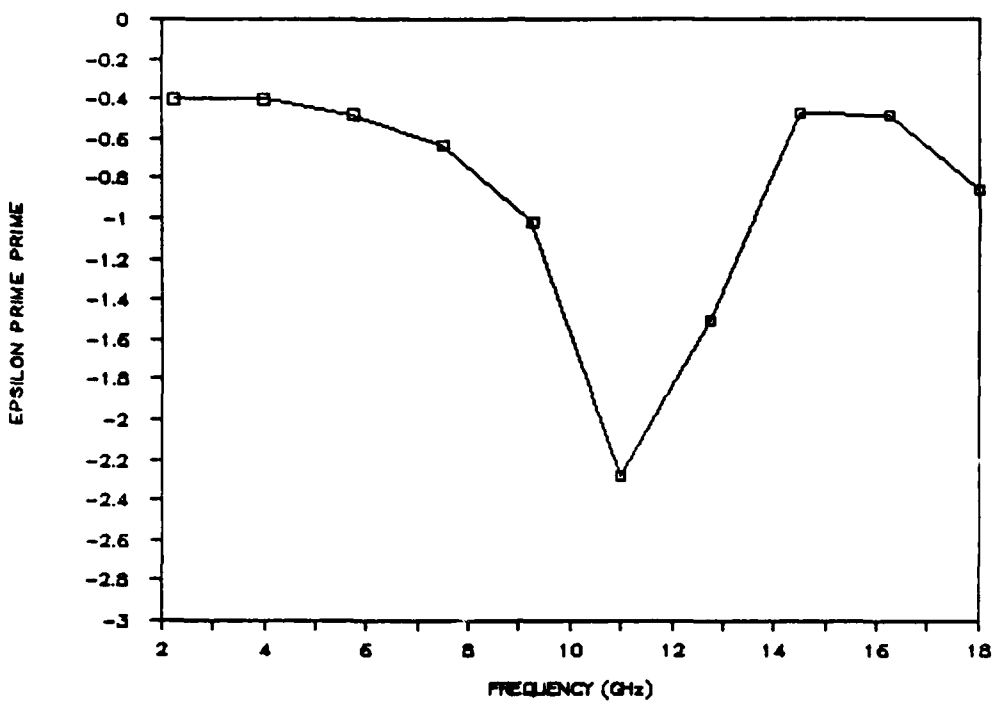


Figure 8b. The imaginary part of the dielectric constant for a 25 weight % composite of Sample 8 (Mobay Chemical Silver-Coated Microspheres) in a Castolite binder.

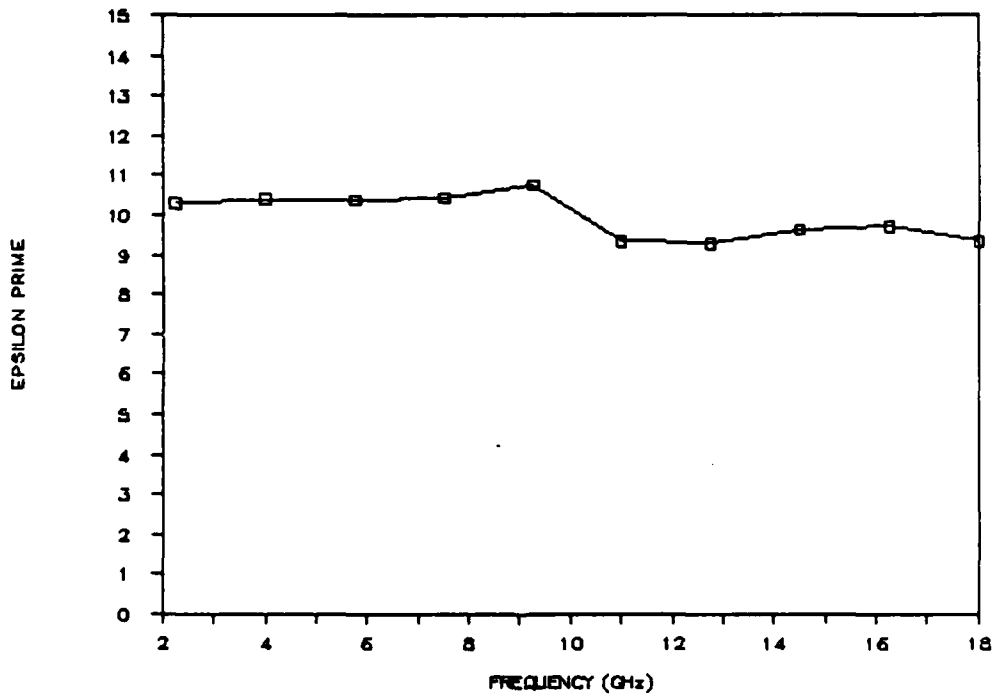


Figure 9a. The real part of the dielectric constant for a 25 weight % composite of Sample 9 (Mobay Chemical Iron-Coated Microspheres) in a Castolite binder.

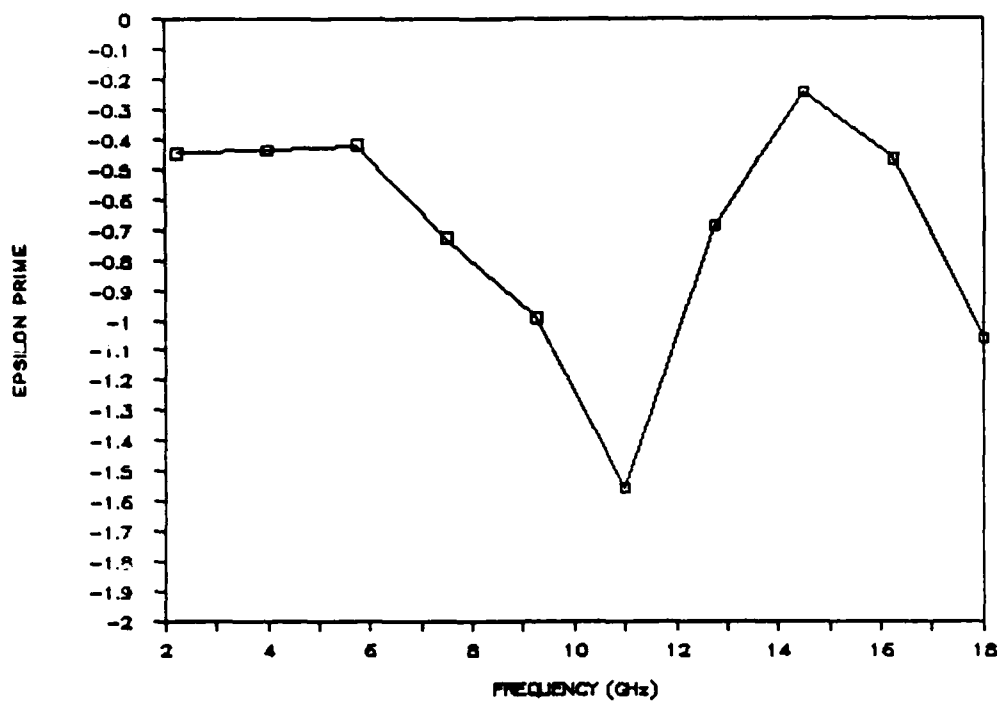


Figure 9b. The imaginary part of the dielectric constant for a 25 weight % composite of Sample 9 (Mobay Chemical Iron-Coated Microspheres) in a Castolite binder.

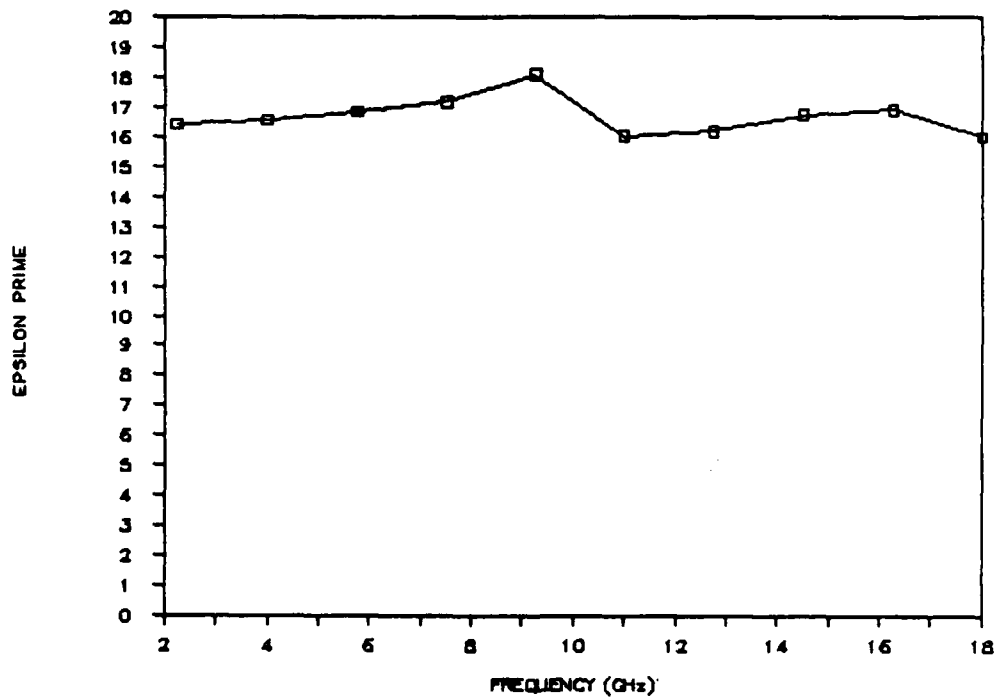


Figure 9c. The real part of the dielectric constant for a 45 weight % composite of Sample 9 (Mobay Chemical Iron-Coated Microspheres) in a Castolite binder.

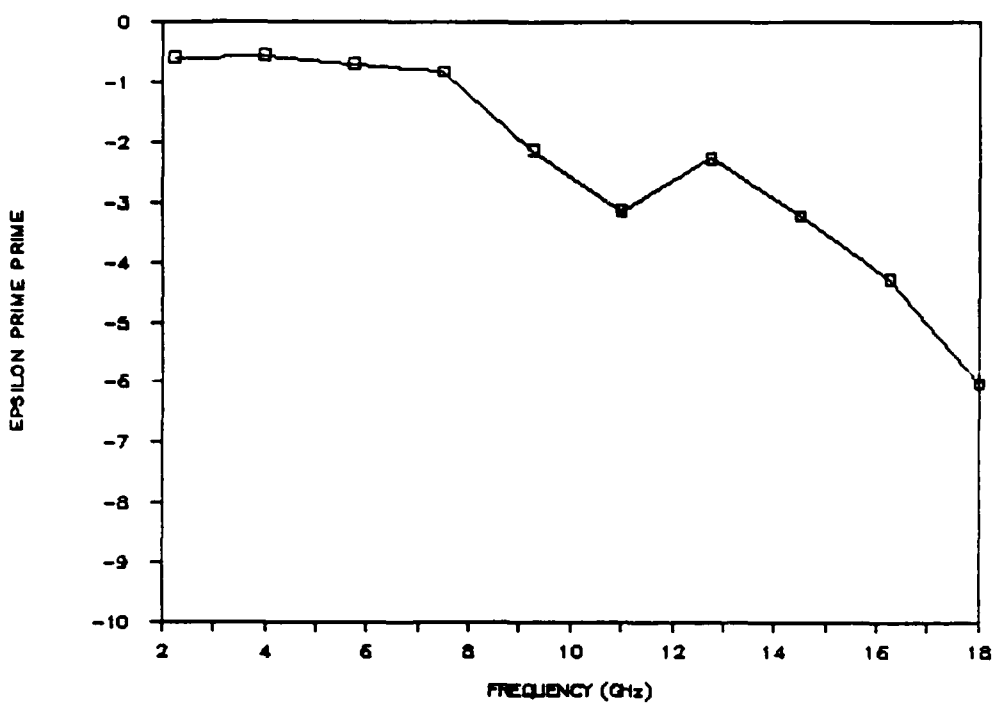


Figure 9d. The imaginary part of the dielectric constant for a 45 weight % composite of Sample 9 (Mobay Chemical Iron-Coated Microspheres) in a Castolite binder.

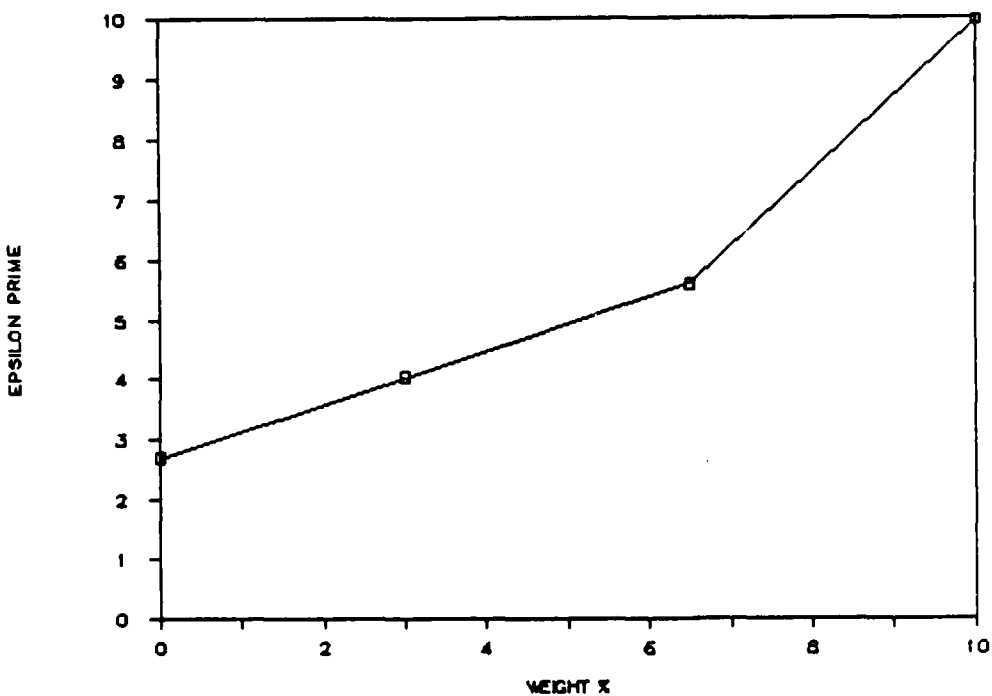


Figure 10a. Variation of the real part of the dielectric constant of Castolite, Type A Carbospheres composites as a function of particle concentration.

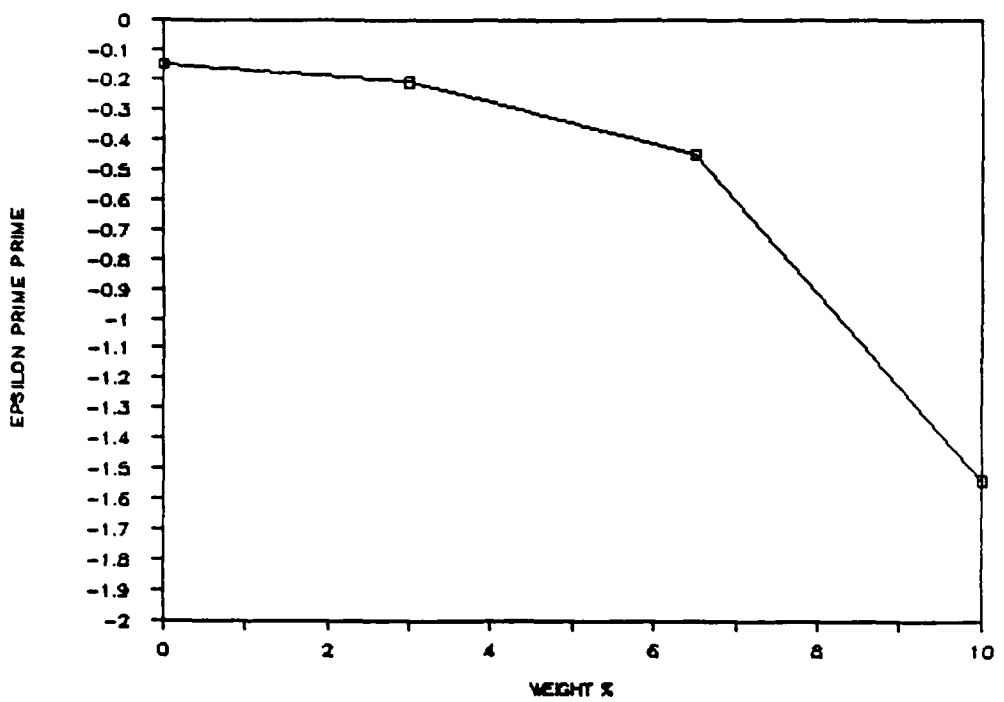


Figure 10b. Variation of the imaginary part of the dielectric constant of Castolite, Type A Carboespheres composites as a function of particle concentration.

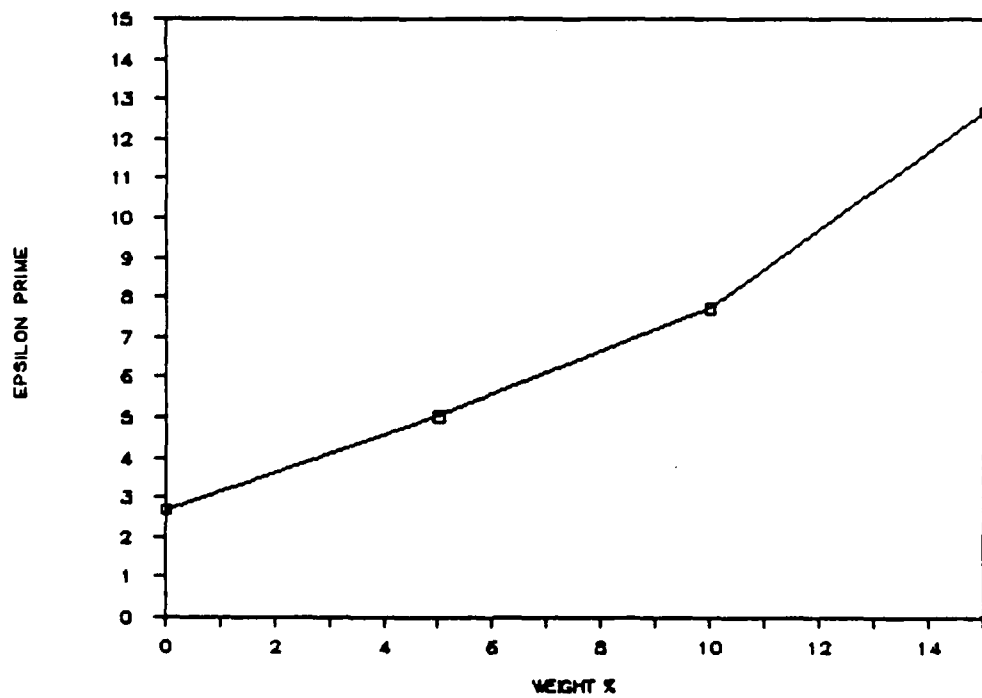


Figure 11a. Variation of the real part of the dielectric constant of Castolite, Type D Carboespheres composites as a function of particle concentration.

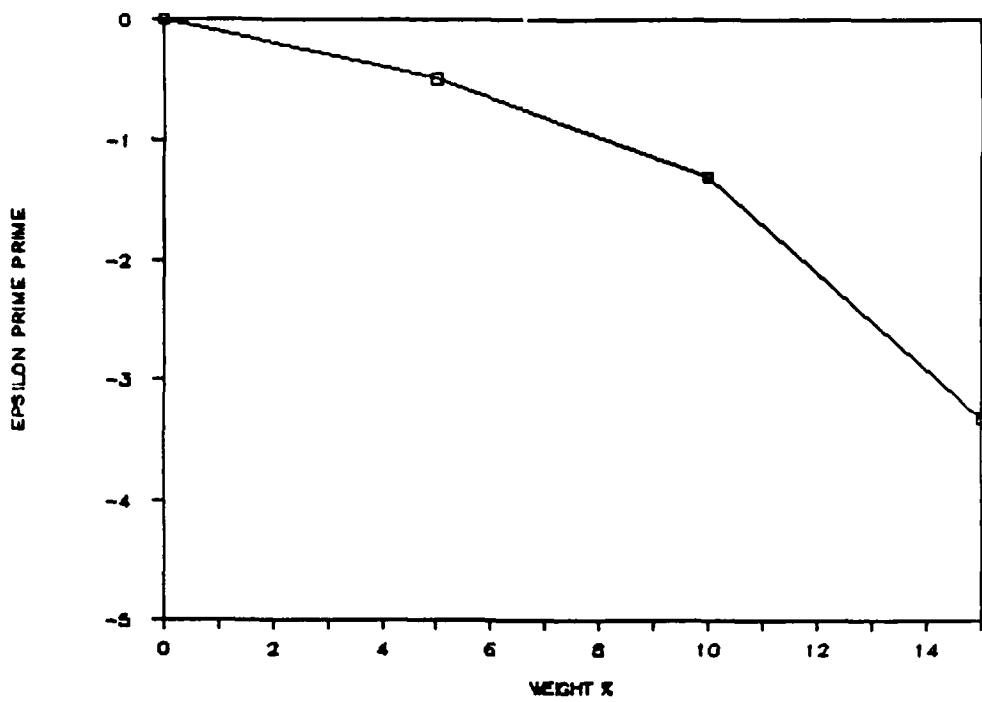


Figure 11b. Variation of the imaginary part of the dielectric constant of Castolite, Type D Carbospheres composites as a function of particle concentration.

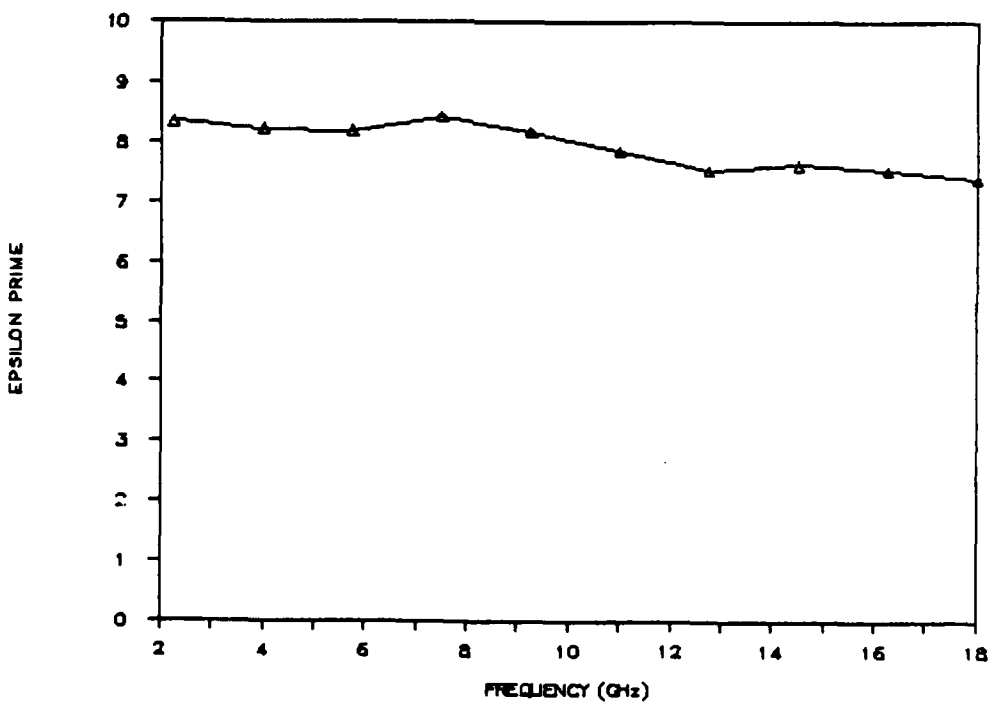


Figure 12a. The real part of the dielectric constant for a 25 weight % composite of iron-coated carbospheres in a Castolite binder. The data is the average of three determinations.

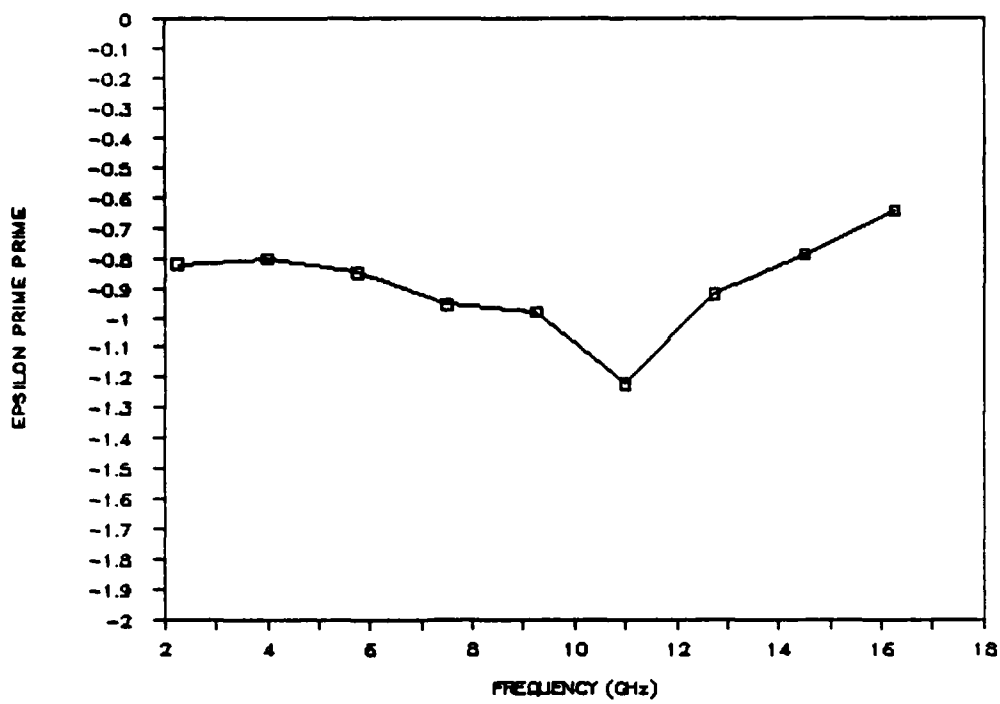


Figure 12b. The imaginary part of the dielectric constant for a 25 weight % composite of iron-coated carbospheres in a Castolite binder. The data is the average of three determinations.

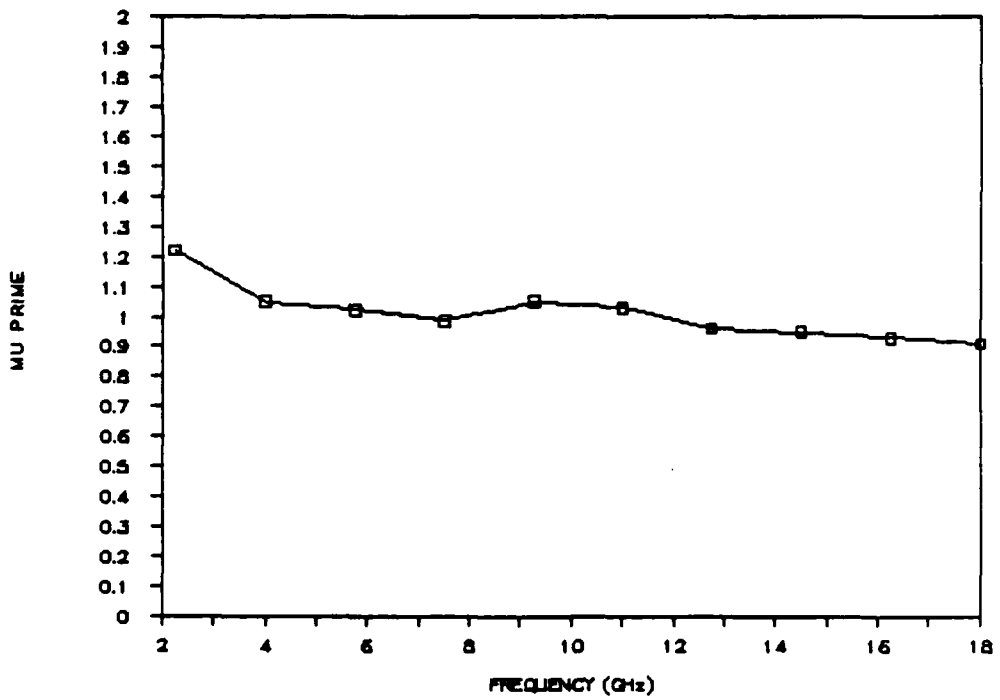


Figure 12c. The real part of the permeability constant for a 25 weight % composite of iron-coated carbospheres in a Castolite binder. The data is the average of three determinations.

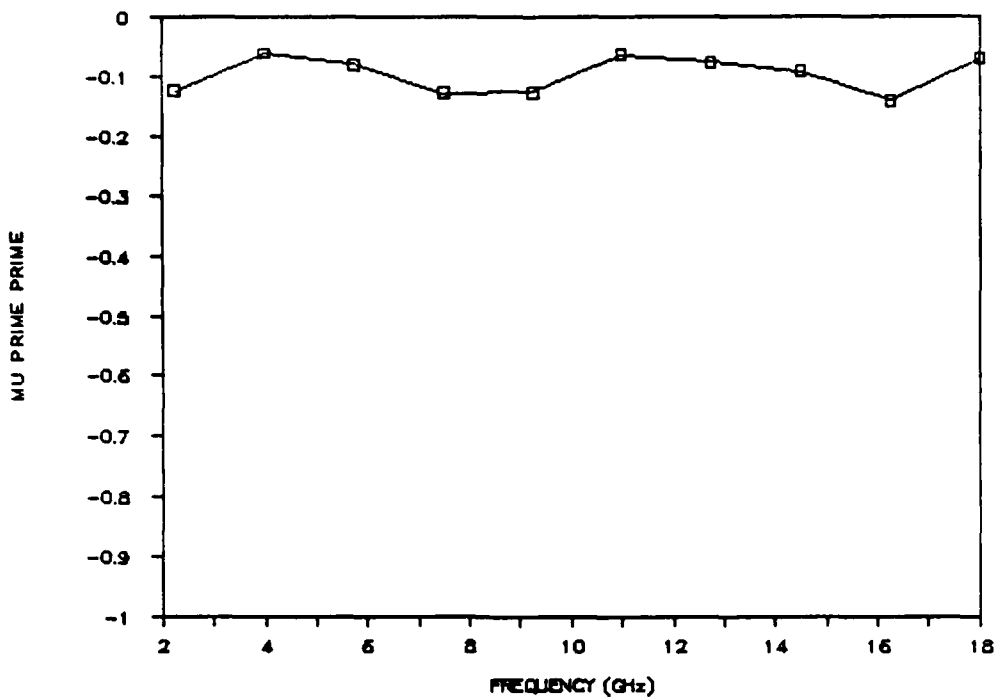


Figure 12d. The imaginary part of the permeability constant for a 25 weight % composite of iron-coated carboospheres in a Castolite binder. The data is the average of three determinations.

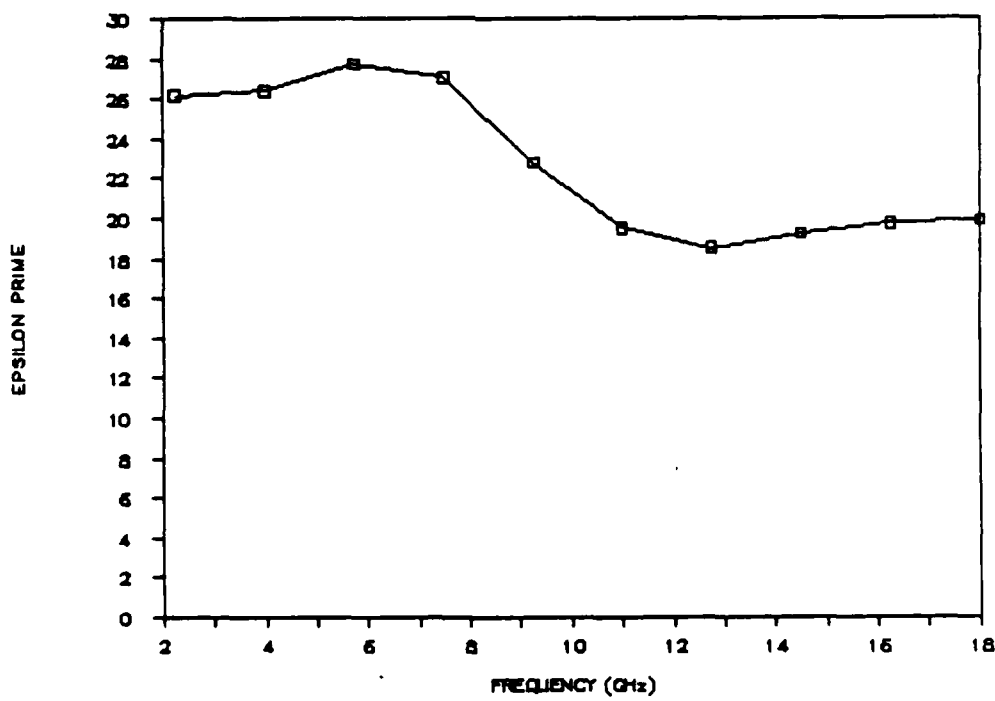


Figure 13a. The real part of the dielectric constant for a 20 weight % composite of nickel-coated carboospheres in a Castolite binder. The data is the average of two determinations.

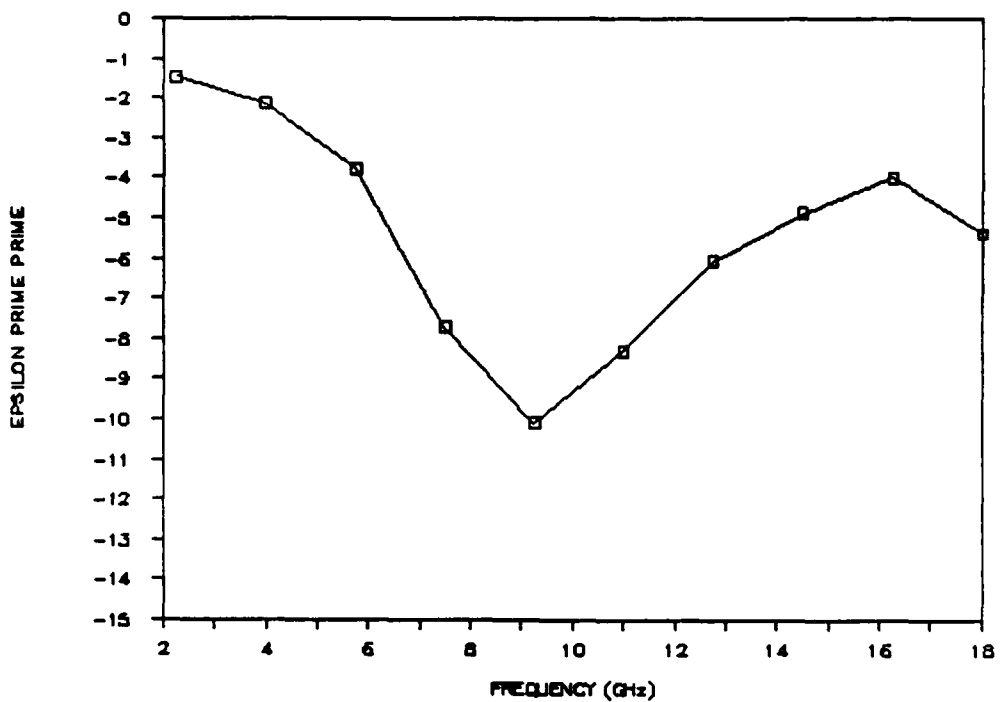


Figure 13b. The imaginary part of the dielectric constant for a 20 weight % composite of nickel-coated carboespheres in a Castolite binder. The data is the average of two determinations.

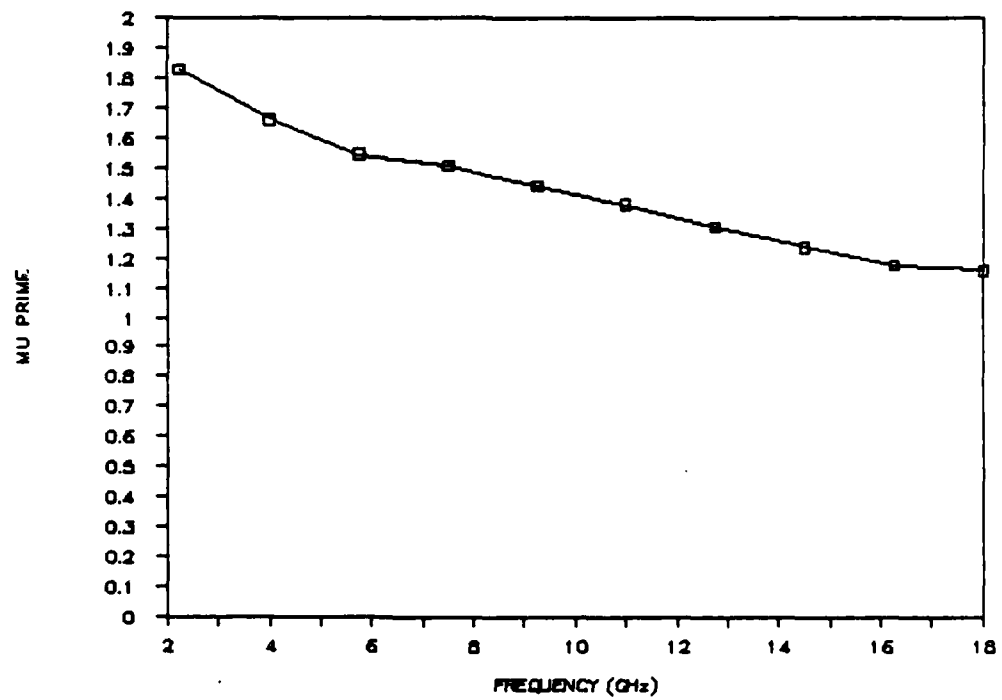


Figure 14a. The real part of the permeability of a 60 weight % composite of Sample 10 (Rockwell Ferrites) in a Castolite binder.

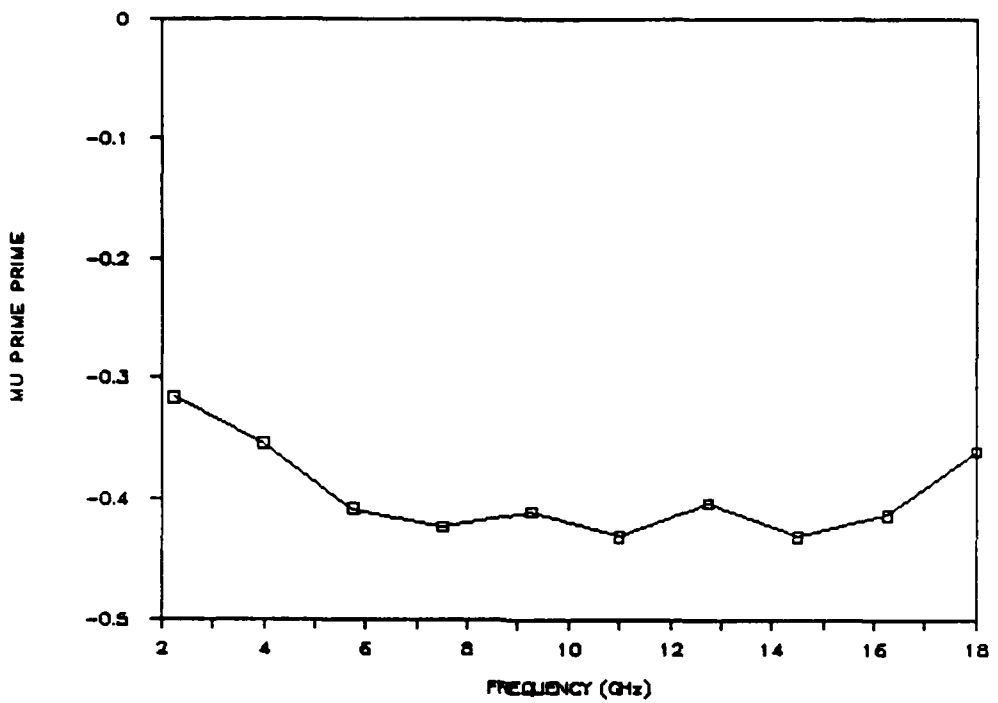


Figure 14b. The imaginary part of the permeability of a 60 weight % composite of Sample 10 (Rockwell Ferrites) in a Castolite binder.

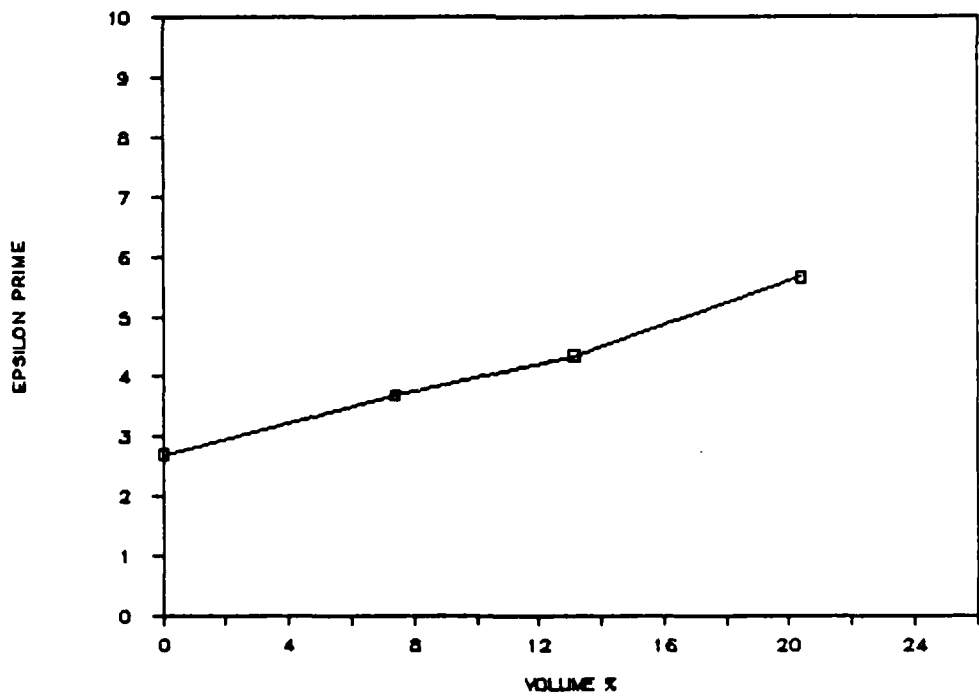


Figure 14c. The real part of the dielectric constant of composites of particles of Sample 10 (Rockwell Ferrites) as a function of volume loading.

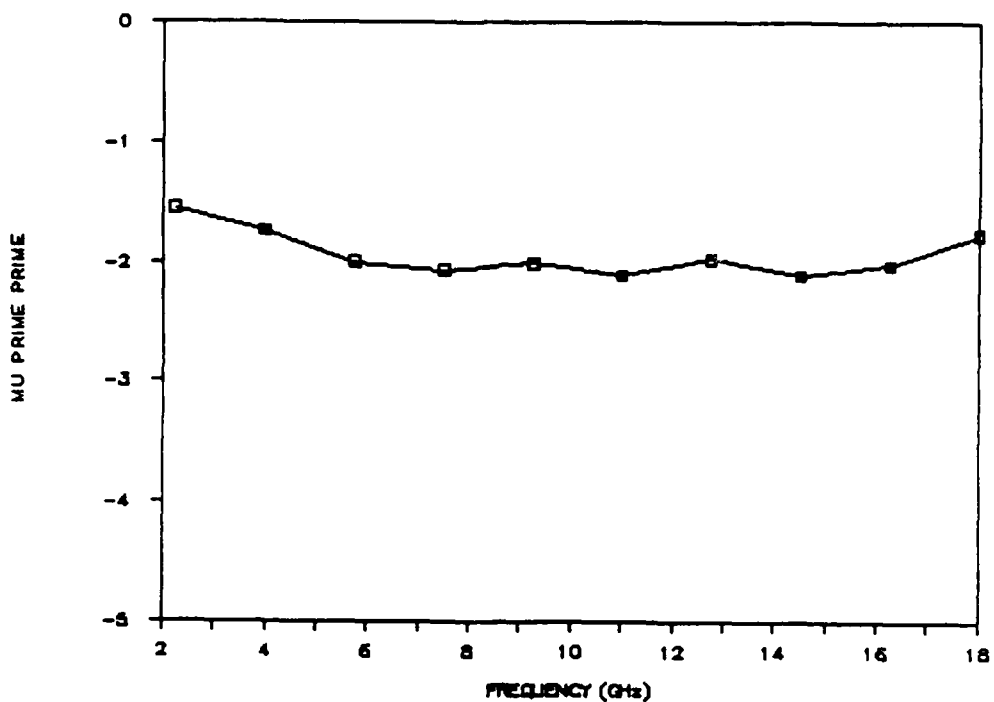


Figure 14d. Composite dielectric constant as a function of particle dielectric constant for 20 volume % composites of spherical particles in a binder of dielectric constant 2.7 calculated using the Maxwell-Garnett theory. Note that the limiting value for the composite dielectric constant is 4.725 for this system.

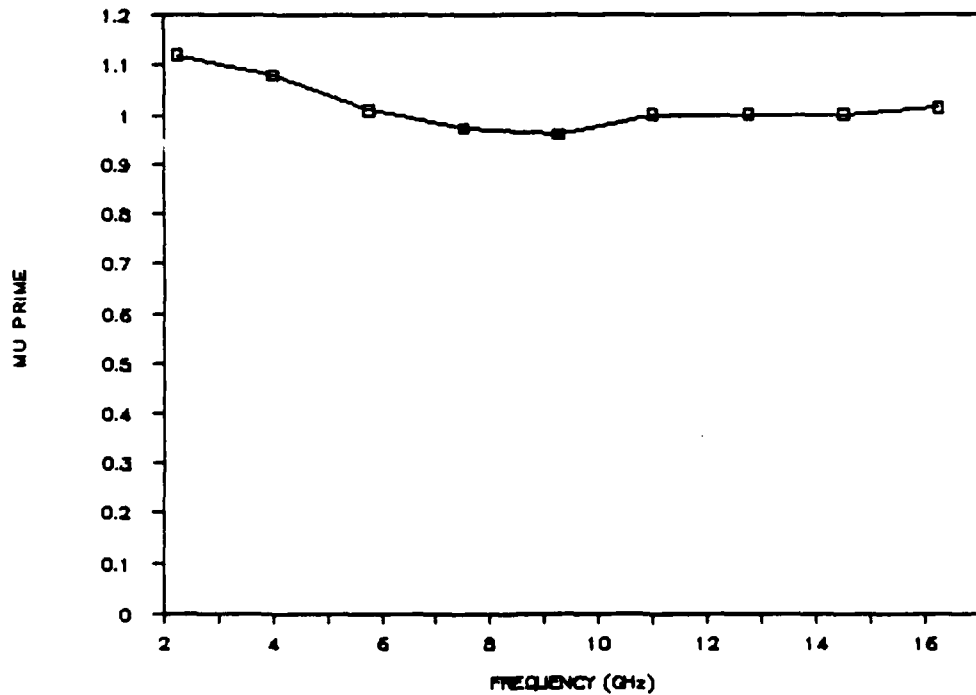


Figure 14e. The real part of the permeability of a particle of Sample 10 (Rockwell Ferrites).

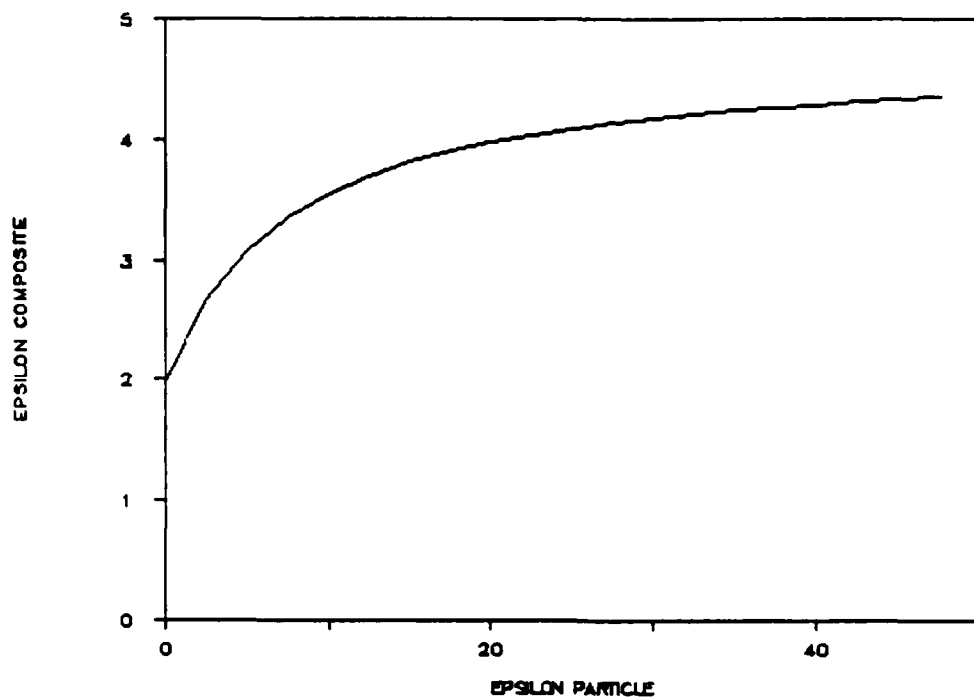


Figure 14f. The imaginary part of the permeability of a particle of Sample 10 (Rockwell Ferrites).

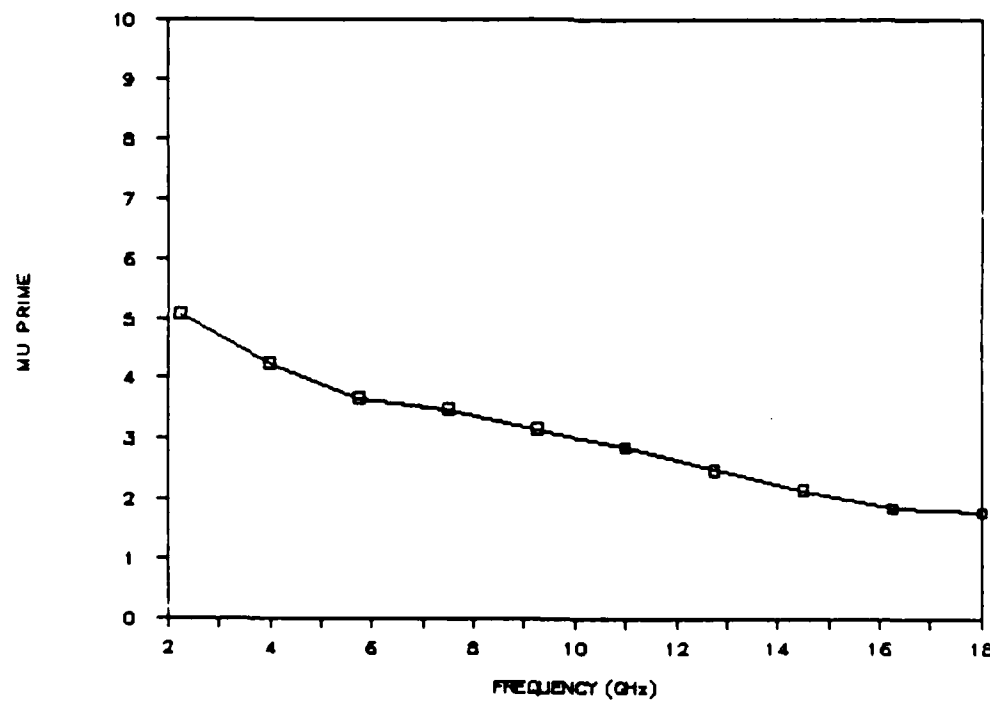


Figure 15a. The real part of the permeability of a 9.8 volume % composite of Sample 13 (Titan Ferrites FCX-1537) in a Castolite binder.

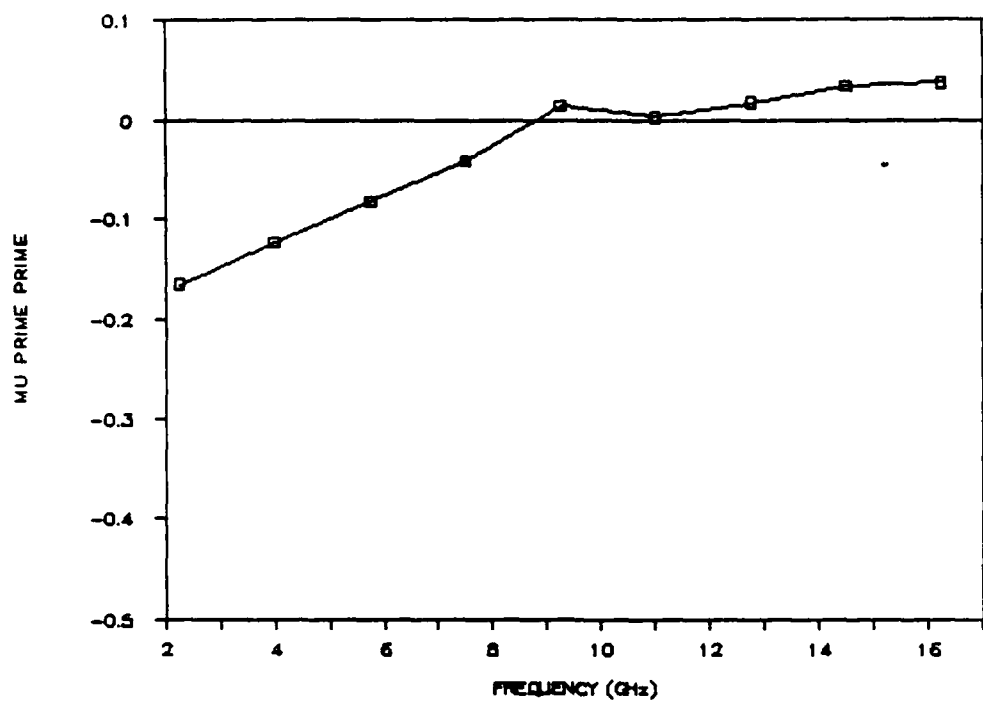


Figure 15b. The imaginary part of the permeability of a 9.8 volume % composite of Sample 13 (Titan Ferrites FCX-1537) in a Castolite binder.

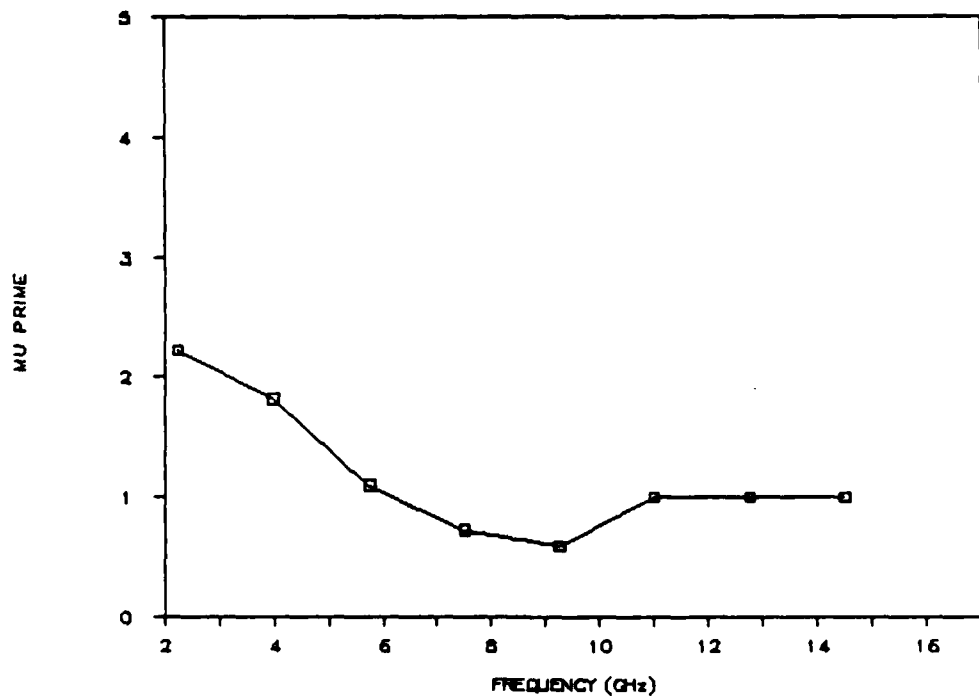


Figure 15c. The real part of the permeability of a particle of Sample 13 (Titan Ferrites FCX-1537).

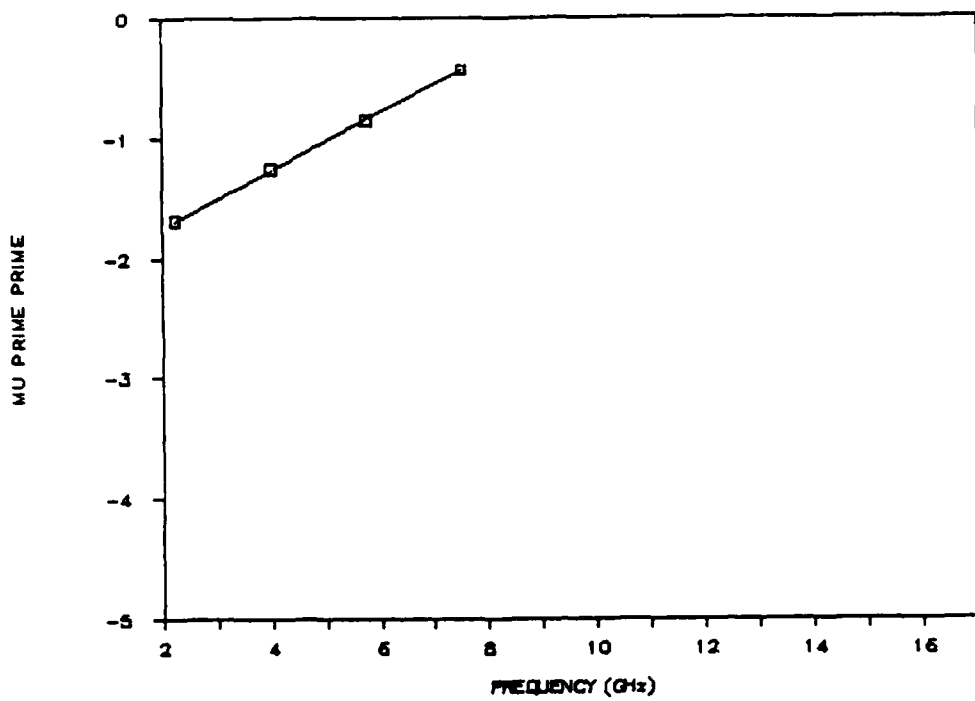


Figure 15d. The imaginary part of the permeability of a particle of Sample 13 (Titan Ferrites FCX-1537).

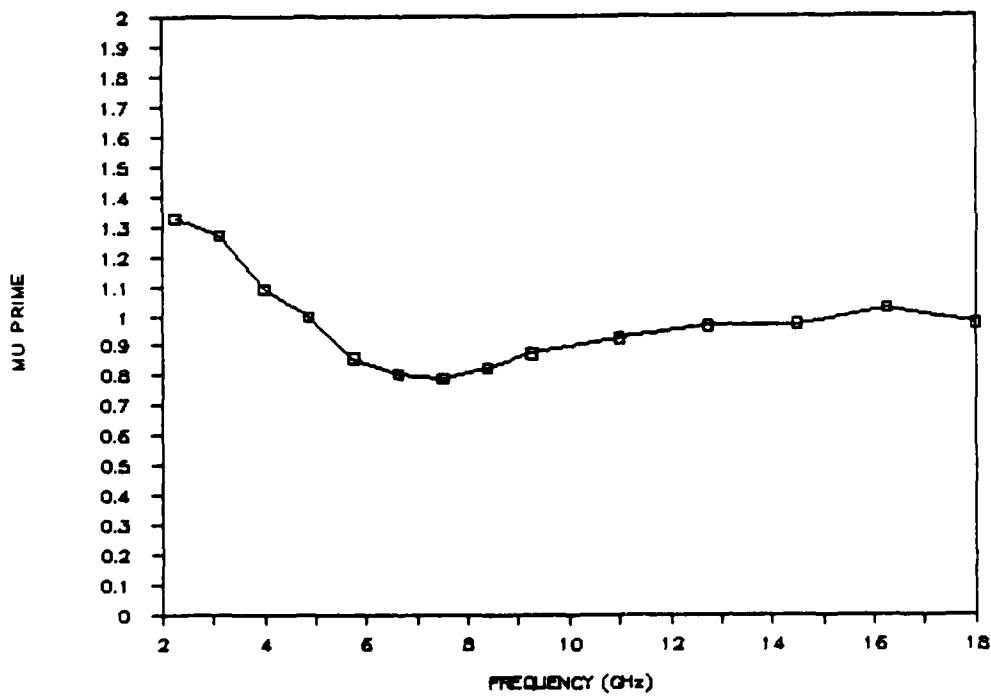


Figure 16a. The real part of the permeability of a 18.9 volume % composite of Sample 14 (Titan Ferrites FCX-1538) in a Castolite binder.

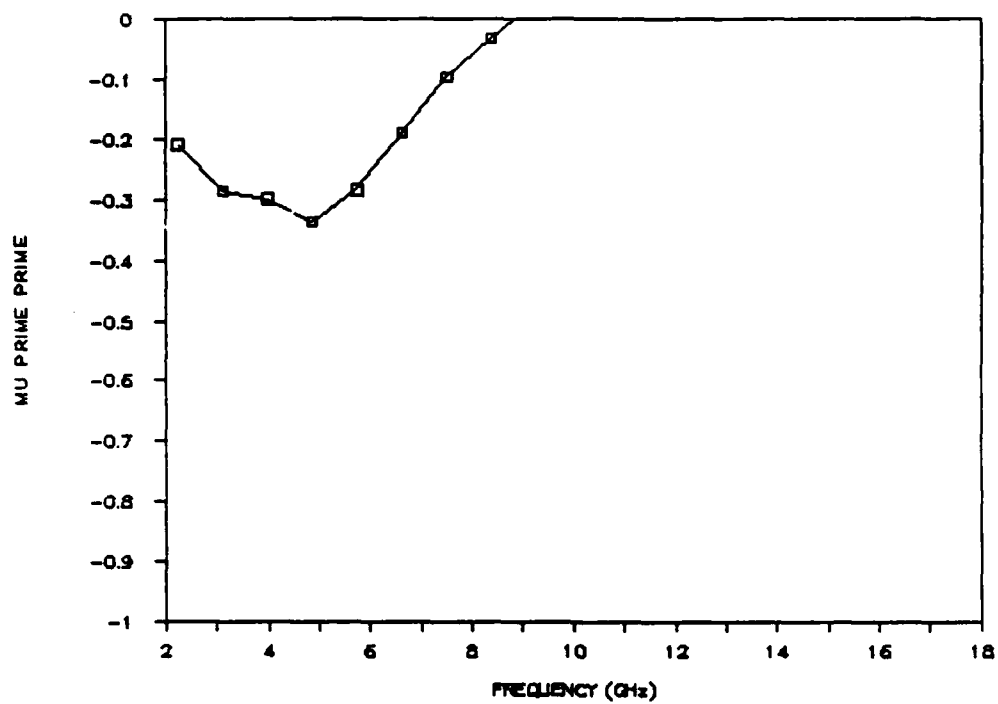


Figure 16b. The imaginary part of the permeability of a 18.9 volume % composite of Sample 14 (Titan Ferrites FCX-1538) in a Castolite binder.

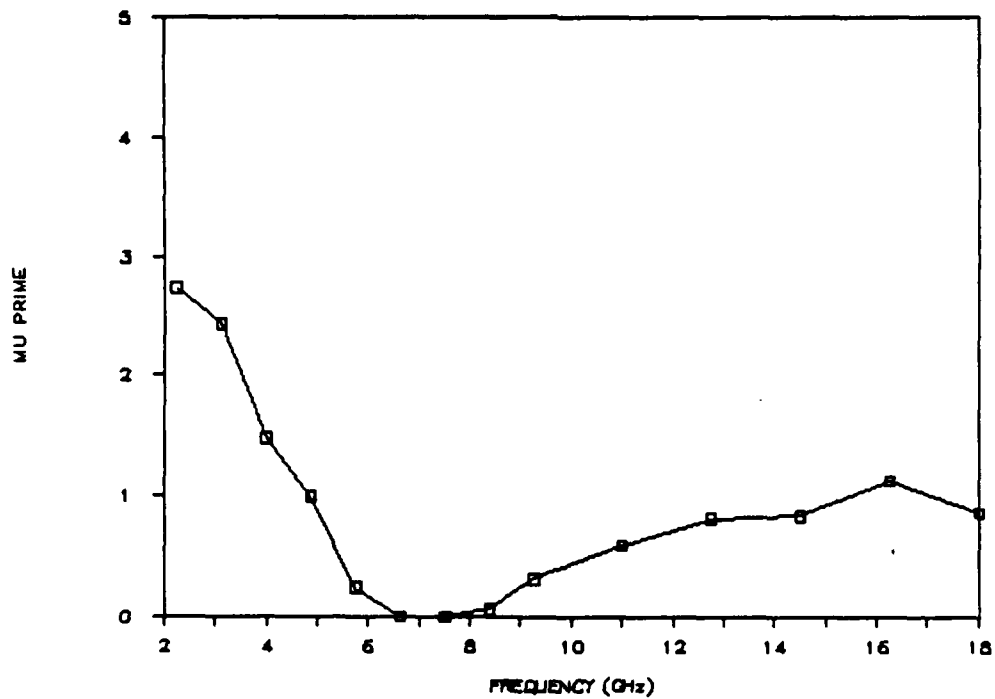


Figure 16c. The real part of the permeability of a particle of Sample 14 (Titan Ferrites FCX-1538).

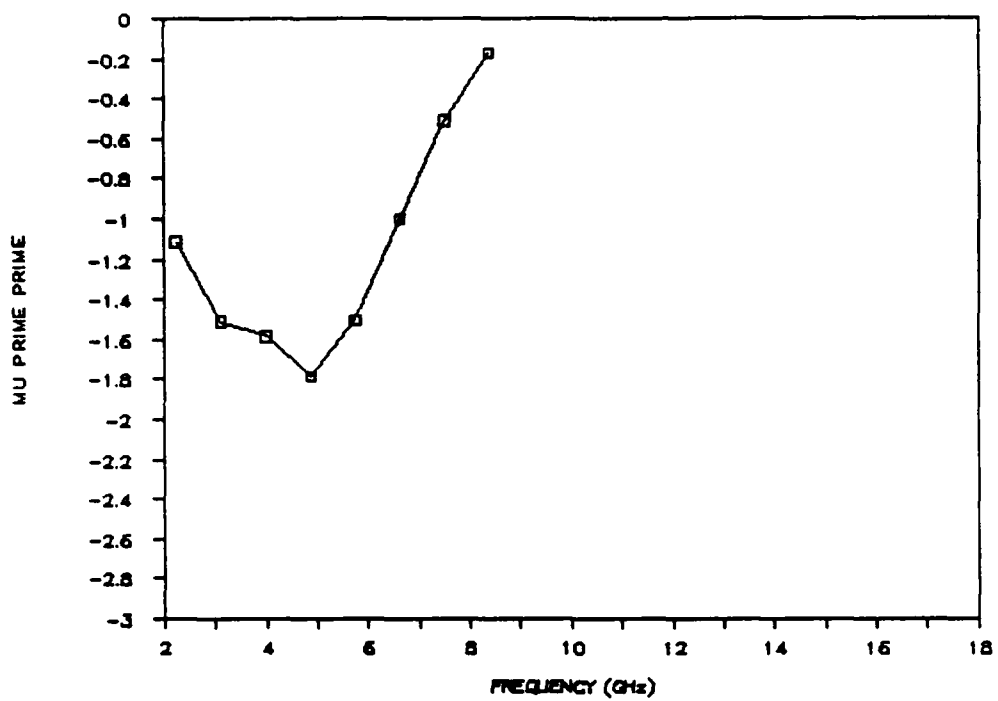


Figure 16d. The imaginary part of the permeability of a particle of Sample 14 (Titan Ferrites FCX-1538).

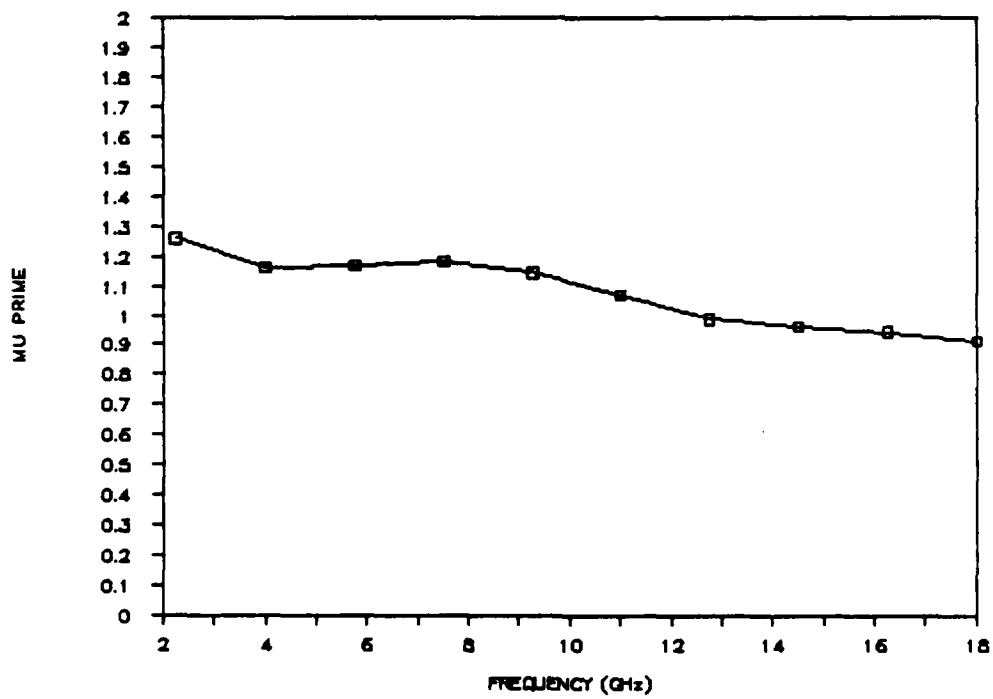


Figure 17a. The real part of the permeability of a 20.1 volume % composite of Sample 15 (Titan Ferrites FCX-1539) in a Castolite binder.

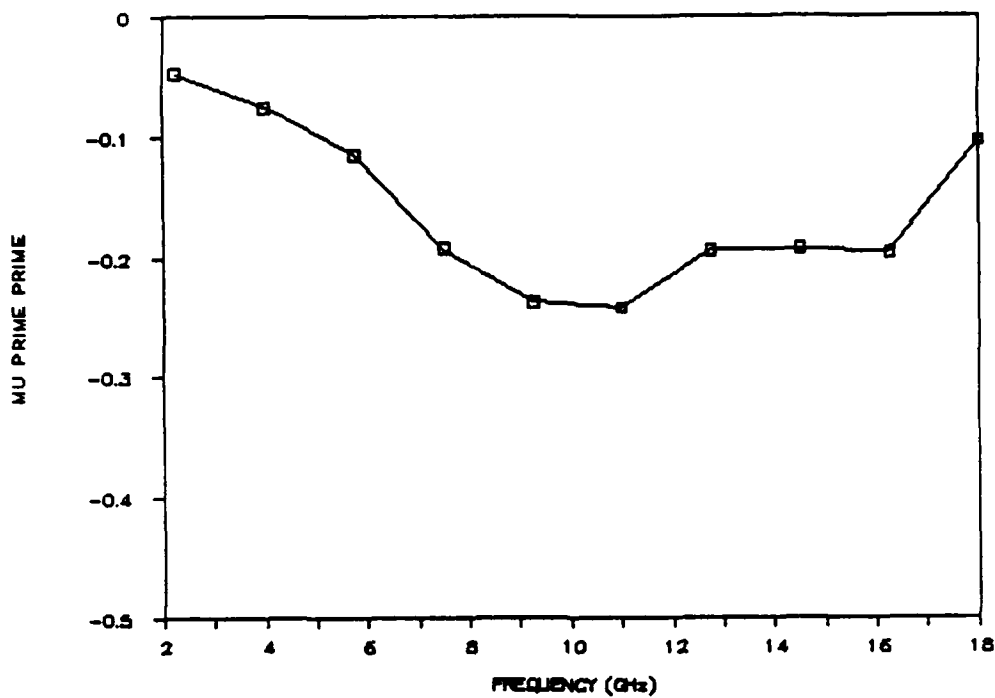


Figure 17b. The imaginary part of the permeability of a 20.1 volume % composite of Sample 15 (Titan Ferrites FCX-1539) in a Castolite binder.

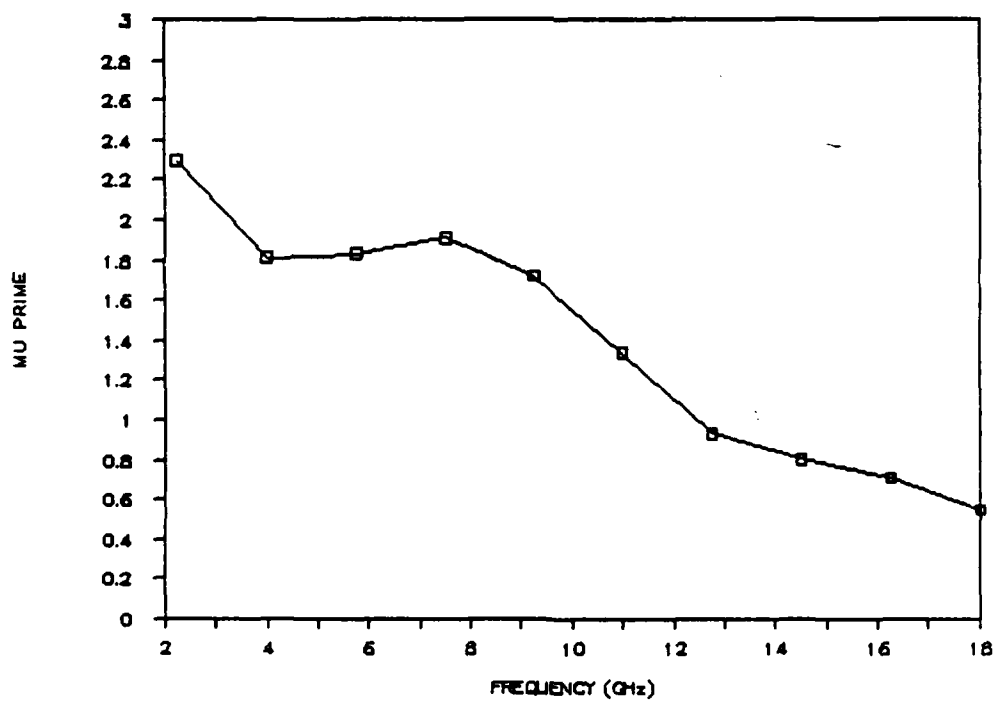


Figure 17c. The real part of the permeability of a particle of Sample 15 (Titan Ferrites FCX-1539).

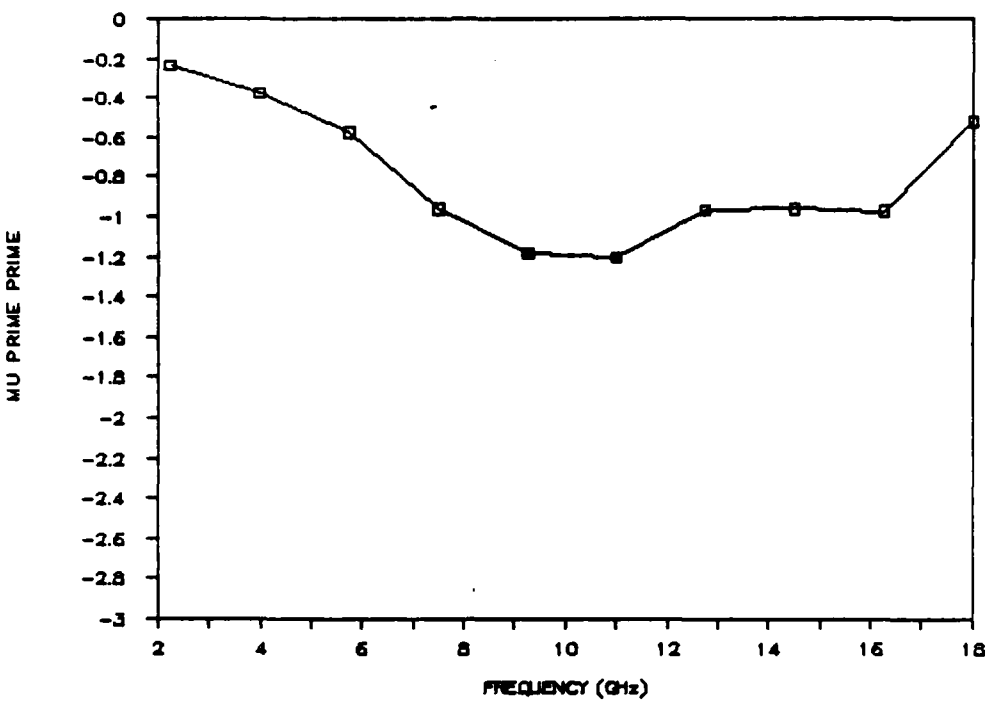


Figure 17d. The imaginary part of the permeability of a particle of Sample 15 (Titan Ferrites FCX-1539).

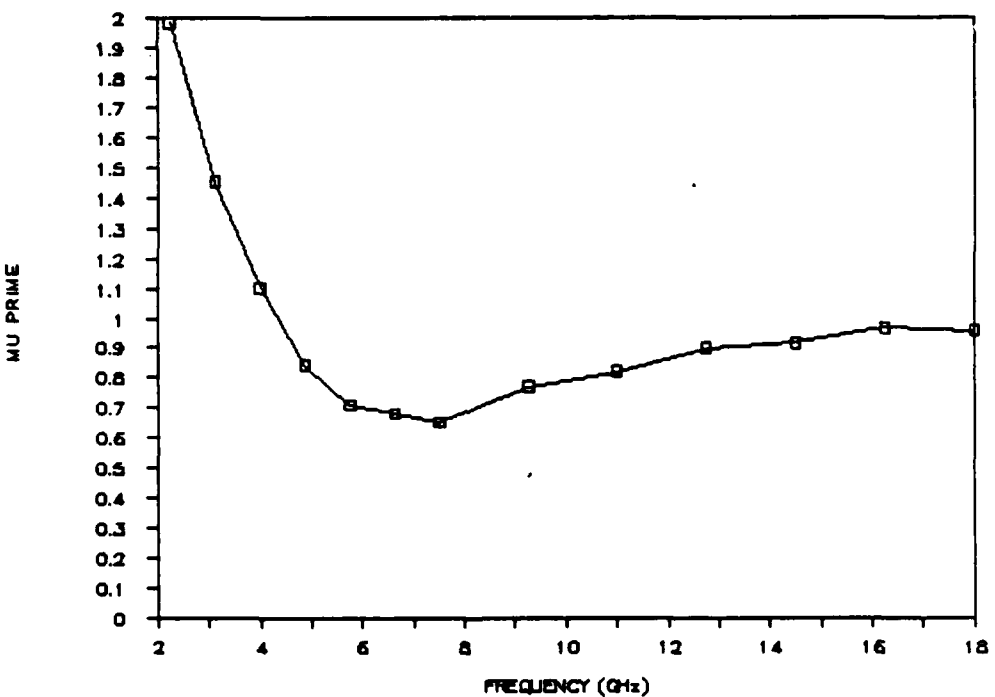


Figure 18a. The real part of the permeability of a 63 weight % composite of Sample 16 (Titan Ferrites FCX-1540) in a Castolite binder.

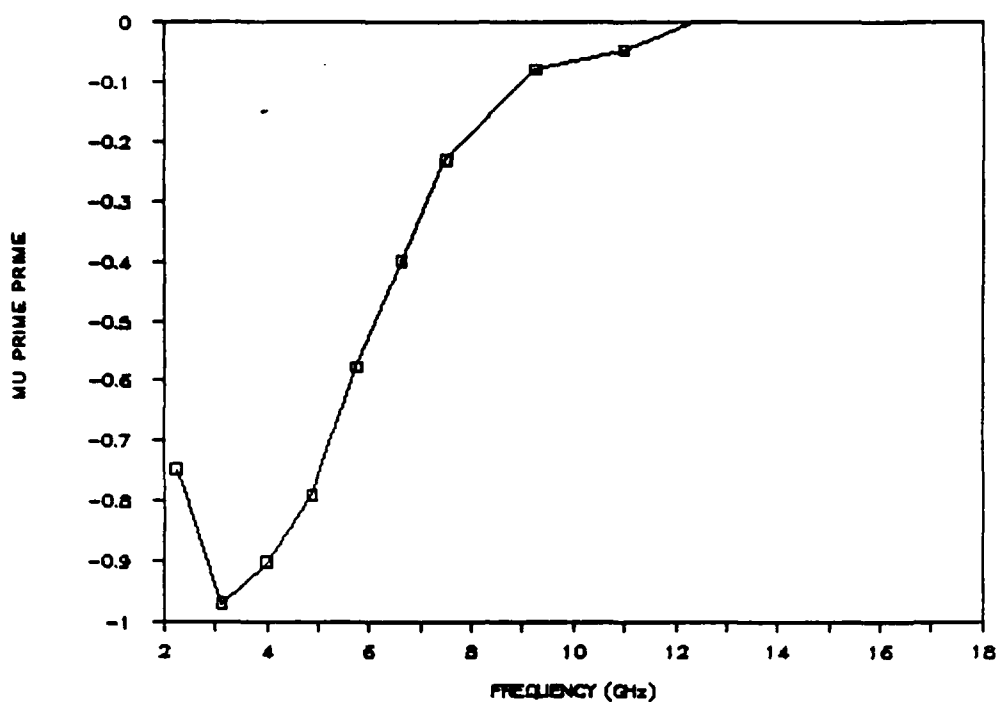


Figure 18b. The imaginary part of the permeability of a 63 weight % composite of Sample 16 (Titan Ferrites FCX-1540) in a Castolite binder.

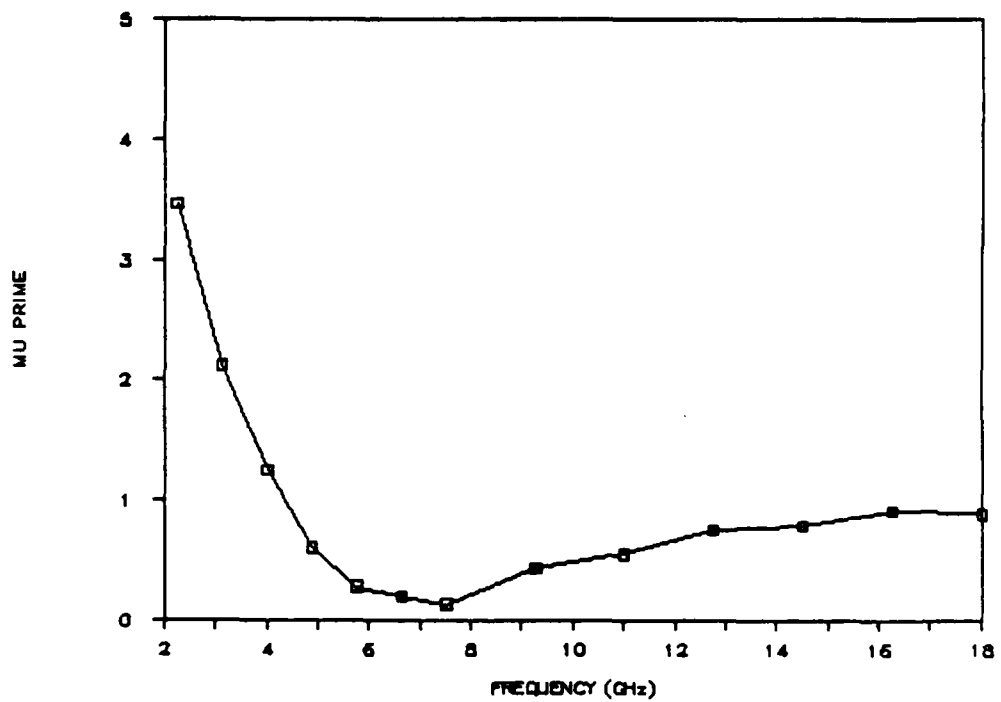


Figure 18c. The real part of the permeability of a particle of Sample 16 (Titan Ferrites FCX-1540).

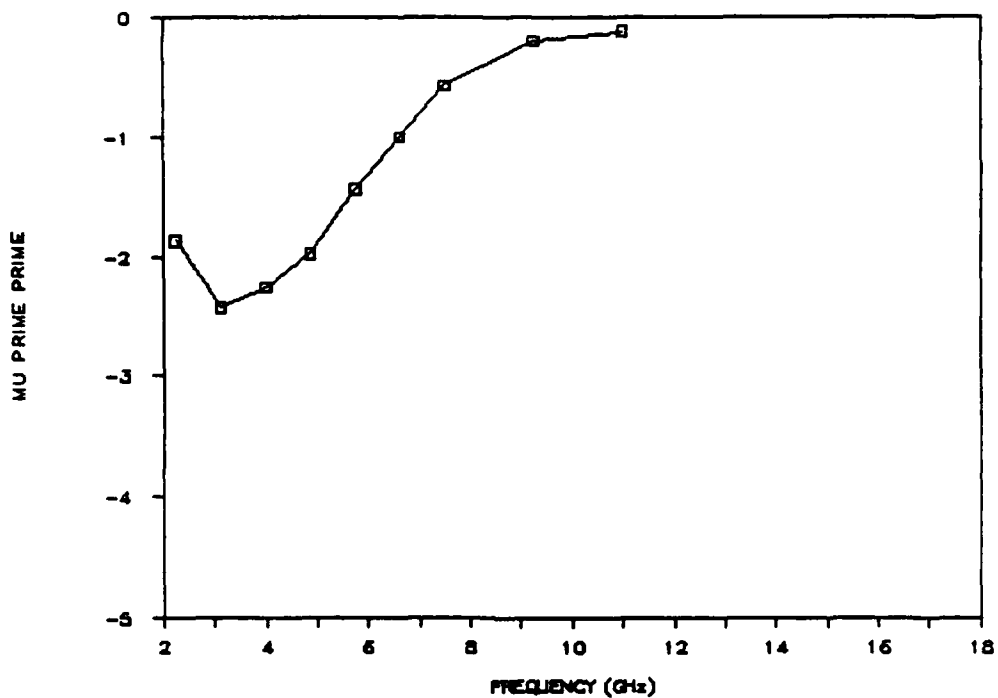


Figure 18d. The imaginary part of the permeability of a particle of Sample 16 (Titan Ferrites FCX-1540).

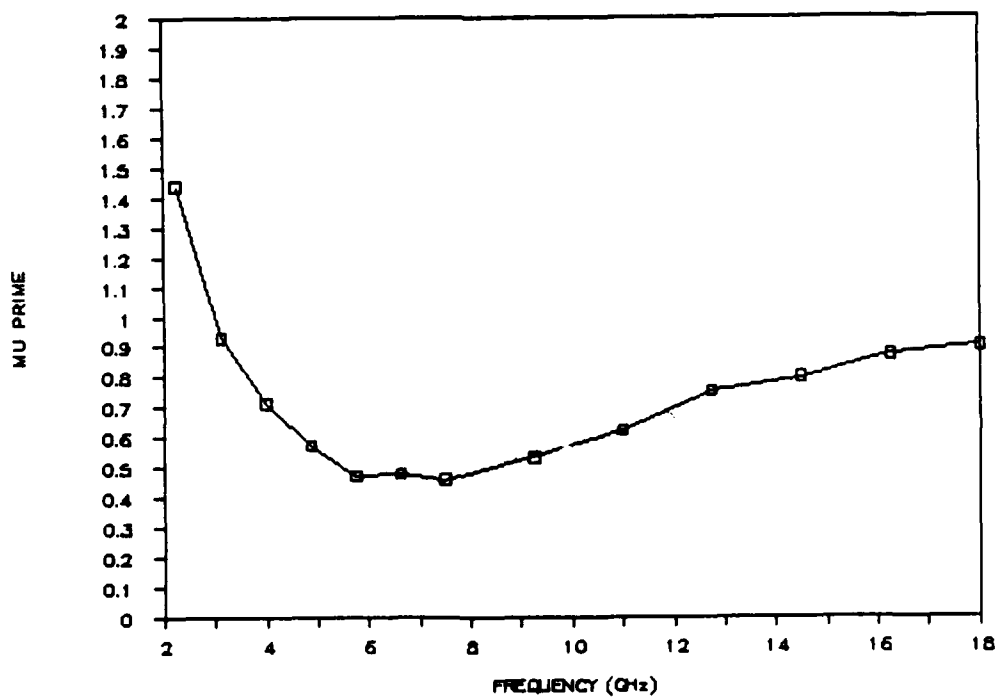


Figure 19a. The real part of the permeability of a 45 volume % composite of Sample 17 (Titan Ferrites FCX-1541) in a Castolite binder.

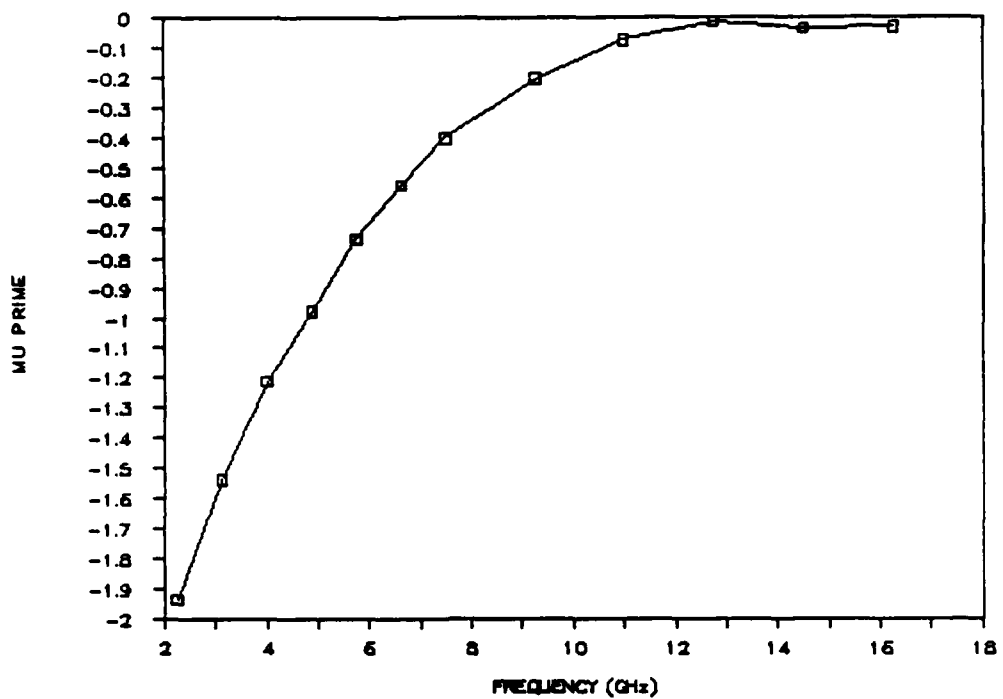


Figure 19b. The imaginary part of the permeability of a 45 volume % composite of Sample 17 (Titan Ferrites FCX-1541) in a Castolite binder.

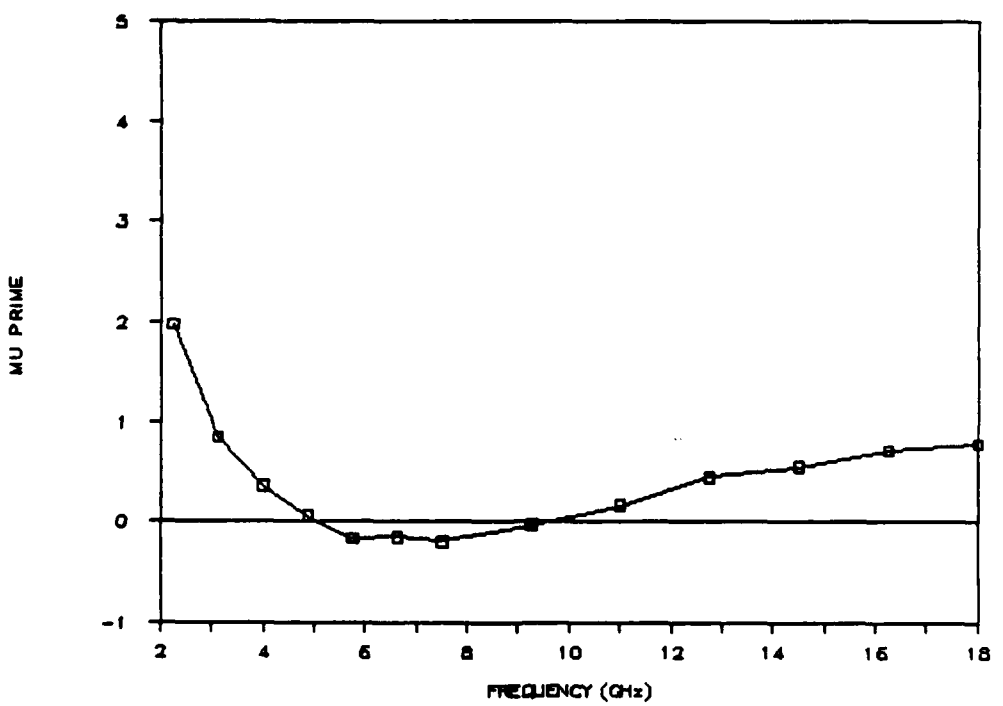


Figure 19c. The real part of the permeability of a particle of Sample 17 (Titan Ferrites FCX-1541).

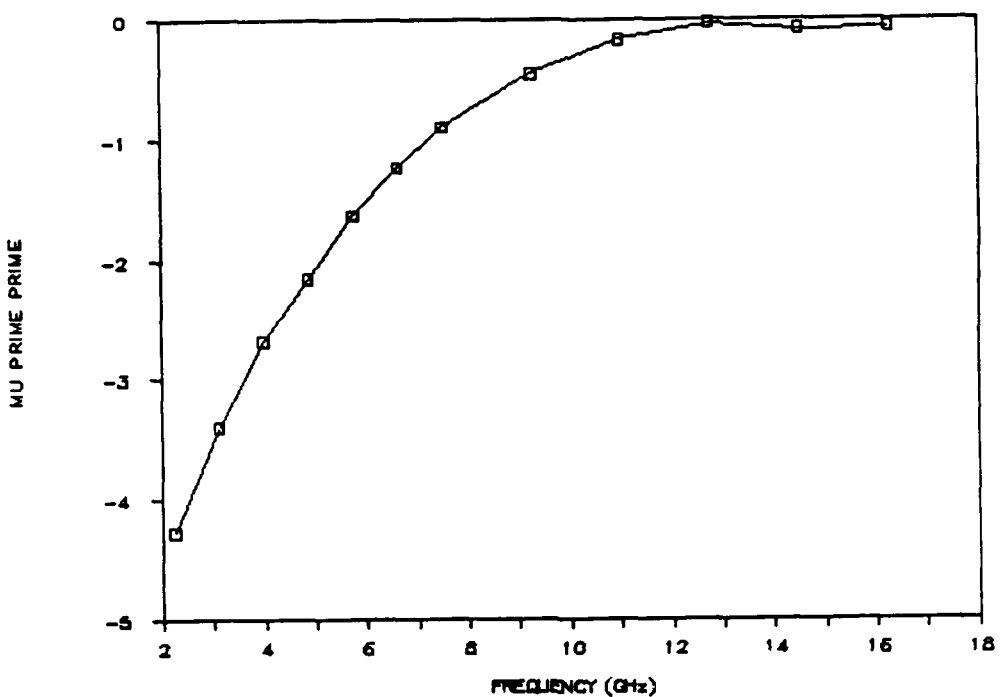


Figure 19d. The imaginary part of the permeability of a particle of Sample 19 (Titan Ferrites FCX-1541).

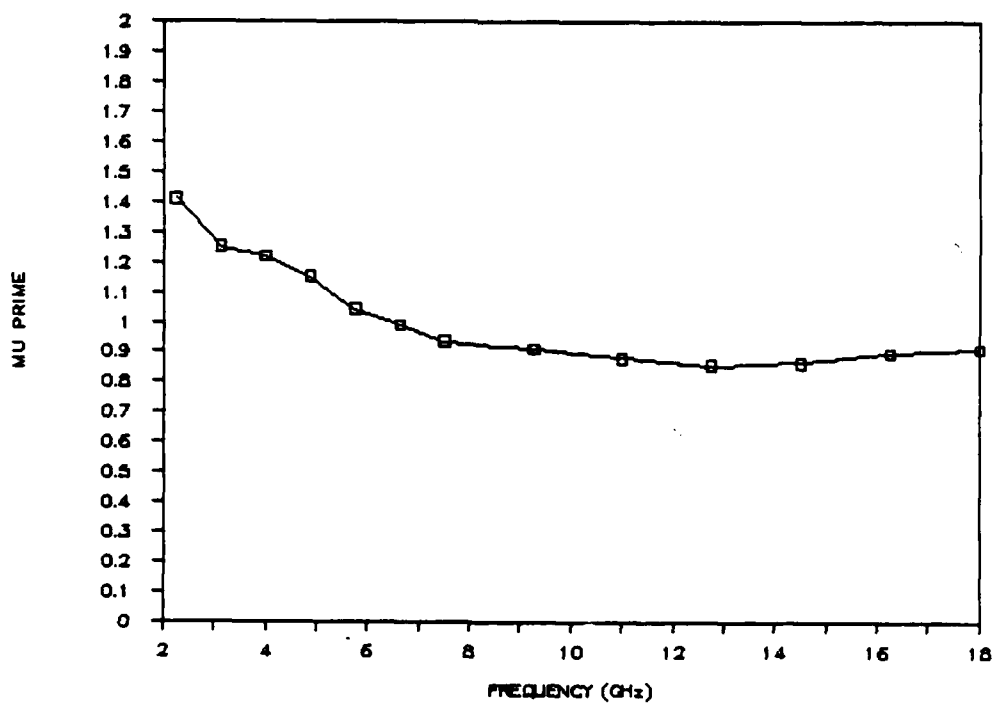


Figure 20a. The real part of the permeability of a 34 volume % composite of Sample 18 (Titan Ferrites FCX-1542) in a Castolite binder.

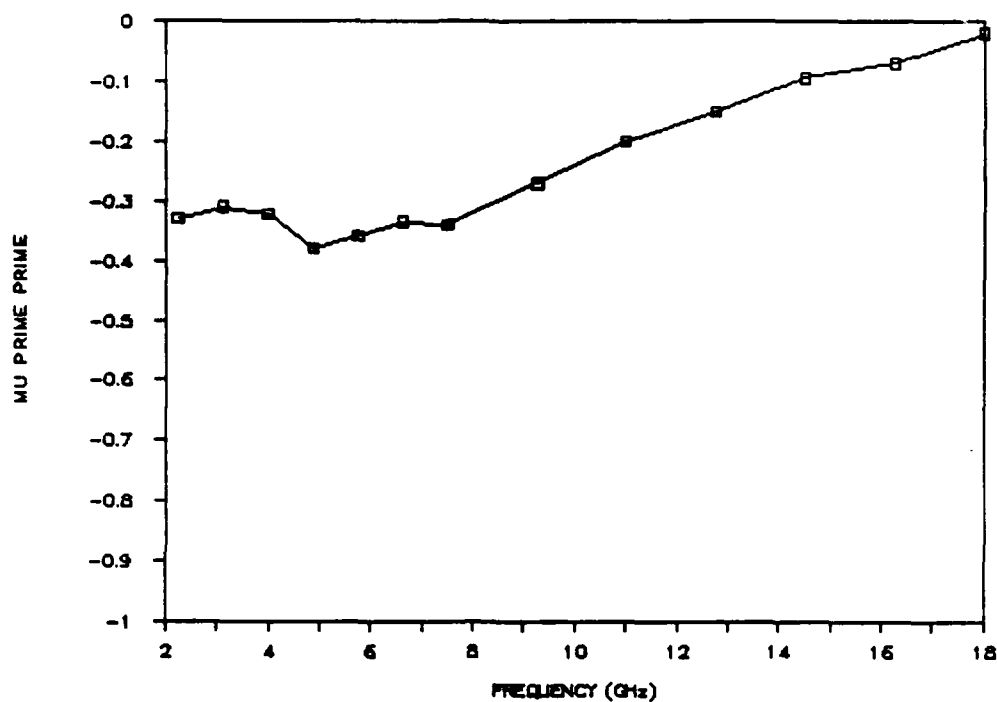


Figure 20b. The imaginary part of the permeability of a 34 volume % composite of Sample 18 (Titan Ferrites FCX-1542) in a Castolite binder.

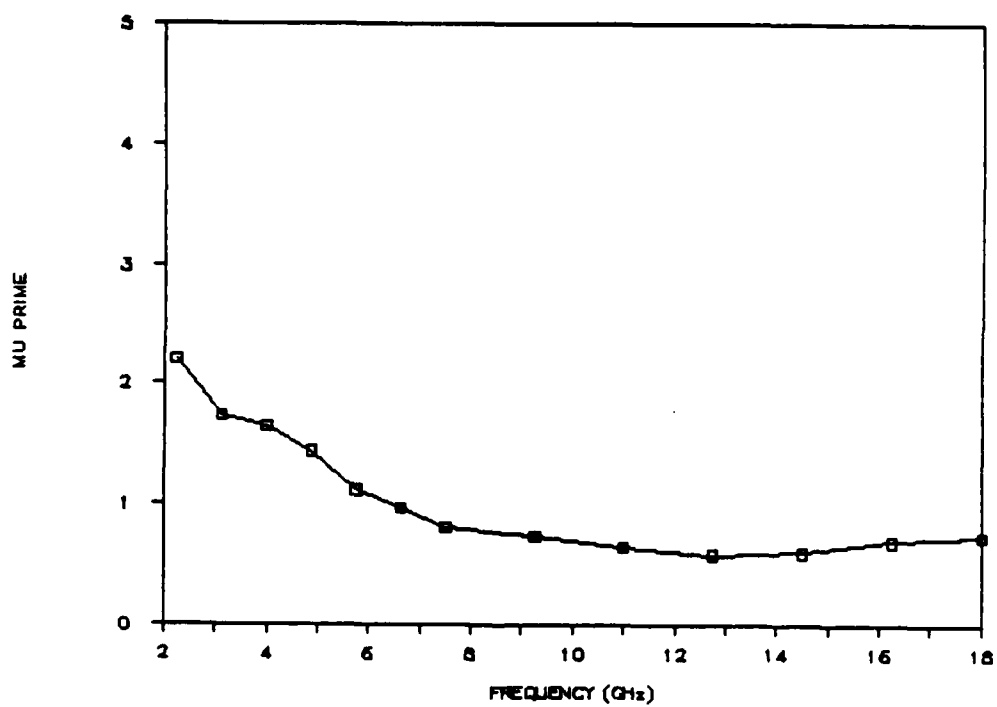


Figure 20c. The real part of the permeability of a particle of Sample 18 (Titan Ferrites FCX-1542).

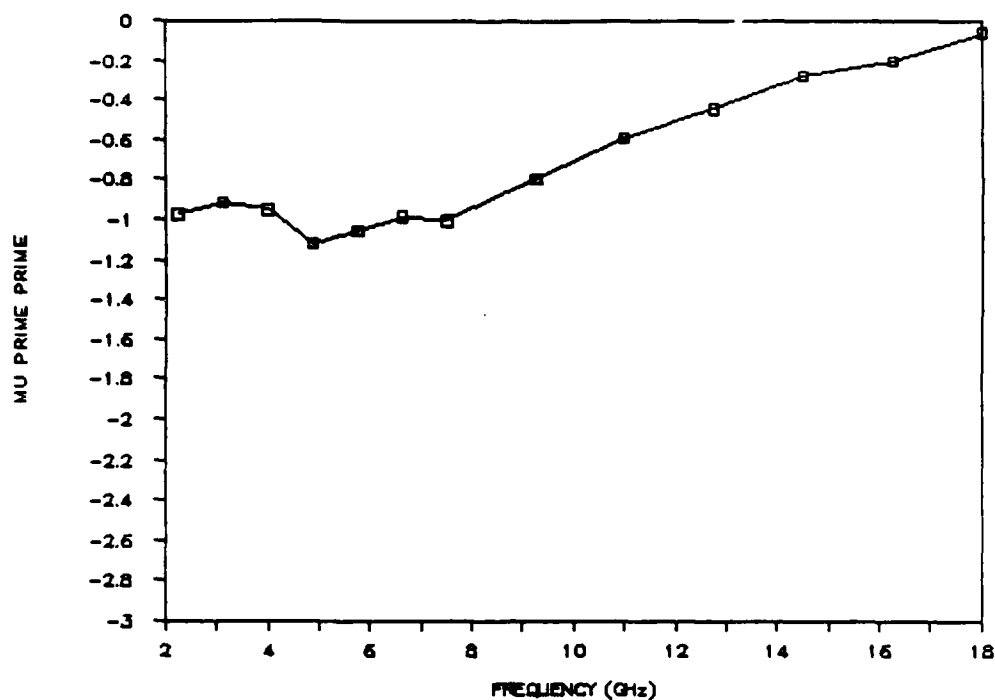


Figure 20d. The imaginary part of the permeability of a particle of Sample 18 (Titan Ferrites FCX-1542).

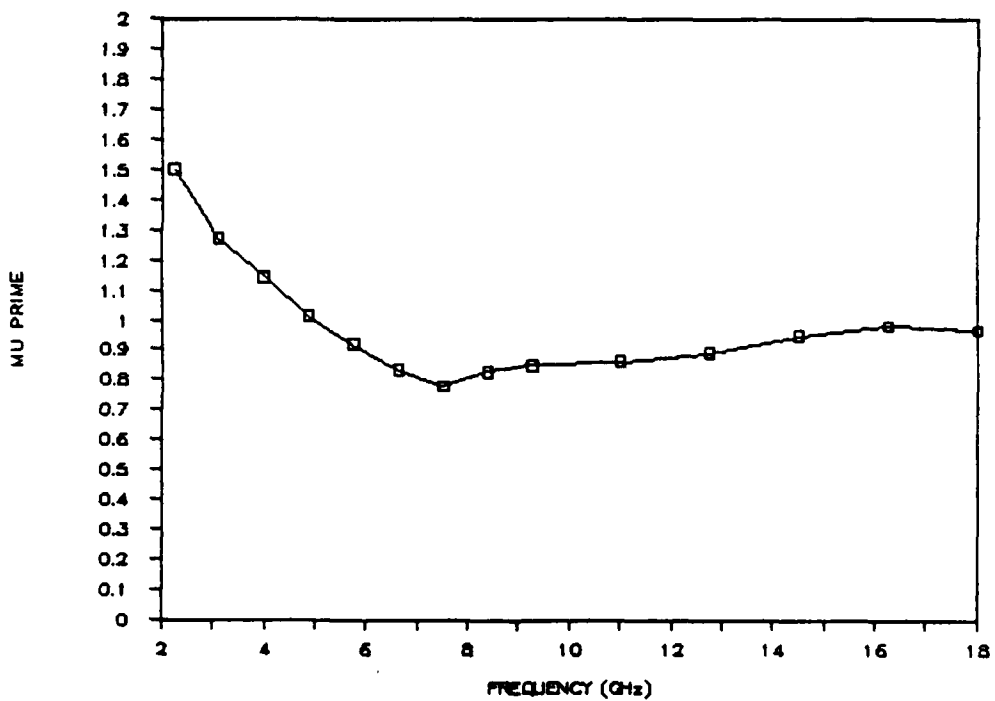


Figure 21a. The real part of the permeability of a 21.7 volume % composite of Sample 20 (Titan Ferrites FCX-1544) in a Castolite binder.

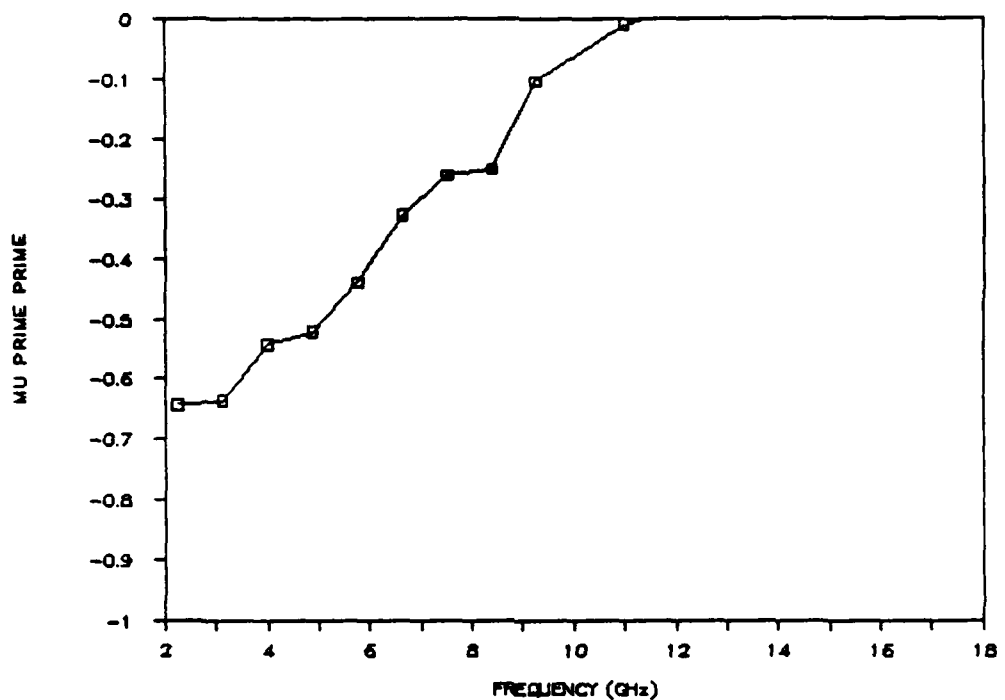


Figure 21b. The imaginary part of the permeability of a 21.7 volume % composite of Sample 20 (Titan Ferrites FCX-1544) in a Castolite binder.

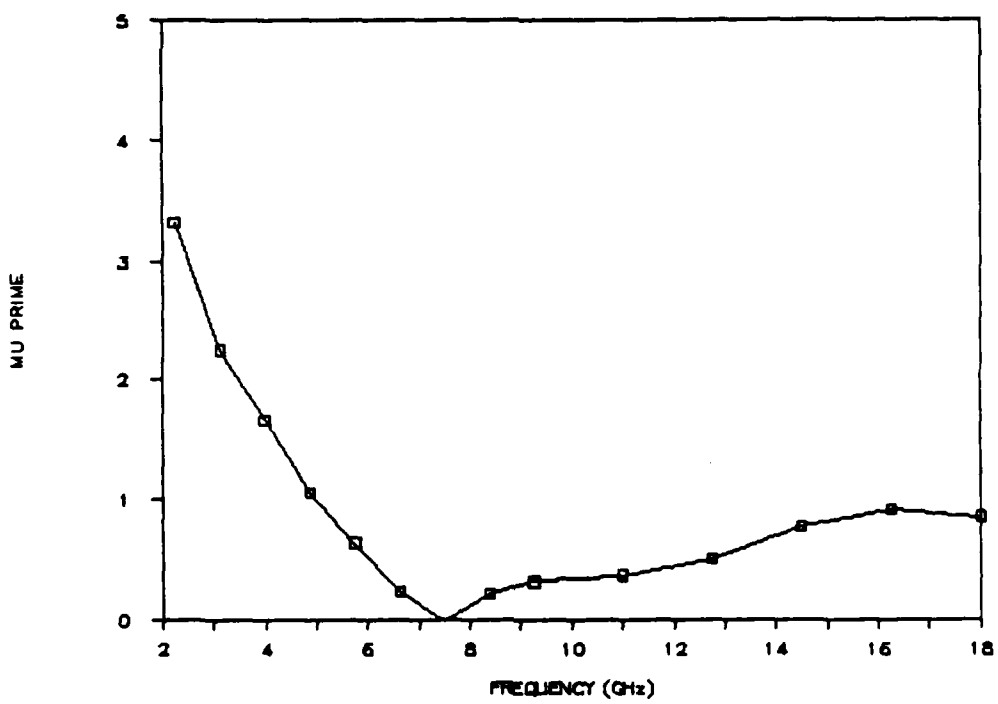


Figure 21c. The real part of the permeability of a particle of Sample 20 (Titan Ferrites FCX-1544).

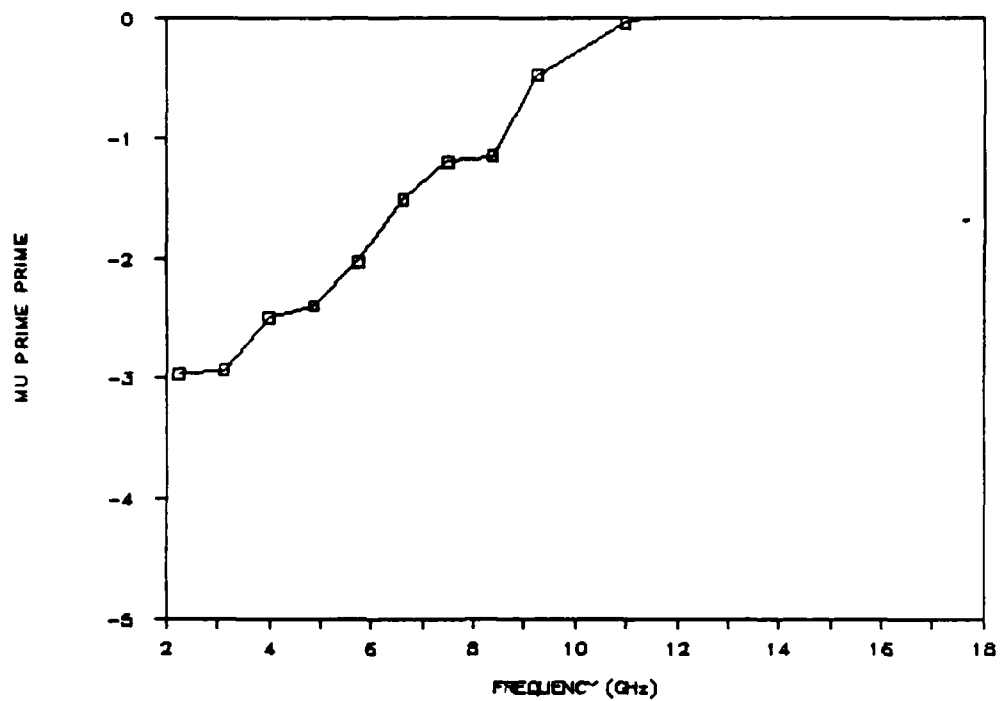


Figure 21d. The imaginary part of the permeability of a particle of Sample 20 (Titan Ferrites FCX-1544).

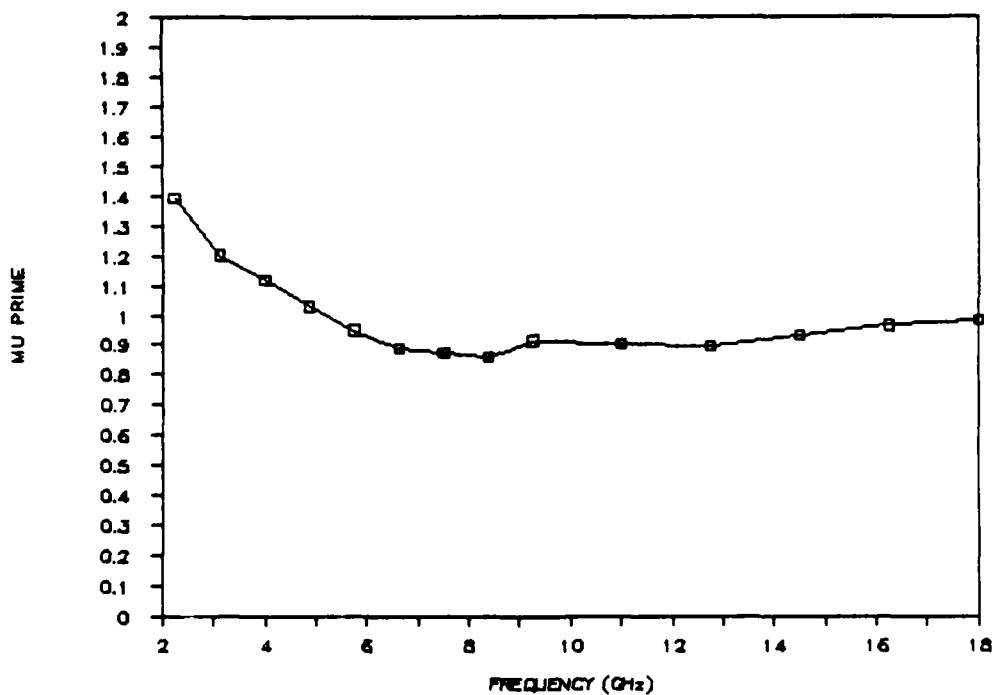


Figure 22a. The real part of the permeability of a 18.1 volume % composite of Sample 22 (Titan Ferrites FCX-1546) in a Castolite binder.

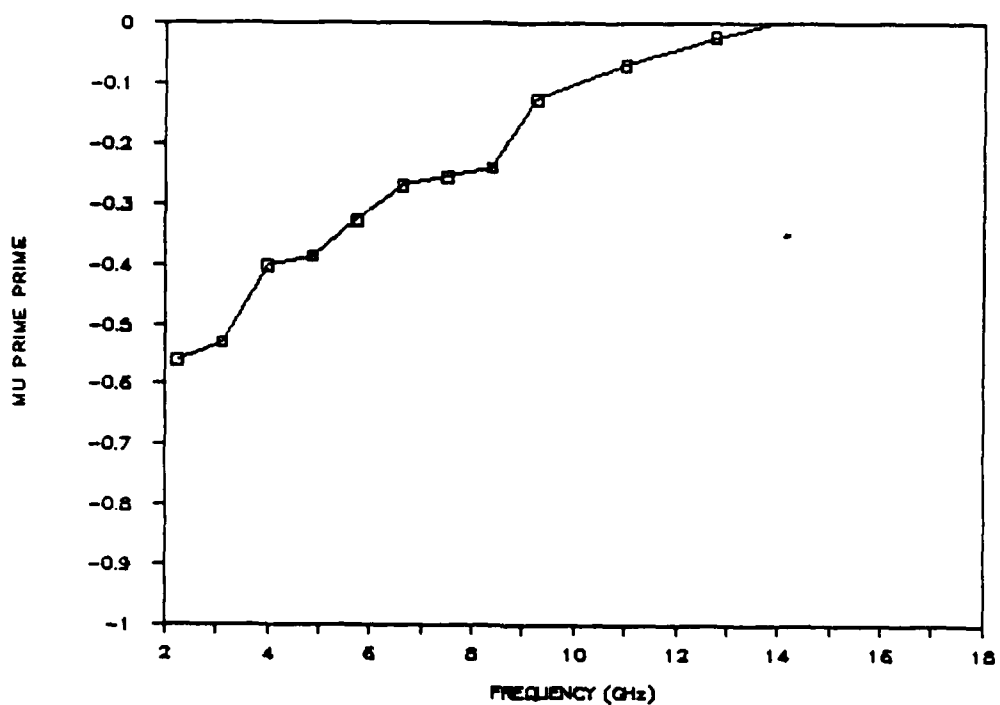


Figure 22b. The imaginary part of the permeability of a 18.1 volume % composite of Sample 22 (Titan Ferrites FCX-1546) in a Castolite binder.

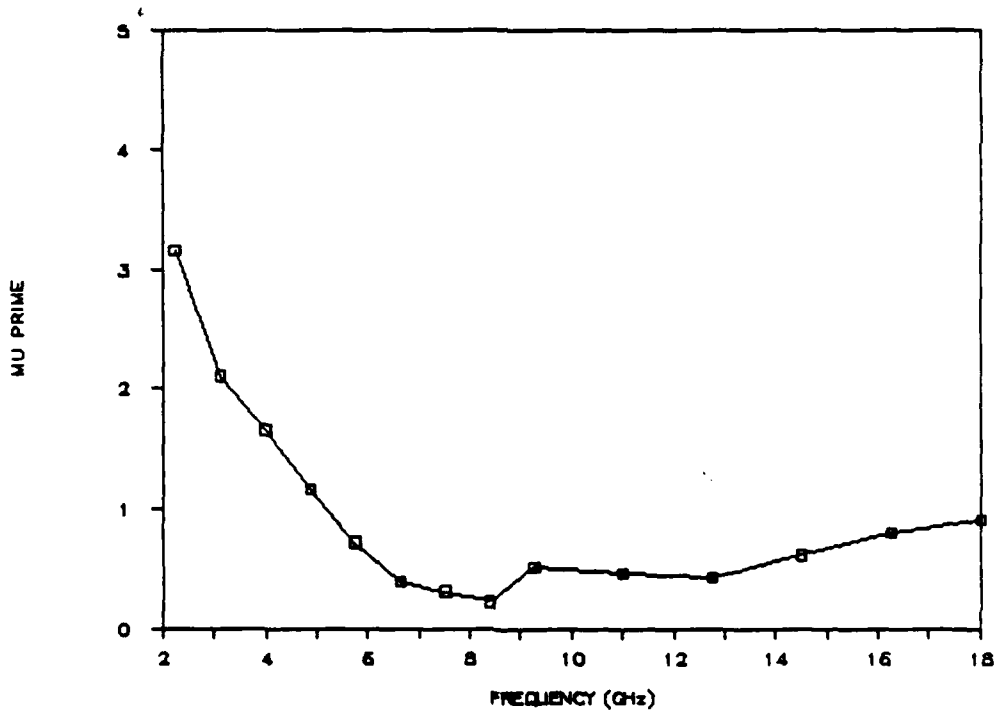


Figure 22c. The real part of the permeability of a particle of Sample 22 (Titan Ferrites FCX-1546).

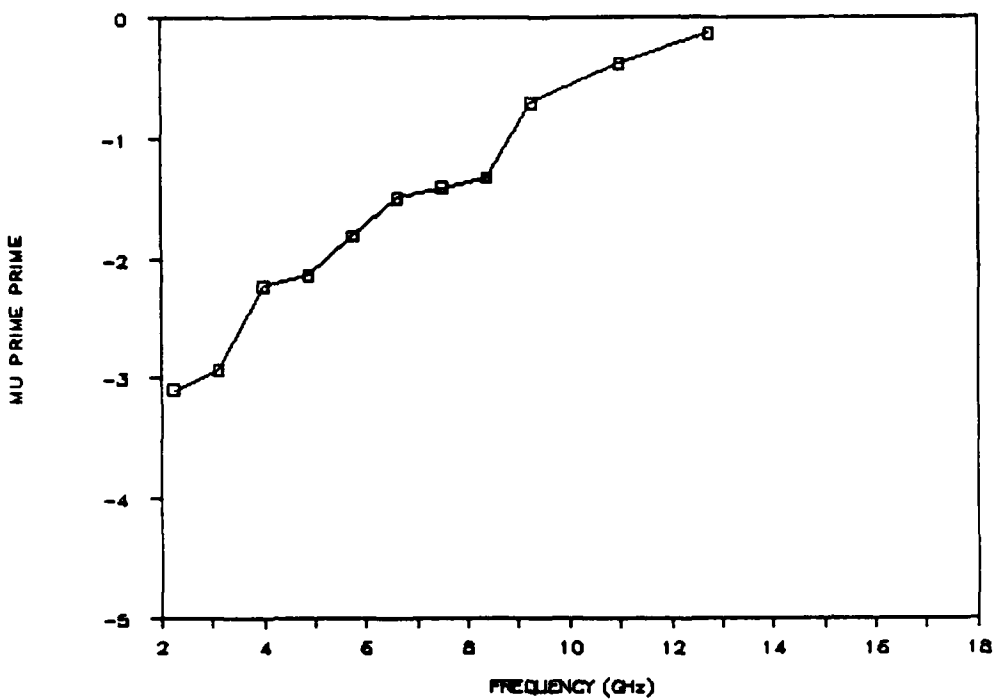


Figure 22d. The imaginary part of the permeability of a particle of Sample 22 (Titan Ferrites FCX-1546).

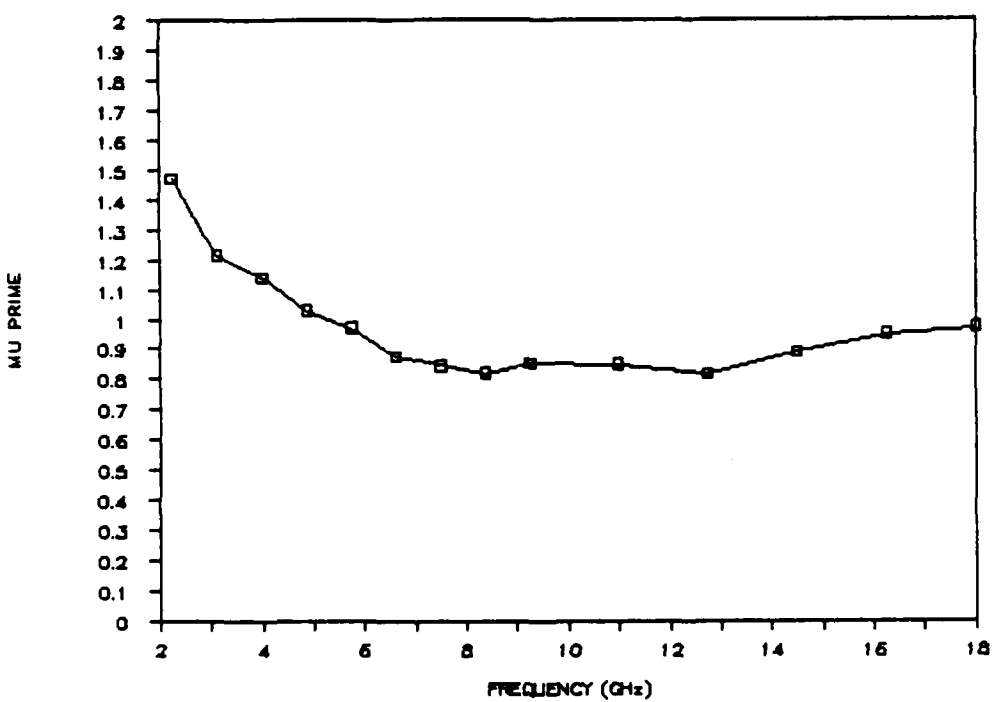


Figure 23a. The real part of the permeability of a 19.5 volume % composite of Sample 23 (Titan Ferrites FCX-1547) in a Castolite binder.

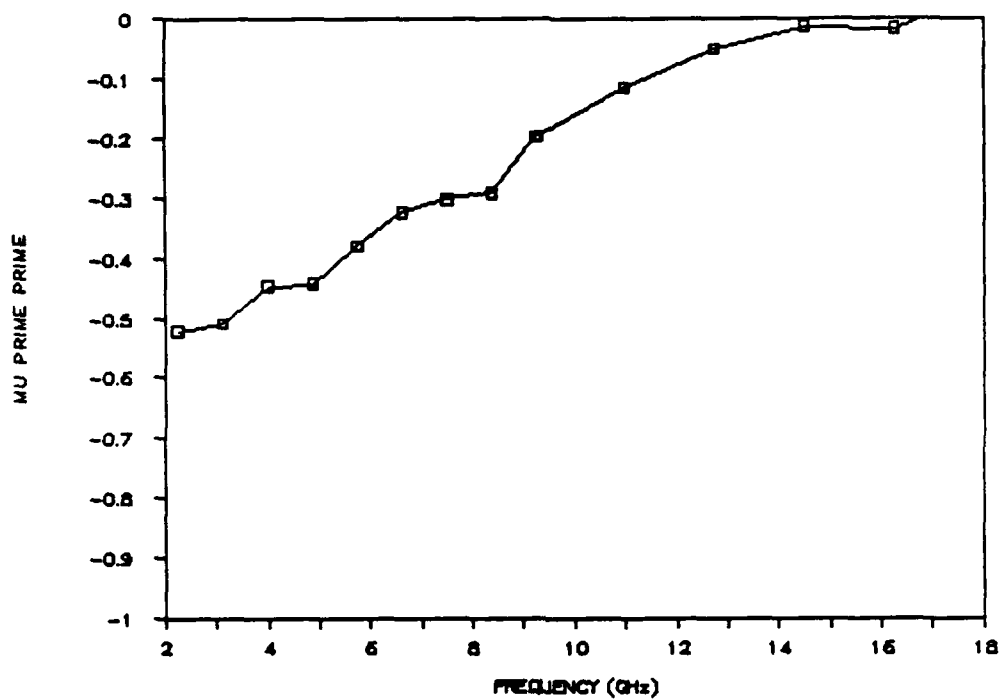


Figure 23b. The imaginary part of the permeability of a 19.5 volume % composite of Sample 23 (Titan Ferrites FCX-1547) in a Castolite binder.

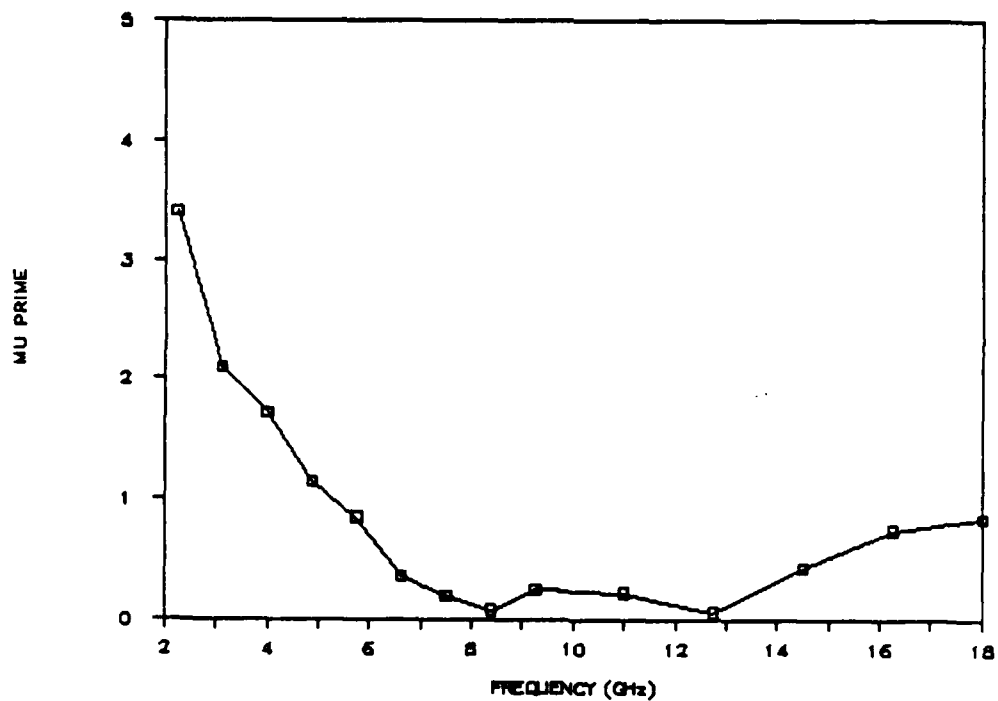


Figure 23c. The real part of the permeability of a particle of Sample 23 (Titan Ferrites FCX-1547).

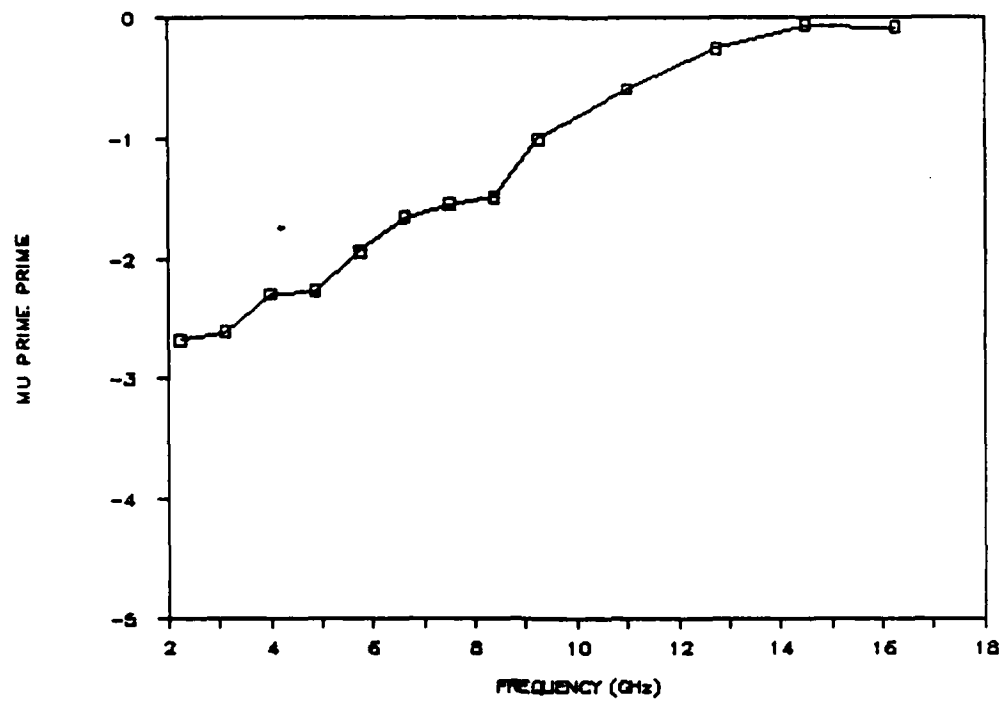


Figure 23d. The imaginary part of the permeability of a particle of Sample 23 (Titan Ferrites FCX-1547).

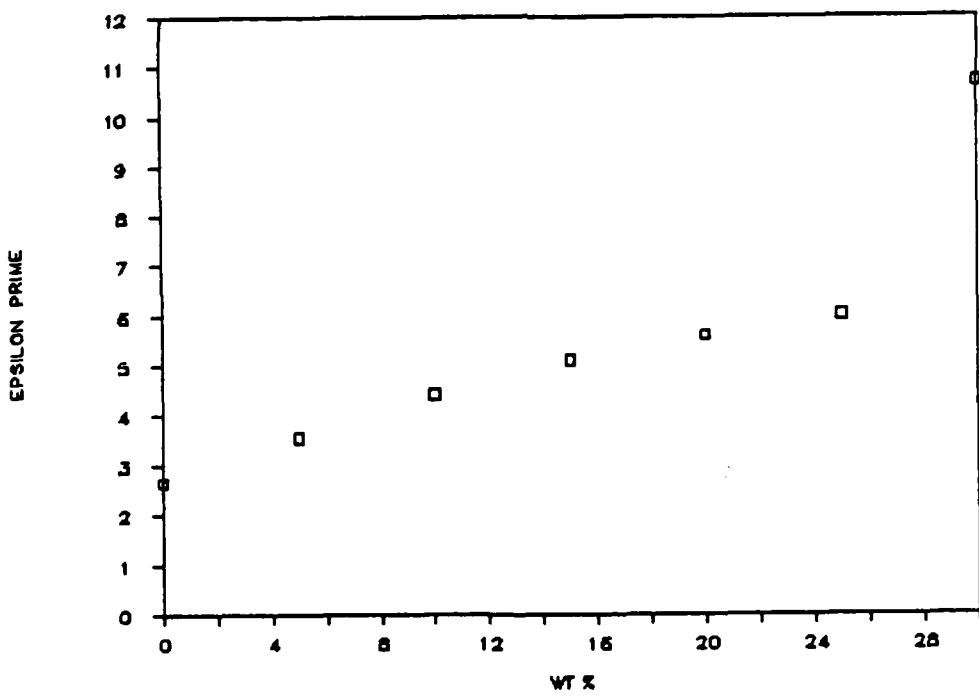


Figure 24a. Variation of the real part of the dielectric constant of a Castolite 50/50 ferronickel flake composite with particle concentration.

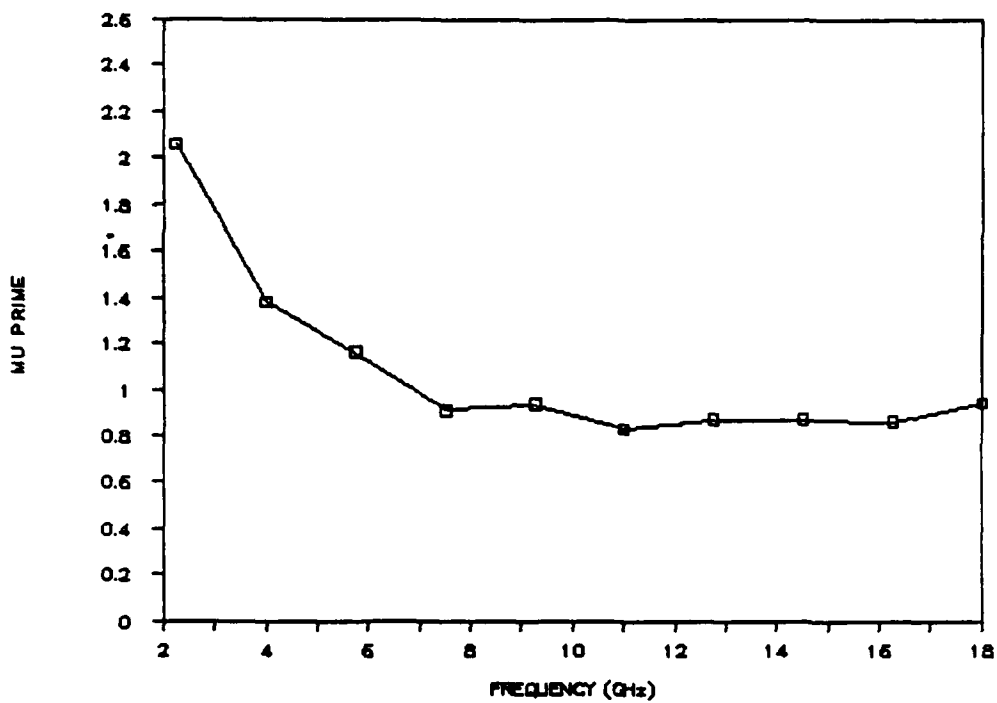


Figure 24b. The real part of the permeability of a composite of 25 weight % 50/50 ferronickel flake in Castolite.

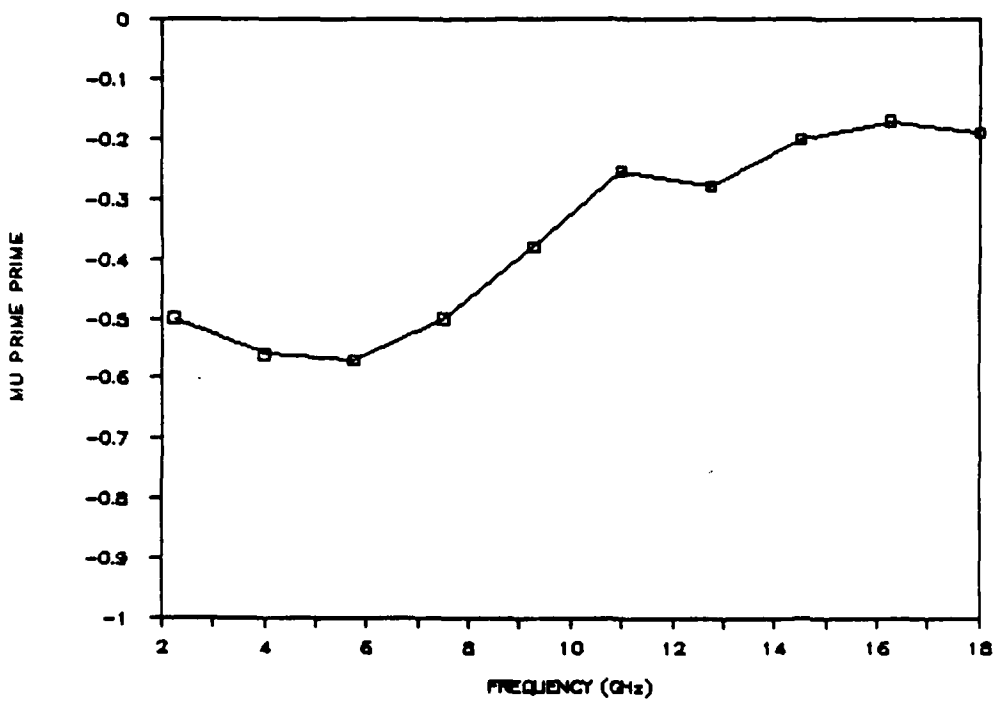


Figure 24c. The imaginary part of the permeability of a composite of 25 weight % 50/50 ferronickel flake in Castolite. Note that there is some magnetic loss from 2 to 18 GHz.

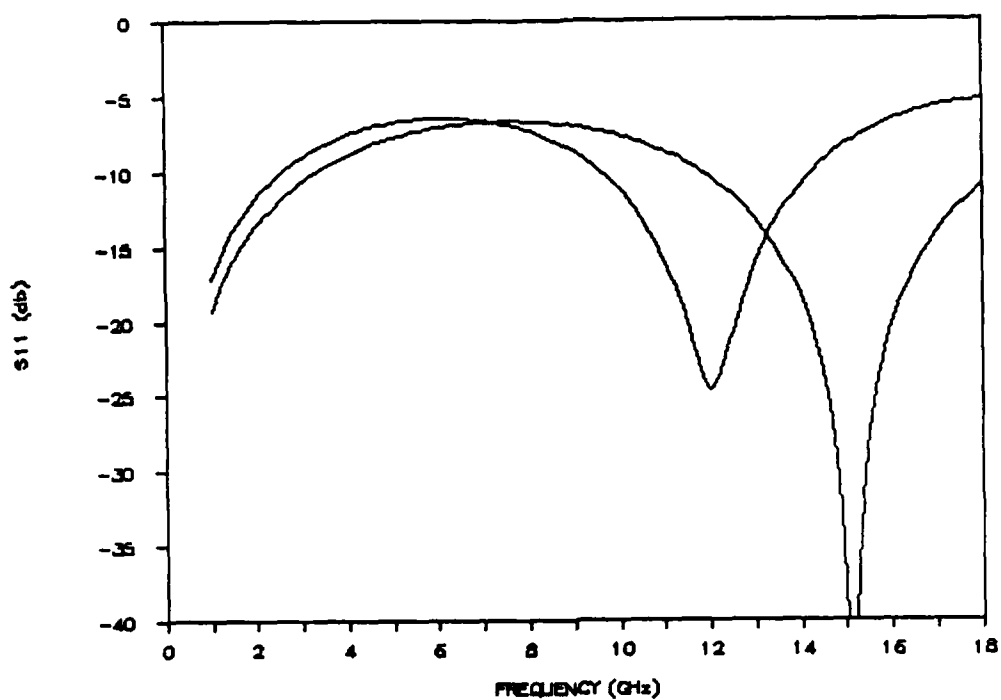


Figure 25. Calculated S<sub>11</sub> for a Castolite sample 0.236 inch long with a layer of green paint 0.036 inch thick of dielectric constant 4.2 on top.

APPENDIX 1 -- PERMEABILITY DATA FOR FERRITES

SAMPLE 10

F(GHz)	COMPOSITE		PARTICLE	
	MU'	MU''	MU'	MU''
2.25	1.83	-0.316	5.07	-1.55
4	1.661	-0.354	4.24	-1.74
5.75	1.544	-0.408	3.67	-2.001
7.5	1.507	-0.423	3.49	-2.07
9.25	1.443	-0.41	3.17	-2.01
11	1.38	-0.431	2.86	-2.11
12.75	1.305	-0.403	2.5	-1.98
14.5	1.237	-0.431	2.16	2.11
16.25	1.177	-0.413	1.87	-2.02
18	1.16	-0.36	1.78	-1.76

SAMPLE 13

F(GHz)	COMPOSITE		PARTICLE	
	MU'	MU''	MU'	MU''
2.25	1.12	-0.166	2.224489	-1.69387
4	1.08	-0.124	1.816326	-1.26530
5.75	1.01	-0.083	1.102040	-0.84693
7.5	0.973	-0.042	0.724489	-0.42857
9.25	0.96	0.014	0.591836	
11	1	0.003		1
12.75	1	0.017		1
14.5	1	0.033		1
16.25	1.014	0.0375		
18	1.09	0.148		

## SAMPLE 14

F(GHz)	COMPOSITE		PARTICLE	
	MU'	MU''	MU'	MU''
2.2500	1.3270	-0.2103	2.7302	-1.1127
3.1250	1.2700	-0.2860	2.4286	-1.5132
4.0000	1.0900	-0.2996	1.4762	-1.5852
4.8750	0.9980	-0.3370	0.9894	-1.7831
5.7500	0.8560	-0.2840	0.2381	-1.5026
6.6250	0.8040	-0.1890	0.0000	-1.0000
7.5000	0.7880	-0.0964	0.0000	-0.5101
8.3750	0.8230	-0.0320	0.0635	-0.1693
9.2500	0.8710	0.0249	0.3175	
11.0000	0.9227		0.5910	
12.7500	0.9650		0.8148	
14.5000	0.9690		0.8360	
16.2500	1.0240		1.1270	
18.0000	0.9730		0.8571	

## SAMPLE 15

F(GHz)	COMPOSITE		PARTICLE	
	MU'	MU''	MU'	MU''
2.2500	1.2600	-0.0476	2.2935	-0.2368
4.0000	1.1630	-0.0758	1.8109	-0.3771
5.7500	1.1670	-0.1150	1.8308	-0.5721
7.5000	1.1830	-0.1930	1.9104	-0.9602
9.2500	1.1446	-0.2372	1.7194	-1.1801
11.0000	1.0680	-0.2414	1.3383	-1.2010
12.7500	0.9860	-0.1940	0.9303	-0.9652
14.5000	0.9600	-0.1930	0.8010	-0.9602
16.2500	0.9412	-0.1960	0.7075	-0.9751
18.0000	0.9088	-0.1040	0.5463	-0.5174

## SAMPLE 16

F(GHz)	COMPOSITE		PARTICLE	
	MU'	MU''	MU'	MU''
2.2500	1.9840	-0.7481	3.4600	-1.8703
3.1250	1.4500	-0.9700	2.1250	-2.4250
4.0000	1.1020	-0.9022	1.2550	-2.2555
4.8750	0.8400	-0.7900	0.6000	-1.9750
5.7500	0.7100	-0.5767	0.2750	-1.4418
6.6250	0.6800	-0.4000	0.2000	-1.0000
7.5000	0.6510	-0.2300	0.1275	-0.5750
9.2500	0.7710	-0.0790	0.4275	-0.1975
11.0000	0.8200	-0.0462	0.5500	-0.1155
12.7500	0.8990	0.0126	0.7475	
14.5000	0.9160	0.0190	0.7900	
16.2500	0.9650	0.0132	0.9125	
18.0000	0.9562	0.0660	0.8905	

## SAMPLE 17

F(GHz)	COMPOSITE		PARTICLE	
	MU'	MU''	MU'	MU''
2.2500	1.4370	-1.9350	1.9847	-4.2715
3.1250	0.9300	-1.5400	0.8455	-3.3996
4.0000	0.7123	-1.2120	0.3649	-2.6755
4.8750	0.5740	-0.9800	0.0596	-2.1634
5.7500	0.4730	-0.7385	-0.1634	-1.6302
6.6250	0.4800	-0.5600	-0.1479	-1.2362
7.5000	0.4600	-0.4040	-0.1921	-0.8918
9.2500	0.5350	-0.2040	-0.0265	-0.4503
11.0000	0.6235	-0.0737	0.1689	-0.1627
12.7500	0.7535	-0.0123	0.4558	-0.0272
14.5000	0.7979	-0.0361	0.5539	-0.0797
16.2500	0.8721	-0.0300	0.7177	-0.0662
18.0000	0.9010	0.0077	0.7815	0.0170

## SAMPLE 18

F(GHz)	COMPOSITE		PARTICLE	
	MU'	MU''	MU'	MU''
2.2500	1.4100	-0.3300	2.2059	-0.9706
3.1250	1.2500	-0.3100	1.7353	-0.9118
4.0000	1.2200	-0.3230	1.6471	-0.9500
4.8750	1.1500	-0.3800	1.4412	-1.1176
5.7500	1.0410	-0.3580	1.1206	-1.0529
6.6250	0.9900	-0.3350	0.9706	-0.9853
7.5000	0.9350	-0.3412	0.8088	-1.0035
9.2500	0.9090	-0.2700	0.7324	-0.7941
11.0000	0.8790	-0.2000	0.6441	-0.5882
12.7500	0.8560	-0.1510	0.5765	-0.4441
14.5000	0.8650	-0.0940	0.6029	-0.2765
16.2500	0.8960	-0.0690	0.6941	-0.2029
18.0000	0.9100	-0.0200	0.7353	-0.0588

## SAMPLE 20

F(GHz)	COMPOSITE		PARTICLE	
	MU'	MU''	MU'	MU''
2.2500	1.5020	-0.6430	3.3134	-2.9631
3.1250	1.2710	-0.6370	2.2488	-2.9355
4.0000	1.1453	-0.5420	1.6696	-2.4977
4.8750	1.0130	-0.5220	1.0599	-2.4055
5.7500	0.9200	-0.4410	0.6313	-2.0323
6.6250	0.8340	-0.3280	0.2350	-1.5115
7.5000	0.7806	-0.2616	-0.0111	-1.2055
8.3750	0.8300	-0.2510	0.2166	-1.1567
9.2500	0.8510	-0.1040	0.3134	-0.4793
11.0000	0.8620	-0.0085	0.3641	-0.0392
12.7500	0.8920	0.0300	0.5023	0.1382
14.5000	0.9500	0.0510	0.7696	0.2350
16.2500	0.9810	0.0186	0.9124	0.0857
18.0000	0.9670	0.0920	0.8479	0.4240

## SAMPLE 22

F(GHz)	COMPOSITE		PARTICLE	
	MU'	MU''	MU'	MU''
2.2500	1.3900	-0.5600	3.1547	-3.0939
3.1250	1.2000	-0.5300	2.1050	-2.9282
4.0000	1.1180	-0.4030	1.6519	-2.2265
4.8750	1.0300	-0.3870	1.1657	-2.1381
5.7500	0.9500	-0.3270	0.7238	-1.8066
6.6250	0.8900	-0.2700	0.3923	-1.4917
7.5000	0.8754	-0.2550	0.3116	-1.4088
8.3750	0.8600	-0.2400	0.2265	-1.3260
9.2500	0.9135	-0.1270	0.5221	-0.7017
11.0000	0.9030	-0.0690	0.4641	-0.3812
12.7500	0.8970	-0.0232	0.4309	-0.1282
14.5000	0.9310	0.0135	0.6188	0.0746
16.2500	0.9655	0.0011	0.8094	0.0061

## SAMPLE 23

F(GHz)	COMPOSITE		PARTICLE	
	MU'	MU''	MU'	MU''
2.2500	1.4690	-0.5220	3.4051	-2.6769
3.1250	1.2140	-0.5090	2.0974	-2.6103
4.0000	1.1400	-0.4470	1.7179	-2.2923
4.8750	1.0280	-0.4430	1.1438	-2.2718
5.7500	0.9700	-0.3790	0.8462	-1.9436
6.6250	0.8750	-0.3240	0.3590	-1.6615
7.5000	0.8440	-0.3020	0.2000	-1.5487
8.3750	0.8200	-0.2910	0.0769	-1.4923
9.2500	0.8535	-0.1970	0.2487	-1.0103
11.0000	0.8480	-0.1150	0.2205	-0.5897
12.7500	0.8160	-0.0500	0.0564	-0.2564
14.5000	0.8890	-0.0130	0.4308	-0.0667
16.2500	0.9490	-0.0160	0.7385	-0.0821
18.0000	0.9690	0.0370	0.8410	

DISTRIBUTION LIST

---

No. of Copies	To
	Office of the Director of Research, Assistant Secretary of the Army (RDA) The Pentagon, Washington, DC 20301-0103
1	ATTN: SARD-TR, K. Gabriel
	Office of the Under Secretary of Defense for Research and Engineering, The Pentagon, Washington, DC 20301
1	ATTN: Mr. J. Persh
	Commander, U.S. Army Laboratory Command, 2800 Powder Mill Road, Adelphi, MD 20783-1145
2	ATTN: AMSLC-DL, Mr. R. Vitali
1	AMSLC-CT
1	SLCSM, LTC W. Probka
1	SLCLT, D. Woodbury
1	SLCLT, G. Roffman
	Commander, Defense Technical Information Center, Cameron Station, Bldg. 5, 5010 Duke Street, Alexandria, VA 22304-6145
2	ATTN: DTIC-FDAC
	Commander, Army Research Office, P.O. Box 12211, Research Triangle Park, NC 27709-2211
1	ATTN: Information Processing Office
1	SLCRO, J. Prater
	Commander, U.S. Army Materiel Command, 5001 Eisenhower Avenue, Alexandria, VA 22333
1	ATTN: AMCLD
1	AMCDE-SR, Dr. R. Chait
	Commander, Chemical Research and Development Engineering Center, Aberdeen Proving Ground, MD 21010-5423
1	ATTN: Mrs. E. Riley
	Commander, U.S. Army Materiel Systems Analysis Activity, Aberdeen Proving Ground, MD 21005
1	ATTN: AMXSY-MP, H. Cohen
	Director, U.S. Army Ballistic Research Laboratory, Aberdeen Proving Ground, MD 21005-5066
1	ATTN: SLCBR-TB-EP, A. Gauss, Jr.
1	SLCBR-TB-EP, S. Cornelison
1	SLCBR-TB-EP, R. Bossoli
1	SLCBR-SE-W, H. B. Wallace
	Commander, U.S. Army Belvoir RD&E Center, Ft. Belvoir, VA 22060-5606
1	ATTN: STRBE-JDR, G. Walker
1	STRBE-JDR, E. Jacobs
1	STRBE-JDR, N. Fontana

---

No. of  
Copies

To

---

Director, U.S. Army VAL, White Sands Missile Range, NM 88002-5513  
1 ATTN: SLCVA-TAC, J. Arthur

Commander, U.S. Army Missile Command, Redstone Scientific Information Center, Redstone Arsenal, AL 35898-5241  
1 ATTN: AMSMI-RD-CS-R/Doc  
1 AMSMI-RLM  
1 AMSMI-RD-ST, L. Mixon

Commander, U.S. Armament, Munitions and Chemical Command, Dover, NJ 07801-5000  
2 ATTN: Technical Library  
1 SMCAR-FSP-A(2), P. Kisatsky

Commander, U.S. Army Natick Research, Development, and Engineering Center, Natick, MA 01760  
1 ATTN: Technical Library  
1 Dr. R. Lewis  
1 STRNC-ITC, S. Seashultz  
1 STRNC-ITC, T. Commerford

Commander, U.S. Army Tank-Automotive Command, Warren, MI 48397-5000  
2 ATTN: AMSTA-TSL, Technical Library  
1 AMSTA-RSL, I. Lozon

Commander, U.S. Army Materials Systems Analysis Activity, Aberdeen Proving Ground, MD 21005-5071  
1 ATTN: AMXSY-GI, Gary Holloway

Commander, Combat Systems Test Activity, Aberdeen Proving Ground, MD 21005-5059  
1 ATTN: STECS-AA-R, Roy Falcone

Commander, U.S. Army Aviation Systems Command, Aviation Research and Technology Activity, Aviation Applied Technology Directorate, Fort Eustis, VA 23604-5577  
1 ATTN: SAVRT-TY-ASV, L. Dikant

Commander, U.S. Army Aviation Systems Command, 4300 Goodfellow Boulevard, St. Louis, MO 63120-1798  
1 ATTN: AMSAV-GTD

1 Dr. Michael Alexander, Chief, RADC/ESMO, Hanscom Air Force Base, MA 01731

Commander, U.S. Army Foreign Science Technology Center, 220 7th Street N.E., Charlottesville, VA 22901-5956  
1 ATTN: AIFREA, S. Eitelman  
1 D. Leiter

Chromerics, Inc., 77 Dragon Court, Woburn, MA 01888  
1 ATTN: Mr. David Smith  
1 Mr. Michael Kocsik

---

No. of  
Copies

To

Fiber Materials Incorporated, Biddeford Industrial Park, Biddeford, ME 04005  
1 ATTN: Mr. Paul Chayka

Textron Bell Helicopter, P.O. Box 482, Ft. Worth, TX 76101  
1 ATTN: Mr. Steven Webster

Director, U.S. Army Materials Technology Laboratory, Watertown,  
MA 02172-0001  
2 ATTN: SLCMT-TML, Library  
4 Authors

U.S. Army Materials Technology Laboratory  
Watertown, Massachusetts 02172-0001  
A SUMMARY OF MEASUREMENTS OF  
PERMITTIVITIES AND PERMEABILITIES OF  
SOME MICROWAVE ABSORBING MATERIALS -  
W. A. Spurgeon, M. El Rayess, P. Dorsey, and  
C. Vittoria

AD UNCLASSIFIED  
UNLIMITED DISTRIBUTION

Technical Report MTL TR 90-26, May 1990, 63 pp-  
illus

Key Words  
Permittivity  
Permeability  
Metal plastic composites

This report presents results of measurements of permittivities and permeabilities of assorted materials collected by the U.S. Army Office of Low Observables Technology and Applications (LOTA), and by the U.S. Army Materials Technology Laboratory (MTL). This will be one of a planned series of annual reports prepared by MTL for LOTA describing the results of such tests. The samples fall into the following categories: (1) Pure materials (teflon, plexiglasses and casting plastic); (2) Metal-coated microspheres; (3) Carbospheres, both uncoated and metal coated; (4) Ferrites; (5) Magnetic metal flake; (6) Ceramic matrix composites; (7) A standard paint. The data and its limitations and plans for additional testing are presented in the text. The most interesting results were obtained for a Rockwell Ferrite and for a 50/50 ferronickel flake which showed magnetic loss from 2 to 18 GHz.

U.S. Army Materials Technology Laboratory  
Watertown, Massachusetts 02172-0001  
A SUMMARY OF MEASUREMENTS OF  
PERMITTIVITIES AND PERMEABILITIES OF  
SOME MICROWAVE ABSORBING MATERIALS -  
W. A. Spurgeon, M. El Rayess, P. Dorsey, and  
C. Vittoria

AD UNCLASSIFIED  
UNLIMITED DISTRIBUTION

Technical Report MTL TR 90-26, May 1990, 63 pp-  
illus

Key Words  
Permittivity  
Permeability  
Metal plastic composites

This report presents results of measurements of permittivities and permeabilities of assorted materials collected by the U.S. Army Office of Low Observables Technology and Applications (LOTA), and by the U.S. Army Materials Technology Laboratory (MTL). This will be one of a planned series of annual reports prepared by MTL for LOTA describing the results of such tests. The samples fall into the following categories: (1) Pure materials (teflon, plexiglasses and casting plastic); (2) Metal-coated microspheres; (3) Carbospheres, both uncoated and metal coated; (4) Ferrites; (5) Magnetic metal flake; (6) Ceramic matrix composites; (7) A standard paint. The data and its limitations and plans for additional testing are presented in the text. The most interesting results were obtained for a Rockwell Ferrite and for a 50/50 ferronickel flake which showed magnetic loss from 2 to 18 GHz.

U.S. Army Materials Technology Laboratory  
Watertown, Massachusetts 02172-0001  
A SUMMARY OF MEASUREMENTS OF  
PERMITTIVITIES AND PERMEABILITIES OF  
SOME MICROWAVE ABSORBING MATERIALS -  
W. A. Spurgeon, M. El Rayess, P. Dorsey, and  
C. Vittoria

AD UNCLASSIFIED  
UNLIMITED DISTRIBUTION

Technical Report MTL TR 90-26, May 1990, 63 pp-  
illus

Key Words  
Permittivity  
Permeability  
Metal plastic composites

This report presents results of measurements of permittivities and permeabilities of assorted materials collected by the U.S. Army Office of Low Observables Technology and Applications (LOTA), and by the U.S. Army Materials Technology Laboratory (MTL). This will be one of a planned series of annual reports prepared by MTL for LOTA describing the results of such tests. The samples fall into the following categories: (1) Pure materials (teflon, plexiglasses and casting plastic); (2) Metal-coated microspheres; (3) Carbospheres, both uncoated and metal coated; (4) Ferrites; (5) Magnetic metal flake; (6) Ceramic matrix composites; (7) A standard paint. The data and its limitations and plans for additional testing are presented in the text. The most interesting results were obtained for a Rockwell Ferrite and for a 50/50 ferronickel flake which showed magnetic loss from 2 to 18 GHz.

U.S. Army Materials Technology Laboratory  
Watertown, Massachusetts 02172-0001  
A SUMMARY OF MEASUREMENTS OF  
PERMITTIVITIES AND PERMEABILITIES OF  
SOME MICROWAVE ABSORBING MATERIALS -  
W. A. Spurgeon, M. El Rayess, P. Dorsey, and  
C. Vittoria

AD UNCLASSIFIED  
UNLIMITED DISTRIBUTION

Technical Report MTL TR 90-26, May 1990, 63 pp-  
illus

Key Words  
Permittivity  
Permeability  
Metal plastic composites

This report presents results of measurements of permittivities and permeabilities of assorted materials collected by the U.S. Army Office of Low Observables Technology and Applications (LOTA), and by the U.S. Army Materials Technology Laboratory (MTL). This will be one of a planned series of annual reports prepared by MTL for LOTA describing the results of such tests. The samples fall into the following categories: (1) Pure materials (teflon, plexiglasses and casting plastic); (2) Metal-coated microspheres; (3) Carbospheres, both uncoated and metal coated; (4) Ferrites; (5) Magnetic metal flake; (6) Ceramic matrix composites; (7) A standard paint. The data and its limitations and plans for additional testing are presented in the text. The most interesting results were obtained for a Rockwell Ferrite and for a 50/50 ferronickel flake which showed magnetic loss from 2 to 18 GHz.